

P0101. POSTER SESSION I

ADAPTIVE OPTICS IMAGES OF KEPLER OBJECTS OF INTEREST. E. R. Adams¹, D. R. Ciardi², A. K. Dupree¹, T. N. Gautier III³, C. Kulesa⁴, and D. McCarthy⁴, ¹Harvard-Smithsonian Center for Astrophysics (60 Garden St., Cambridge, MA, 02138, eadams@cfa.harvard.edu, adupree@cfa.harvard.edu), ²NASA Exoplanet Science Institute/Caltech (ciardi@ipac.caltech.edu), ³Jet Propulsion Laboratory/Caltech (thomas.n.gautier@jpl.nasa.gov), ⁴University of Arizona (ckulesa@as.arizona.edu, dmccarthy@as.arizona.edu).

Introduction: High-resolution images are a critical component of the Kepler validation effort. With sub-arcsecond resolution, it is possible to detect very close companion stars, which can dilute the transit signal or even introduce false positive signals. Here we present adaptive optics (AO) images of 90 Kepler Objects of Interest (KOIs) observed with two instruments: ARIES, a near-infrared PI instrument using adaptive optics on the MMT, and PHARO on Palomar. Most objects (60%) had at least one star within 6", and 20 objects (22%) had one or more companion within 2" of the target star, the closest with separations of only 0.1". We also place limits on the allowed magnitudes of still-undetected stars from 0.1-4" of each star.

Ruling Out False Positives: A variety of complementary methods are used to vet each Kepler candidate. When possible, high quality radial velocity measurements can uniquely confirm planetary mass, but they are unfortunately quite difficult or impossible to obtain for the smallest, most interesting objects or those around faint stars. A variety of other tests are used for such objects. The centroid of each candidate star is examined both in and out of transit to be sure there is no motion, indicating that the correct transit host has been identified. High-resolution images are used to search for close companion stars, ideally in multiple wavelengths to provide additional color constraints on blend scenarios. All of these parameters are used in BLENDER analyses, a comprehensive approach that is used to validate the planetary nature of Kepler Objects of Interest, such as Kepler-9d [1]. The magnitude limits placed at a range of distances by high-resolution images are particularly important, since they are used to decrease the area in which background events can exist and dramatically decrease the false positive probability.

Accurate Sizes: Even if the object that transits is still a planet, the dilution caused by another star will make the planet appear smaller than it actually is. Accounting for even a little dilution could make a big difference in determining whether a candidate planet is actually Earth-sized.

Examples: Two objects that have benefitted from AO images are shown in Figure 1. Kepler-7, aka KOI-97, has a stellar companion at 1.8" that is 4 mag fainter in J and Ks [2]. This results in a dilution factor of 2.7% in

both the primary transit and the planetary occultation. A larger effect can be seen for Kepler-14, aka KOI-98, which has a stellar neighbor 0.3" away that is 0.3 and 0.4 mag fainter in J and Ks respectively [3]. Complementary speckle images were also taken in optical wavelengths [4]. When combined with an analysis of the centroids, it was determined that the planetary candidate orbits the brighter star, and, while still planetary, the object is both 10% larger in radius and 60% more massive than would be estimated without knowledge of the companion star.

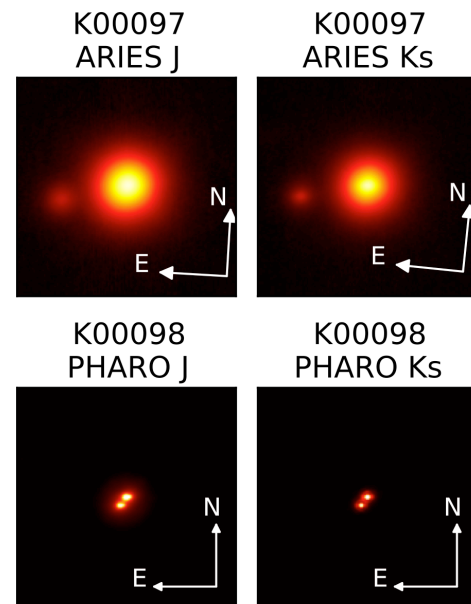


Figure 1. Inner 4" field of view of AO images of Kepler-7, aka K00097, and Kepler-14, aka K00098. In both cases a nearby companion star is present, affecting the planetary parameters determined. The companion to K00097 is 1.8" away and 4 mag fainter in J and Ks, while the companion to K00098 is 0.3" away and 0.3 and 0.4 mag fainter in J and Ks.

References: [1] Torres, G. et al. (2011) *ApJ*, 727, 24. [2] Demory, B.-O., et al. (2011) *ApJL* 735, L12. [3] Buchhave, L. A., et al. (2011) *arXiv:1106.5510*. [4] Howell, S. B. et al. (2011) *AJ*, 142, 19.

P0102. POSTER SESSION I

The NASA Exoplanet Archive and support for the Kepler science community. Rachel Akeson¹ and the Exoplanet Archive Team, ¹NASA Exoplanet Science Institute, California Institute of Technology, 1200 E. California Blvd, Pasadena, CA, 91125, rla@ipac.caltech.

Introduction: The NASA Exoplanet Science Institute (NExSci) will be releasing the first version of the NASA Exoplanet Archive in late fall 2011. One of the primary goals for this archive is to support the astronomical community in utilizing Kepler data for exoplanet searches and other astrophysics and to support the Kepler project during the extended mission.

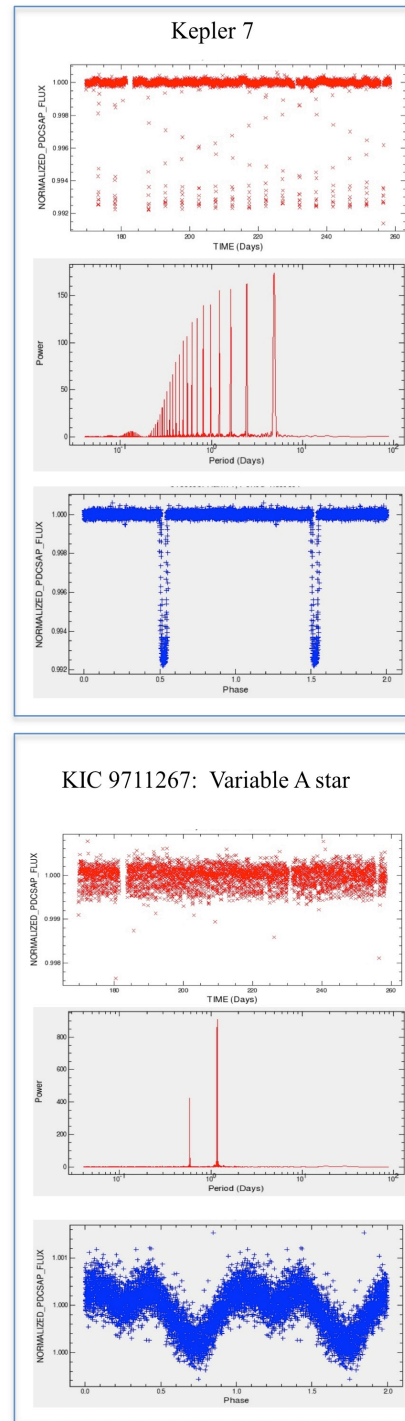
I will describe both the near-term capabilities of this archive and the longer-term plans which include:

- Tools for viewing and working with light curves (phasing, normalization, periodogram, see figure)
- Integrated table of Kepler planets and candidates including mission data validation values and follow-up data
- Support for community-wide follow-up observing of Kepler candidates
- Support for new Kepler candidates during the extended mission

Community Input: At the Kepler Science conference we will be soliciting feedback for future development and support of the Exoplanet Archive such as:

- How should the community be organized for the follow-up observing of Kepler candidates during the extended mission to minimize duplication of effort?
- What additional tools are needed to work with Kepler data?
- What additional data products should be integrated into the environment?

Figure 1: The normalized light curve, periodogram and phased light curve for Kepler 7 and a variable A star, KIC 9711267.



P0103. POSTER SESSION I

Radial velocity follow-up of CoRoT transiting candidates with HARPS.

F. Bouchy^{1,2}, A. Santerne³, C. Moutou³, G. Hébrard^{1,2}, R. Diaz^{1,2}, M. Deleuil³, D. Queloz⁴, A. Hatzes⁵

¹Institut d'Astrophysique de Paris, UMR7095, CNRS/UPMC, 98bis Bd Arago, 75014 Paris, France (bouchy@iap.fr, hebrard@iap.fr, diaz@iap.fr) ²Observatoire de Haute-Provence, CNRS/OAMP, 04870 St Michel l'Observatoire, France, ³Laboratoire d'Astrophysique de Marseille, CNRS/OAMP, 38 rue Frederic Joliot-Curie, 13388 Marseille, France (claire.moutou@oamp.fr, magali.deleuil@oamp.fr), ⁴Thüringer Landessternwarte, Sternwarte 5, Tautenburg 5, D-07778 Tautenburg, Germany (artie@tls-tautenburg.de), ⁵Observatoire de l'Université de Genève, 51 chemin des Maillettes, 1290 Sauverny, Switzerland (didier.quelez@unige.ch)

Abstract: Radial velocity follow-up is essential and mandatory to establish or exclude the planetary nature of a transiting companion as well as to accurately determine its mass. Here we present our large program of Doppler follow-up conducted these 5 last years with the high-precision spectrograph HARPS (3.6-m ESO) on the CoRoT transiting candidates. We discuss and present our observing strategy, the main difficulties and limitations, as well as the obtained and on-going results. We also discuss the different diagnostics to reveal the impostors among the transiting exoplanet candidates and we point out the high rate of false positives revealed by our Doppler follow-up.



P0104. POSTER SESSION I

Measuring the Rate of Non-Planetary Background Transit Events in Kepler Data. S. T. Bryson¹, M. R. Haas², J. M. Jenkins³, C. J. Burke⁴, and D. A. Caldwell⁵, ¹MS 244-30 NASA Ames Research Center Moffett Field, CA 94035 steve.bryson@nasa.gov, ²NASA Ames Research Center, michael.r.haas@nasa.gov, ³SETI Institute, jon.jenkins@nasa.gov, ⁴SETI Institute, christopher.j.burke@nasa.gov, ⁵SETI Institute, douglas.caldwell@nasa.gov.

Introduction: The *Kepler* mission finds exoplanets through the detection of transit signatures. However, transit-like signatures can be due to phenomena other than exoplanets. One of the dominant sources of such false-positive transit signatures is an eclipsing binary nearly aligned with the observed target star, referred to as a Background Eclipsing Binary (BGEb). While eclipsing binaries in isolation generally have eclipses that are much deeper than a planetary transit, dilution by the flux of the target star can reduce the apparent depth of the eclipse so it appears very similar to a planetary transit.

The *Kepler* data analysis pipeline uses a variety of methods to detect BGEbs, primarily by detecting an offset of the transit signal from the target star. This method fails when the BGEb is very well aligned with the target star. Therefore it is critical to know the probability of an aligned BGEb when determining the confidence that a transit signal is due to an exoplanet orbiting the target star. Available binary density models [1] provide an estimate of the expected background binary density, but these models have a high degree of uncertainty because they are based on the observed bright binary population.

We describe a direct measurement of the density of eclipsing binary signals in the Kepler field of view that would appear as planetary transits if diluted by a foreground target star. We expect that some of these signals are due to extremely faint binary systems that cannot be distinguished from the general stellar background. We do not attempt to characterize these binary systems, as we are interested only in the density of possibly confounding BGEb signatures.

The Observed Data: Starting in quarter 5 (Spring 2010) a 36 x 60 pixel (143 x 239 arcsec) region (Fig. 1) on each of the 80 active channels of the *Kepler* focal plane has been observed with the standard *Kepler* 30-minute long cadence. These regions contain relatively few bright stars. The size of these regions was dictated by the number of pixels that became available when four channels of the *Kepler* focal plane failed in quarter 4.

These regions total 0.2% of the focal plane, compared with 6% of the focal plane observed in the planetary search. Eclipsing binary density models predict that the number of BGEb signatures in each region will range from a few for channels towards the Galactic plane to less than one for channels away from the Galactic plane.

Measuring the BGEb Signal Density: BGEb signals will be detected by tiling each region with overlapping 2x2 pixel apertures and searching these apertures for eclipsing binary signatures using the standard *Kepler* data analysis pipeline. This search will be part of standard *Kepler* processing [2] beginning in mid 2012. Preliminary searches are underway and available results will be presented. The 2x2 tiling produces about 130,000 targets to be searched.

The use of 2x2 pixel apertures is driven by the desire to minimize background noise while still capturing the flux of the BGEb in at least one aperture. We expect that the resulting search will be complete to about *Kepler* magnitude $K_p = 22$. For comparison, Zodiacal light is about $K_p = 20$.

This study will provide an estimate of the density per square arc second of eclipsing binary signals that would appear planetary (have depth < 1%) when diluted by a target star as a function of eclipse period and depth. This estimate can be used to calibrate binary population models.

Several challenges arise in this study. Channels away from the Galactic plane are predicted to have fewer than 1 BGEb in each region, so our result will be based on small statistics. We will discuss the completeness of our study, specifically the detectability of very dim BGEbs.

We welcome collaborators in the analysis of this background data. Formal collaborators will have access to all background data.

References: [1] Raghavan, D. et. Al. (2011) *ApJ*, to appear. [2] Jenkins, J. J., et al. (2010) *Proc. SPIE*, Vol. 7740, 77400D.

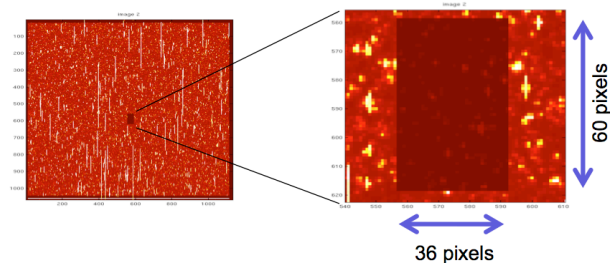


Fig 1: All *Kepler* channels averaged together, showing the BGEb search region as the shaded rectangle. Left: all 1024 x 1100 pixels per channel. Right: close-up of the BGEb search region.

P0105. POSTER SESSION I

Efficient formation of terrestrial planets around low-metallicity stars inferred from Kepler data. Lars A. Buchhave^{1,2}, David W. Latham³, Anders Johansen⁴, Jason F. Rowe⁵, G. Torres³, ¹Niels Bohr Institute, University of Copenhagen, DK-2100, Copenhagen, Denmark, buchhave@astro.ku.dk, ²Centre for Star and Planet Formation, Natural History Museum of Denmark, University of Copenhagen, DK-1350 Copenhagen, Denmark, buchhave@astro.ku.dk, ³Harvard-Smithsonian Center for Astrophysics, Cambridge, MA 02138, USA, latham@cfa.harvard.edu, torres@cfa.harvard.edu, ⁴Lund Observatory, Lund University, Box 43, 221 00 Lund, Sweden, anders@astro.lu.se, ⁵SETI Institute/NASA Ames Research Center, Moffett Field, CA 94035, USA, jason.rowe@nasa.gov

Ground-based exoplanet surveys find that the probability for a star to be orbited by a gas-giant planet increases with the abundance of heavy elements (metallicity) in the stellar photosphere. This is in agreement with theoretical models of accumulation of dust grains and planetesimals into gas-giant cores. However, how the planet-metallicity relationship extends to terrestrial planets is unknown. The unprecedented sensitivity of the Kepler mission provides a unique opportunity to probe the planet-metallicity correlation down to low-radius planets. Here we report spectral observations yielding an abundance analysis of the host stars of 250 exoplanets discovered by the Kepler mission. The data reveal with statistical significance that planets with small radii orbit stars that are on the average of lower metallicity than planets with larger radii. This implies that the planet formation process converts dust much more efficiently into terrestrial planets than into cores of gas giants around low-metallicity stars.

We thank all the Kepler follow-up observers who have worked hard to obtain reconnaissance spectra of Kepler Objects of Interest, which were the basis for this study: William D. Cochran, Michael Endl, Phillip J. MacQueen, Paul Robertson, Erik J. Brugamyer, Caroline Caldwell, Anita L. Cochran, Geoff Marcy, Andrew Howard, Debra Fischer, Christian Schwab, Julien Spronck, John Johnson, Tim Morton, Justin Crepp, John Pineda, Mike Bottom, Chris Clanton, Gaspar Bakos and Guillermo Torres. We also thank the Kepler team for the remarkable photometry that has provided the planet radius estimates. Kepler was competitively selected as the tenth Discovery mission. Funding for this mission is provided by NASA's Science Mission Directorate.

P0106. POSTER SESSION I

The Search for Jupiter Analogs in Kepler’s First Three Quarters J. A. Burt¹, G. Laughlin², P. Nutzman², ¹University of California at Santa Cruz, Santa Cruz, CA, 95064; jaburt@ucsc.edu ²Lick Observatory; laugh@ucolick.org, pnutzman@ucolick.org

In the past three years the Kepler team has begun to determine the commonality of Earth-like planets in our galaxy through their use of phase-folding lightcurve analysis [1]. While these detections help astronomers to understand the frequency with which short period planets occur, they are insensitive to planets with long orbital periods [2] (figure 1). Thus we are unable to assess the commonality of our solar system as a whole because the data processing method is highly unlikely to detect the signature of planets with periods exceeding the current observational baseline, such as our Jupiter. These “true Jupiter analogs” are an important factor in understanding the dynamics of other star systems and as such merit a focused attempt at detection.

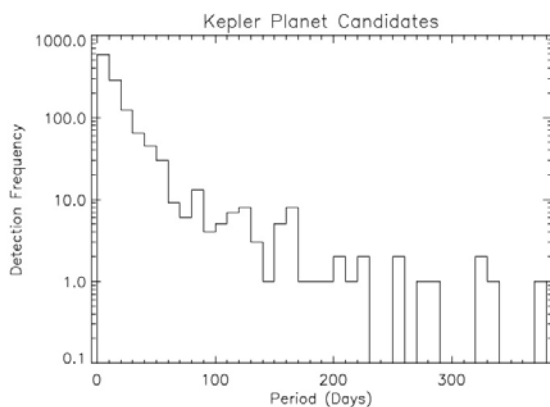


Figure 1: Periods of Kepler’s planet candidates. For comparison, Jupiter’s period is ~4332 days.

We adopt an analysis method focused on detecting long duration, single transit events. The traditional starting point of fitting high order polynomials to the entire lightcurve poses the possibility of also fitting a long duration transit and is therefore avoided. Thus the algorithm must be robust enough to deal with numerous changes in curvature due to both stellar variability and large flux discontinuities caused by the equipment that cannot be divided out. The magnitude of these affects varies strongly between stars, so the algo-

rithm must be able to handle such transitions quickly and proficiently.

Lightcurves are searched piecewise for evidence of large scale changes in the photometric scatter that characterize of planetary transits. Once a transit is detected, the code works through suspected transit points, verifying them one at a time through an iterative fitting process. While the code is currently tuned for Jupiter-sized events, its thresholds can be manipulated to search for planets on shorter-period orbits as well.

Work is currently in progress to apply the algorithm to the publicly released Kepler data (Q1 – Q3). Preliminary results will be presented.

References:

- [1] Jenkins et al. (2010) Proc. of SPIE, 7740. D1-D11
- [2] Borucki et al (2011) ApJ, 736:19

P0107. POSTER SESSION I

LINEAR AND NONLINEAR NOISE REDUCTION TECHNIQUES FOR KEPLER DATA. D. L. Buzasi¹,
¹Eureka Scientific, 2452 Delmer St., Ste. 100, Oakland, CA 94602, dbuzasi@gmail.com.

The Kepler pipeline produces simple aperture photometry on each target, and engineering data and other diagnostics are used to remove systematic errors in the resulting time series. Time series are then searched for planet signatures using an adaptive matched filter (Jenkins et al. 2010), and for stellar oscillations and other astrophysically interesting phenomena using a variety of techniques (Hekker et al. 2011, Mathur et al. 2011). Noise levels found in these time series are up to 50% higher than originally anticipated for the mission, with a large contribution to the noise level coming from intrinsic stellar signals such as activity and granulation (Gilliland et al. 2011).

Buzasi (2007) suggested that use of a Wiener filter based on the known signature of stellar granulation might improve noise characteristics of the time series. However, this appears to be a significant improvement on the current (mostly time domain) filtering approach only in certain portions of parameter space. Alternatively, nonlinear noise reduction techniques can be used for such broad-band noise spectra. In this paper, we compare the performance of linear and nonlinear noise reduction on Kepler data, with both planetary detection and stellar oscillation applications in mind.

P0108. POSTER SESSION I

TRANSIT VERIFICATION PHOTOMETRY WITH THE FAULKES - NORTH TELESCOPE, HAWAII.

E. Chang¹, E. Gaidos¹, J. D. Armstrong², D. Anderson³, J. Beyer¹, S. Lépine⁴, E. Hilton^{1,5}. ¹Department of Geology & Geophysics, University of Hawaii at Manoa, Honolulu, HI 96822 (gaidos@hawaii.edu) ²Institute for Astronomy ATRC, Pukalani, HI 96768, ³Astrophysics Group, Keele University, Keele, Staffordshire ST5 5BG, UK, ⁴American Museum of Natural History, New York, NY 10024. ⁵Institute for Astronomy, University of Hawaii at Manoa, Honolulu, HI 96822.

Introduction: Exoplanet science is important to understanding the formation of planets and stars and the possibility of habitable planets and life elsewhere; [1-2]. Late K and early M dwarf stars are ideal candidates for exoplanets detection because their relatively small size and low stellar noise and lower luminosity increase the possibility of detecting smaller transiting planets around them [3-4]. The *Kepler* Mission is surveying approximately 150,000 stars for transiting planets; despite the bias of its magnitude-limited target catalog, this includes more than 10,000 late K- and early M stars [5]. However most of these stars are too faint for follow-up observations.

Approach: We study nearby late K and early M stars as a comparison/complementary sample to that of *Kepler*. We use SuperWASP lightcurves to identify candidate transiting planets to follow-up with more precise ground-based photometry. SuperWASP consists of two telescope arrays (in La Palma and South Africa) of 8 wide-angle cameras, each with 2048² CCDs having a 61 square degree field of view [6-7]. SuperWASP can detect Neptune-size planets around M dwarfs (transit depth ~5 mmag) but with a high false-positive rate. Our approach is to identify candidates for rapid screening with high-precision (≤ 1 mmag) photometry from 1-2m ground-based telescopes. We identified 1763 late K and early M stars with $V < 14$ or $J < 10$ from the SUPERBLINK proper motion-selected catalog [8] that are within 45" of sources falling in the inaugural (2004) fields of WASP-North: most sources have $> 10,000$ measurements.

Candidate screening: After detrending, each lightcurve was searched for transit-like events in the range 0.3-30 days [7]. Over 1000 candidate transit signals were individually inspected and selected for follow-up using several criteria designed to eliminate false positives due to systematic noise and binary or spotted stars (Figure 1). Selection is based on signal to red-noise ratio (> 3), elliptical variance, signal to red-noise transit/anti-transit (> 1), quality and number of transits, $\Delta\chi^2$, transit width and period, and transit depth. Signals with period within 5% of the alias signals at 1/3, 1/2, 2/3, 2, and 3 days or within 10% of 1 day are rejected.

Follow-up photometry: Transit predictions are based on the SuperWASP-based ephemerides. Events

within 3 hr of sunrise/sunset or at airmass > 1.4 are ignored. The target is observed the entire night, until it sets, or airmass reaches 2. Observations are conducted on the 2-m Faulkes-North telescope on Haleakula, Hawaii with a Spectra Physics 4096² CCD camera. The field of view is 10.5×10.5 arc-minutes. All observations are obtained through a Pan-STARRS Z filter (center wavelength of 870 nm) to maximize signal from these red stars, minimize errors due to atmospheric absorption, and intrinsic stellar variability [9]. Fields are optimized to include one or more comparison stars of similar J magnitude and J-K color and avoid CCD cosmetics. Images are defocused to average out flatfield errors and reduce lightcurve noise to increase duty cycle. Each integration is 2-3 minutes and acquires a few million electrons.

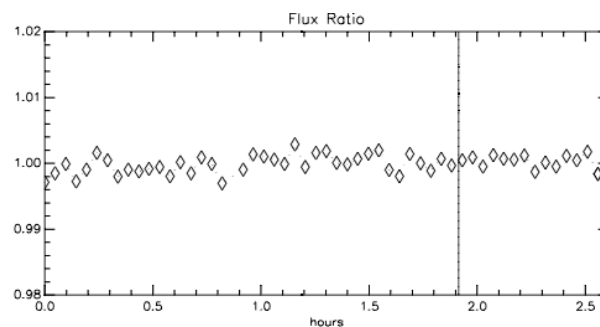


Figure 1. Normalized flux ratio between J=8.5 target and reference stars (RMS= 1.3×10^{-3}). The solid line is the predicted transit time; no transit was detected.

Analysis and results: The images are flat-fielded and aperture photometry is performed on the target and reference stars using a circular aperture and an annular sky aperture. Thus far, usable data has been obtained on 6 nights, and we have achieved photometric stability (RMS) as good as 1.3×10^{-3} per 2 min integration, allowing us to detect Neptune-size planets.

P0109. POSTER SESSION I

Photometric Analysis in the Kepler Science Operations Center Pipeline. B.D. Clarke¹, J.D. Twicken¹, S.T. Bryson², H. Wu¹, J.M. Jenkins¹, F. Girouard³, T.C. Klaus³, ¹SETI Institute/NASA Ames Research Center, M/S 244-30, NASA Ames Research Center, Moffett Field, CA 94035; Bruce.D.Clarke@nasa.gov, Joseph.Twicken@nasa.gov, hayley.wu@gmail.com, Jon.Jenkins@nasa.gov, ²NASA Ames Research Center; Steve.Bryson@nasa.gov, ³Orbital Sciences Corporation; Forrest.Girouard@nasa.gov, todd.klaus@nasa.gov

Introduction: We describe the Photometric Analysis (PA) software component and its context in the *Kepler* Science Operations Center (SOC) Science Processing Pipeline. The primary tasks of this module are to compute the photometric flux and photocenters (centroids) for over 160,000 long cadence (30 minute integration) and 512 short cadence (one minute integration) stellar targets from the calibrated pixels in their respective apertures. We discuss science algorithms for long and short cadence PA: cosmic ray cleaning; background estimation and removal; aperture photometry; and target centroiding. We present examples of photometric apertures, raw flux light curves, and centroid time series from *Kepler* flight data.

Cosmic Ray Cleaning: Outlier values are identified and replaced in each background and target pixel time series. Detrending and median filtering are performed on each time series, the Median Absolute Deviation (MAD) of the residuals after median filtering is computed, and a detection threshold is applied. Outliers may be both positive and negative, although a threshold multiplier may be specified for negative events. The expected cosmic ray flux rate for the *Kepler* CCD array is $5 \text{ cm}^{-2} \text{ sec}^{-1}$ (three direct hits per pixel per day).

Background Estimation and Removal: Background pixels are acquired at the long cadence rate in a grid pattern on each of the focal plane module outputs. A robust two-dimensional polynomial is fit to these background pixels on each cadence, and the polynomial is evaluated at the coordinates of the target pixels in each stellar aperture to estimate the background level for each target pixel. The background is removed by subtracting the background estimates from the respective target pixels. Robust fitting is required because background pixels may be corrupted by flux from nearby targets.

Aperture Photometry: Simple Aperture Photometry (SAP) is the only photometry method supported in the current PA release (SOC 8.0). For SAP, the *unweighted* sum of the background-removed pixels in the *optimal* aperture of each target is computed to obtain the raw flux per target and cadence. Uncertainties in the raw flux values are propagated by standard methods from uncertainties in the calibrated background pixels and calibrated pixels in the optimal apertures of the respective targets.

Target Centroiding: The center of photometric flux is computed for each target and cadence from background-removed pixels in the associated centroid aperture. Two different centroiding methods are supported by PA. Flux-weighted (first moment) centroids are computed for all targets. Centroids may also be computed for select targets by fitting a predetermined Pixel Response Function (PRF) to pixel values in the respective target apertures. Flux-weighted centroids are computed in an aperture that includes the optimal aperture plus a single halo ring for each target. PRF-based centroids are computed in an aperture that includes all available pixels for each target. Uncertainties in the row and column centroid values are propagated by standard methods from uncertainties in the calibrated background pixels and calibrated pixels in the centroid apertures of the respective targets.

Barycentric Timestamp Correction: A barycentric timestamp offset is computed for each stellar target such that the sum of the timestamp plus offset yields the time that flux from the given target would have been captured at the solar system barycenter. Barycentric offsets allow investigators to account for modulation of the timing of observed transits due to the heliocentric orbit of the photometer. This correction also accounts for the small time slice offsets introduced in the multiplexed readout of the focal plane array. The corrections must be computed separately for each target due to the wide field of view of the *Kepler* photometer.

Summary: PA light curves, centroid time series, and barycentric timestamp corrections for each stellar target are exported to the Multi-mission Archive at Space Telescope [Science Institute] (MAST) and are made available to the general public in accordance with the NASA/*Kepler* data release policy.

References:

- [1] Bryson, S.T., et al. (2010), "Selecting pixels for *Kepler* downlink," Proc. SPIE 7740.
- [2] Jenkins, J.M., et al. (2010), "Overview of the *Kepler* Science Processing Pipeline," ApJL, 713 (2), L87-L91.
- [3] Bryson, S.T., et al. (2010), "The *Kepler* Pixel Response Function," ApJL, 713 (2), L97-102.
- [4] Wu, H., et al. (2010), "Data validation in the *Kepler* Science Operations Center pipeline," Proc. SPIE 7740.

P0110. POSTER SESSION I

VETTING KEPLER PLANET CANDIDATES WITH MULTI-COLOR PHOTOMETRY FROM THE GRAN TELESCOPIO CANARIAS. K. D. Colón¹, E. B. Ford², R. C. Morehead³, M. Shabram⁴, ¹Department of Astronomy, University of Florida, 211 Bryant Space Science Center, PO Box 112055, Gainesville, FL 32611; knicole@astro.ufl.edu, ²University of Florida; eford@astro.ufl.edu, ³University of Florida; rmorehead@astro.ufl.edu, ⁴University of Florida; mshabram@astro.ufl.edu.

Introduction: We present multi-color observations of several planet candidates recently identified by the Kepler space mission [1]. By applying the unique capabilities of OSIRIS (installed on the 10.4-meter Gran Telescopio Canarias) for near-simultaneous multi-color photometry, we use the color of Kepler candidates as measured during predicted transit events to reject candidates that are false positives (e.g., a blend with an eclipsing binary either in the background or bound to the target star). Because a majority of Kepler's eclipsing binaries have short orbital periods [2,3], and because hierarchical triple star systems can mimic Neptune-size transits [4], we specifically target small planets (less than ~6 Earth radii in size) with short orbital periods (less than ~6 days). Our results include the identification of KOI 225.01 and KOI 1187.01 as false positives. These observations are part of a program to observationally determine the false positive rate for a subset of Kepler planet candidates (i.e. planets with radii less than ~6 Earth radii and orbital periods of less than ~6 days) and are complementary to a similar program being conducted using warm-Spitzer [e.g., 5,6,7]. The results of this program will be compared to recent estimates made for the false positive rates for the Kepler sample [4,7]. This material is based upon work supported by the National Science Foundation Graduate Research Fellowship under Grant No. DGE-0802270. This work was also aided by grants from the American Philosophical Society and the National Geographic Society.

References: [1] Borucki W. J. et al. (2011) *ApJ*, 736, 19. [2] Prsa A. et al. (2011) *AJ*, 141, 83. [3] Slawson R. W. et al. (2011) submitted to *AJ*, arXiv:1103.1659. [4] Morton T. D. and Johnson J. A. (2011) *ApJ*, 738, 170. [5] Ballard S. et al. (2011) accepted to *AJ*, arXiv:1109.1561. [6] Fressin F. et al. (2011) accepted to *AJ*, arXiv: 1105.4647. [7] Desert J.-M. et al. (2011) Bulletin of the *AAS*, Abstract #211.06.

P0111. POSTER SESSION I

DETECTING CIRCUMBINARY PLANETS BY ECLIPSE ECHOLaurance R. Doyle¹ and Hans-Jörg Deeg²¹SETI Institute, 189 Bernardo Avenue, Mountain View, CA 94043, USA, ldoyle@seti.org,²Instituto de Astrofísica de Canarias, C. Via Lactea S/N, 38205 La Laguna, Tenerife, Spain, hdeeg@iac.es.

A photometric method to detect planets orbiting around short-period binary stars is presented. It is based on the detection of stellar eclipse signatures in the reflected light of circumbinary planets. Amplitudes of such “eclipse echos” (EEs) will depend on the orbital configurations of the stellar binary and circumbinary planet(s) relative to the observer, and theoretically could be detectable even for binary systems not eclipsing along our line-of-sight. These reflected eclipses will occur, to the observer, with a period that is distinct from the binary eclipse periods themselves because, 1) the planet will “see” eclipses at various times different from the observer because of its orbital motion, and 2) by a much smaller effect, the light travel time to/from the planet will cause a variable delay in the reflected EE. At the photometric precision of Kepler, dozens of known eclipsing binary systems may potentially show evidence of such EE signals if short-period circumbinary planets are present.

P0112. POSTER SESSION I

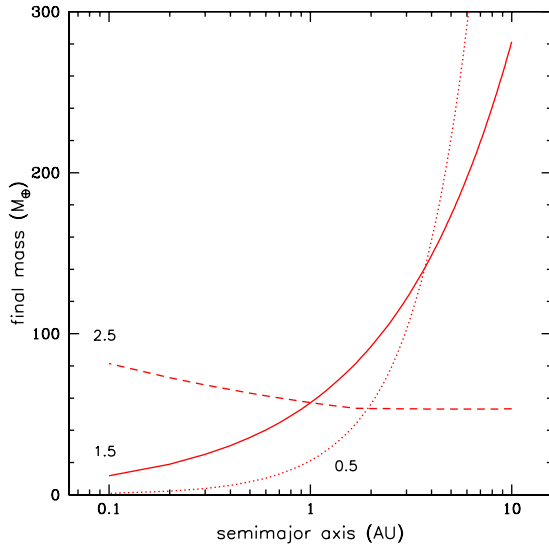
STATISTICS OF NEPTUNE-MASS PLANETS AND SUPER-EARTHS IN A QUIESCENT-DISK PLANET FORMATION MODEL. P. R. Estrada, I. Mosqueira, *Carl Sagan Center, SETI Institute, Mountain View CA 94043, USA, (Paul.R.Estrada@nasa.gov).*


Figure 1: Plot of the final mass for an inviscid disk of the gap-opening masses. We show three different values for the gas surface density powerlaw exponent to cover a reasonable range of potential initial conditions. The solid red curve corresponds to the standard model value $n = 3/2$. Kinks seen are due to transition from the disk back reaction being important to not important.

Introduction: In a weakly turbulent disk the Type I inward migration of objects of $\sim 10 M_{\oplus}$ stalls due to the feedback effect [1,2]. Since in the core-accretion model of planet formation such objects can form in a time ($10^5 - 10^6$ yrs) comparable to their migration time, provided that the nebula was enhanced in solids with respect to solar abundances, gap-opening can explain planet survival. The required enhancement in solids in the planet-forming region can result from the gas-drag migration of planetesimals during the early evolution of the extended solar nebula. Once such a core forms gap-opening occurs both due to rapid gas accretion and because of the tidal interaction with the gas disk. The final mass of an isolated planet then depends on a competition between these two processes; however, multiple giant planets complicate this picture as one planet can replenish the feeding zone of its neighbor. Here we investigate planetary properties using simple parameterized models for the gas accretion rate onto the core and the evolution of the gaseous disk [3] and the results from N-body accretion simulations (e.g., [4]). We will discuss whether this framework of planet formation yields planetary masses that are generally in agreement with recent observational constraints [5].

Methodology: The non-linear evolution of sound waves as they travel away from the planet leads to the formation of a shock [6]. For a planet mass M , the distance at which the wave first begins to deposit its angular momentum (for a constant surface density disk) is given approximately by $l_{sh} \approx \zeta(2H/3)(M/M_1)^{-2/5}$, where H is the local disk scale height, M_1 is the upper limit of the mass that may not open a gap, and $\zeta = 1.4$. More generally, the gap-opening conditions on the limiting mass of the perturber for an inviscid disk [1]

can be expressed in terms of the Toomre parameter Q as

$$M/M_1 > \min[5.2Q^{-5/7}, 3.8(Q/h)^{-5/13}], \quad (1)$$

where $h = H/r$. In the right limit, the feedback reaction of the disk from the density perturbations to the drift velocity causes the migrating protoplanet to stall, eventually stopping migration and begins to open a gap in place [7,8]. The left limit corresponds to the case for which the disk back reaction is unimportant and fails to slow a rapidly migrating protoplanet enough for it to stall. Instead, a gap is opened behind the protoplanet (opposite the direction of migration). In Figure 1 we show the final mass of the giant planet with distance from a solar like star using Eq. (1), for a standard “optically thin” minimum mass model [9, solid curve], under the idealized assumption that the protoplanet can accrete all of the available gas within its shocking distance. These examples demonstrate that gap-opening, and subsequently final masses can decrease sharply as you approach the star.

In order to begin to properly model the physical processes involved in gap-opening by a protoplanet, numerical models are required. We have developed a code that incorporates the growth of the giant planet with the disk evolution. The gas accretion rate of the giant planet is parameterized using $\dot{M}_{gas} = M/\tau_{KH}$, where τ_{KH} is the Kelvin-Helmholtz timescale [e.g., 10], and by drawing gas from the protoplanet’s feeding zone. The half-width of this zone is defined by the minimum of the accretion radius ($R_a = GM/c^2$, where c is the local sound speed), and $2.5 R_{Hill}$.

We solve the self-consistent equation for the surface density evolution by combining the equations of continuity and angular momentum:

$$\frac{\partial \Sigma}{\partial t} = \frac{1}{2\pi r} \frac{\partial}{\partial r} \left\{ \left[\frac{\partial}{\partial r} (\Omega r^2) \right]^{-1} \frac{\partial}{\partial r} (G_\nu - F) \right\}, \quad (2)$$

where G_ν and F are the viscous and gas tidal torque, respectively. For the tidal torque F , we employ two methods. The first is the damping prescription of [6] where the disk is vertically isothermal and the disk response is strictly 2D[1,3,6]. However, the prescription of [6] only takes into account the contribution of the torque from resonances that lie within a (linear) “launch zone”. These authors calculate the form of the wake in the linear zone which they allow to damp in the non-linear region (beyond $\sim (4/3)H$ from the protoplanet). Although this accounts for bulk of the torque, we supplement this treatment by adding those resonant m -numbers that fall in the non-linear region using the tidal torque formulae of [8].

References [1] Rafikov, R. R. 2002. *Astrophys. J.* **572**, 566. [2] Li, H. et al. 2009. *Astrophys. J.* **690**, L52. [3] Estrada, P. R., and I. Mosqueira 2004. 35th LPSC, #1854. [4] Chambers, J. E. 2001. *Icarus* **152**, 205. [5] Howard, A. W. et al. 2010. *Astro ph.* [6] Goodman, J., and R. R. Rafikov 2001. *Astrophys. J.* **552**, 793. [7] Hourigan, K., and W. R. Ward 1984. *Icarus* **60**, 29. [8] Ward, W. R., 1997. *Icarus* **126**, 261. [9] Hayashi, C. 1981. *Prog. Theor. Phys. Supp.* **70**, 35. [10] Ikoma, M., et al. 2000. *Astrophys. J.* **537**, 1013.

P0113. POSTER SESSION I

THE CASE FOR M DWARF STARS IN THE *KEPLER* FIELD. E. Gaidos¹, A. Mann², and S. Lépine³, ¹Dept. of Geology & Geophysics and ²Institute for Astronomy, University of Hawaii at Manoa, Honolulu, HI 96822 (gaidos@hawaii.edu), ³Dept. of Astrophysics, American Museum of Natural History, New York, NY 10024.

M dwarfs are attractive targets for planet searches because planets produce larger, unambiguous transits, and planets within the habitable zone (HZ) are more likely to transit and more frequently. But most M dwarfs are faint and excluded from the magnitude-limited *Kepler* target list, although fainter ($14 < K_p < 16$) proper motion-selected stars were included [1]. Doppler follow-up is difficult and resource-intensive for faint stars ($K_p > 12$), but there are alternatives methods to identify false positives and constrain mass [2-6].

TRILEGAL [7] predictions of M star ($T_e < 4000$ K) counts in the *Kepler* field show that $K_p > 14$ giants are scarce while dwarfs are abundant. Only 4% of these are in the thick disk or halo and thus metal-poor and perhaps lacking planets. The number of stars for which a transiting HZ planet is detectable ($SNR > 7$, 3 transits) in 1 yr, and the total number of detections assuming 1 HZ planet around each star were calculated assuming stellar radius~mass, circular orbits, and uncorrelated noise $2\times$ the nominal limit [8]. We predict that observations of 5000 stars may yield many HZ planets. The prior false positive rate is predicted to be $\leq 10\%$ [9]. Inclusion of late K stars ($T_e < 4500$ K) doubles the number of super-Earth detections but the number of Earth-size planet detections increases by only 7%.

Finally, determinations of M dwarf radii are required for planet radii. Transit data suggest stellar densities/radii are intermediate those of the KIC and of Muirhead et al. [10], and roughly consistent with Yale-Yonsei predictions [12]; further analysis is underway.

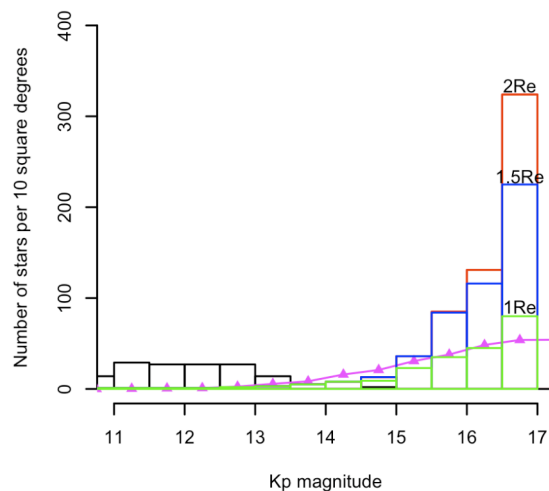


Figure 1. Predicted counts per 10 sq. deg. of M giants (black), M dwarfs around which planets of a given radius could be detected (red/blue/green), and SUPERBLINK [9] proper-motion-selected M dwarfs with $V-J > 2.7$ (purple).

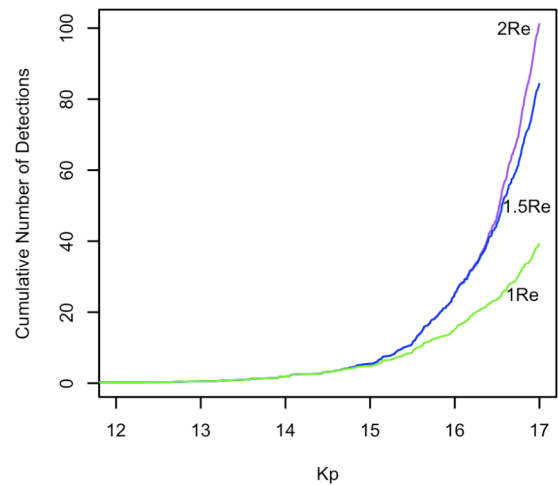


Figure 2. Total number of detections vs K_p magnitude in 1 year if 1 planet of a given radius is in the HZ of each star.

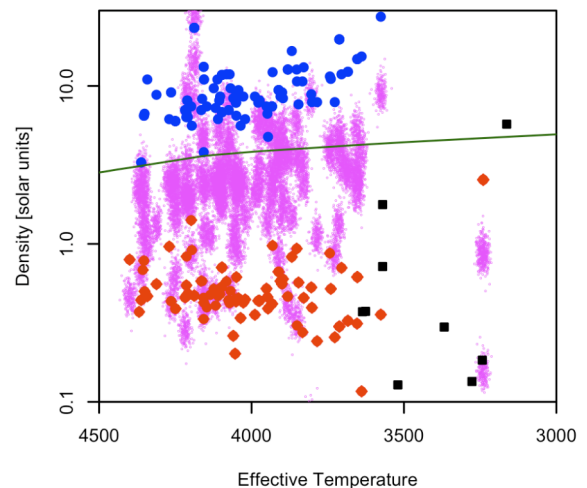


Figure 3. M dwarf densities from the KIC (red), Muirhead [10] (blue), and transit duration assuming Rayleigh-distributed eccentricities with dispersion of 0.05 (purple). Black points are interferometer measurements [11] and solid green is a Yale-Yonsei 5 Gyr $[Fe/H] = 0$ isochrone [12].

References: [1] Batalha N. et al. (2010) *ApJ* 713, L109. [2] Torres G. et al. (2011) *ApJ* 727, 24. [3] Lissauer J. et al. (2011) *Nature* 470, 53. [4] Anderson H. et al. arXiv1103.2541. [5] Gaidos E. et al. arXiv1108.5686. [6] Wolfgang A. & Laughman G. arXiv1108.5842. [7] Girardi L. et al. (2005) *A&A* 436, 895. [8] Koch D. et al. (2010) *ApJ* 713, L79. [9] Morton T. & Johnson J. (2011) *ApJ* 738, 170. [10] Lépine S. (2008) *AJ* 135, 2177. [11] Casagrande (2008) *MNRAS* 389, 585. [12] Demarque et al. (2004) *ApJSS* 155, 667.

P0114. POSTER SESSION I

Transiting planets search and characterization with the SOPHIE spectrograph at OHP.

G. Hébrard^{1,2}, F. Bouchy^{1,2}, R. F. Diaz^{1,2}, C. Moutou³, A. Santerne^{2,3}

¹ Institut d'Astrophysique de Paris (hebrard@iap.fr, bouchy@iap.fr, diaz@iap.fr)

² Observatoire de Haute-Provence

³ Laboratoire d'Astrophysique de Marseille (claire.moutou@oamp.fr, Alexandre.Santerne@oamp.fr)

The SOPHIE environmentally stabilized echelle spectrograph at Haute-Provence Observatory, France, is widely used for the radial velocity follow-up of space- and ground-based photometric surveys for transiting planets, including Kepler, CoRoT, SuperWASP or HAT. Such spectroscopic observations are mandatory to establish the planetary nature of transiting candidates for most of the systems, then to characterize the detected planets. The performances of SOPHIE have been dramatically improved in June 2011 with the use of octagonal optical fibers for the injection of the spectrograph. Latest SOPHIE results will be presented here.

P0115. POSTER SESSION I

Safronov Numbers for Transiting Exoplanets. J. Hodgson II¹, M. Lund¹, and D.J. Christian^{1,1} California State University, Department of Physics and Astronomy, Northridge, CA, USA, 91330, John.Hodgson.71@my.csun.edu

Introduction: Planetary radii can be derived from the transits of Extra-solar planets (ESPs). The resulting mass-radius relations promise information on their internal structures. In the present work, we calculate Safronov numbers for the current sample of 147 transiting ESPs and find the distinction between Class I and Class II Safronov numbers (Hansen et al. 2007) to be significant based on the Kolmogorov-Smirnov statistic. We also present the search for correlations of other planet parameters with Safronov numbers. Although the usefulness of Safronov numbers has been the topic of recent discussion (e.g. Southworth 2010), it may still be useful to investigate possible correlations between them and other planet parameters that may give insights into different ESP populations and formation mechanisms.

[1] Hansen B. M. and Barman T. (2007) *ApJ.*, 671, 861. [2] Southworth J. K. et al. (2010) *MNRAS*, 408, 1689.

P0116. POSTER SESSION I

Kepler 21b – Kepler’s Brightest Host Star Harbors a 1.6 R_{Earth} Planet.

Steve B. Howell and the Kepler Team; NASA Ames Research Center; steve.b.howell@nasa.gov

Introduction: We present *Kepler* observations of the bright ($V=8.3$), oscillating star HD 179070. The observations show transit-like events that reveal that the star is orbited every 2.8 days by a small, 1.6 R_{Earth} object. The planet’s mass is likely to be 6-10 M_{Earth} .

Seismic studies of HD 179070 using short cadence *Kepler* observations show that HD 179070 has a frequency-power spectrum consistent with solar-like oscillations that are acoustic p-modes. Asteroseismic analysis provides robust values for the mass and radius of HD 179070, $1.34 \pm 0.06 M_{\text{Sun}}$ and $1.86 \pm 0.04 R_{\text{Sun}}$ respectively, as well as yielding an age of 2.84 ± 0.34 Gyr for this F5 subgiant.

Together with ground-based follow-up observations, analysis of the *Kepler* light curves and image data, and blend scenario models, we conservatively show at the $>99.7\%$ confidence level (3 sigma) that the transit event is caused by a $1.64 \pm 0.04 R_{\text{Earth}}$ exoplanet in a 2.785755 ± 0.000032 day orbit.

The exoplanet is only 0.04 AU away from the star and our spectroscopic observations provide an upper limit to its mass of $\sim 10 M_{\text{Earth}}$ (2 sigma).

HD 179070 is the brightest exoplanet host star yet discovered by *Kepler*.

Limits to the Density and Mass for Kepler-21b:

To determine a statistically firm upper limit to the planet mass, we carried out an MCMC analysis of the Keck radial velocities with a Keplerian model for the planet’s orbit. The resulting 2-sigma upper limit to the mass the following upper limits: RV amplitude of $K < 3.9 \text{ m s}^{-1}$; a planet mass of $M = 10.4 M_{\text{Earth}}$ (2 sigma), and a corresponding density of $< 12.9 \text{ g cm}^{-3}$.

This upper limit to the density of 12.9 g cm^{-3} is so high that the planet could be (compressed) solid or composed of admixtures of rocky, water, and gas in various amounts, unconstrained by this large upper limit to density. The 1-sigma upper limit to density is 7.4 g cm^{-3} , still consistent with all types of interior compositions and would yield a planet mass of $\sim 5.9 M_{\text{Earth}}$.

If Kepler-21b contains a large rocky core, the high pressure inside such a massive planet would cause the silicate mantle minerals to compress to dense phases of post-perovskite; the iron core is also at higher density than inside Earth. However, Kepler-21b could also have a small rocky core, be mostly gas and not be nearly as massive. The maximum core fraction expected for rocky planets of this radius corresponds to a planet with mass of $10.0 M_{\text{Earth}}$ and a mean density of

12.5 g/cc with a corresponding RV semi-amplitude of 2.3 m sec^{-1} still below our detection limit. If Kepler-21b were a water planet with low silicate-to-iron ratio and 50% water by mass, its mass would be merely $2.2 M_{\text{Earth}}$, similar to that of Kepler-11f, but at mean density of 2.7 g/cc . The measured radial velocities provide neither a confirmation nor a robust limit (~ 10 Earth-masses) on the mass of Kepler-21b but suggests an upper limit near that of the maximum rocky core fraction theoretically allowed.

The full paper (Howell et al. 2011) will be published in the *Astrophysical Journal*.

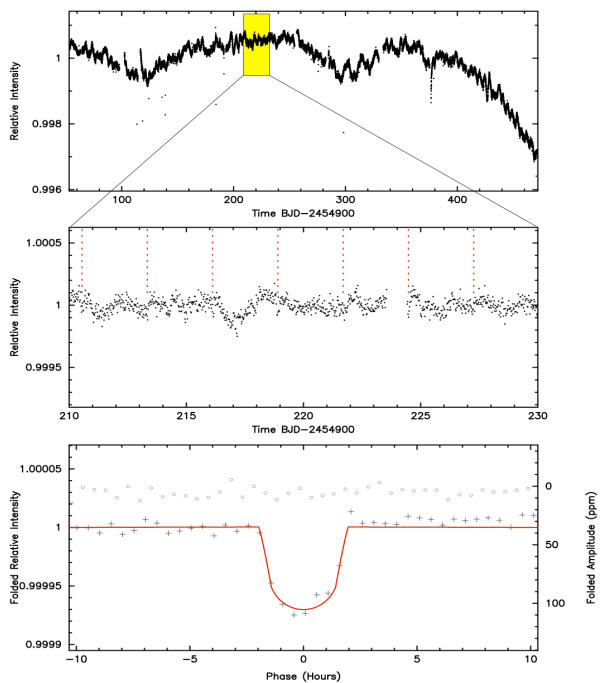


Fig 1: *Kepler* light curve of HD 179070 covering Quarters 0 to 5. The top raw light curve covers 164 separate transit events for the small exoplanet orbiting the star. The middle panel shows a typical normalized section from the full light curve in which transits are visible (positions marked with dotted lines). The bottom panel shows the detrended, binned, and phase folded-data overlotted by our model fit (red line).

Dynamic Black-Level Correction and Artifact Flagging for Kepler Pixel Time Series. J. J. Kolodziejczak¹, B. D. Clarke² and D. A. Caldwell², ¹Space Science Office, NASA Marshall Space Flight Center, Huntsville, AL 35812; kolodz@nasa.gov, ²SETI Institute, NASA Ames Research Center; bruce.d.clarke@nasa.gov; Douglas.Caldwell@nasa.gov.

Introduction: Methods applied to the calibration stage of Kepler pipeline data processing [1] (CAL) do not currently use all of the information available to identify and correct several instrument-induced artifacts. These include time-varying crosstalk from the fine guidance sensor (FGS) clock signals, and manifestations of drifting moiré pattern as locally correlated nonstationary noise, and rolling bands in the images which find their way into the time series [2], [3]. As the Kepler Mission continues to improve the fidelity of its science data products, we are evaluating the benefits of adding pipeline steps to more completely model and dynamically correct the FGS crosstalk, then use the residuals from these model fits to detect and flag spatial regions and time intervals of strong time-varying black-level which may complicate later processing or lead to misinterpretation of instrument behavior as stellar activity.

FGS Crosstalk: This artifact appears in the images as a pattern like that shown in figure 1. To mitigate prelaunch risk, we defined a set of long cadence artifact removal pixel (ARP) targets and continue to collect them throughout the mission. These pixels are read out at the same time as the offending periods of FGS readout and are fit cadence-by-cadence, along with the trailing black collateral data, to extract the time-dependent profile of the crosstalk. Examples of this variation over nearly 2 years are shown in figure 2.

Rolling Bands: The residuals of the FGS crosstalk spatial model fits reveal time-varying features in the black level caused by the drifting moiré patterns and scene dependent response to variable stars. These fea-

tures are too complex to correct, but the presence of the largest variations, the rolling bands, can be flagged in the pixel time series and the flags can then be carried forward to the light curves to provide end users with knowledge of affected time intervals. Figure 3 shows an example of recurring strong rolling bands in the trailing black over a 2 year interval. The band repeats annually, but not at precisely the same time in the same region.

Summary: The FGS crosstalk pixels are present in 20-25% of targets but typically vary slowly enough to create a very small risk of reduced sensitivity or increased false positive rate in the transit search. They do have the potential to complicate or reduce the effectiveness of cotrending algorithms by introducing additional cotrending terms into the light curves which are not associated with prior relations. We will present results regarding the improvement in cotrending performance as a result of including FGS corrections in the calibration.

The rolling bands appear in only ~10% of channels and are present only in 3% of the total exposure, but we estimate that because of the rotation of stars through the affected sky groups, about 30% of light curves are ultimately affected. Thus the utility of this is expected to be high. We will discuss the effectiveness of the proposed flagging and illustrate with some affected light curves.

References: [1] J. M. Jenkins, et al. (2010) *ApJ*, 713, L87. [2] D. A. Caldwell et al. (2010) *ApJ*, 713, L92. [3] J. J. Kolodziejczak. (2010) *Proc. SPIE*, 7742, 38.

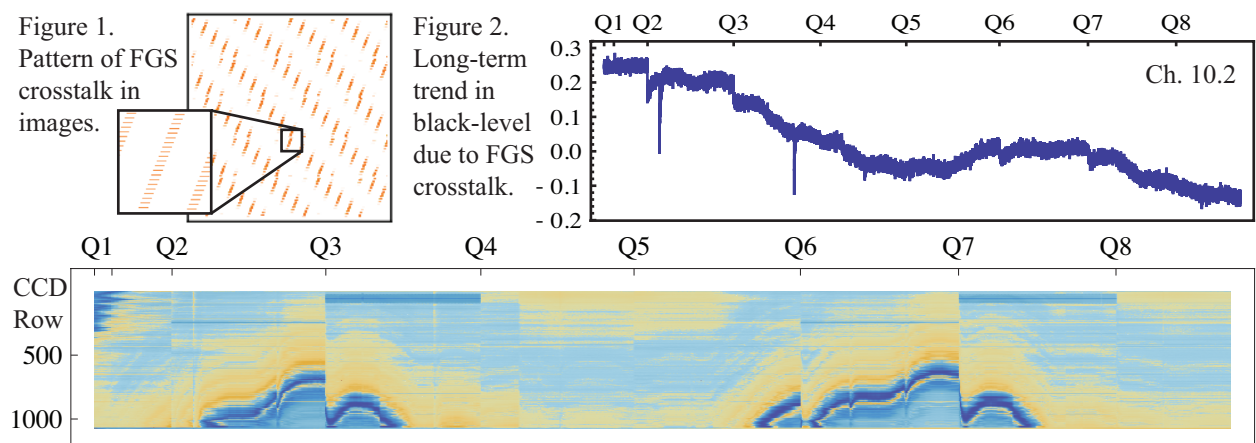


Figure 3. Channel 9.2 color map of trailing black residuals, indicating annually recurring rolling bands.

P0118. POSTER SESSION I

TRANSIT MODEL FITTING IN THE KEPLER SCIENCE OPERATIONS CENTER PIPELINE. J. Li*, C. J. Burke, J. M. Jenkins, E. V. Quintana, J. F. Rowe, S. E. Seader, P. Tenenbaum, J. D. Twicken, SETI Institute/NASA Ames Research Center, MS 244-30, Moffett Field, CA , 94035, USA, *jie.li-1@nasa.gov.

Light curves of long cadence targets are subjected to the Transiting Planet Search (TPS) [1] component of the *Kepler* Science Operations Center (SOC) Pipeline. Those targets for which a Threshold Crossing Event (TCE) is generated in the transit search are subsequently processed in the Data Validation (DV) Pipeline component [2], [3]. The light curves may span one or more Kepler observing quarters, and data may not be available for any given target in all quarters.

Transit model parameters are fitted in DV to transit-like signatures in the light curves of target stars with TCEs. The fitted parameters are used to generate a predicted light curve based on the transit model. The residual flux time series of the target star, with the predicted light curve removed, is fed back to TPS to search for additional TCEs. The iterative process of transit model fitting and transiting planet search continues until no TCE is generated from the residual flux time series or a planet candidate limit is reached.

The transit model includes five parameters to be fitted: transit epoch time (i.e. central time of first transit), orbital period, impact parameter, ratio of planet radius to star radius and ratio of semi-major axis to star radius. The initial values of the fit parameters are determined from the TCE values provided by TPS. A limb darkening model is included in the transit model to generate the predicted light curve. The limb darkening coefficients are interpolated in multiple dimensions from tables provided by Prsa [4].

For each TCE generated by TPS, the transit fitting is implemented with a loop which includes a whitening filter and robust Levenberg-Marquardt fitter. The whitening filter removes the colored noise in the flux time series. The predicted light curve is subjected to the same whitening filter, so the parameters of the transit model are determined by least-squares fitting in the whitened domain. The fit residual is utilized to update the parameters of the whitening filter on each iteration. Robust weights are assigned to each point of the flux time series so that data with large errors are assigned small weights in the least-squares fitting algorithm. The iterative whitening and fitting loop is terminated when both the whitening filter and the robust fitter converge or a predefined iteration limit is reached.

After the whitening filter and robust fitter converge, a metric of signal-to-noise ratio is calculated to determine the strength of the planet candidate. A covariance matrix describing variances and correlations in the fitted parameters is produced by computation of

numerical Jacobians and standard propagation of uncertainty methodology.

To demonstrate the performance of the transit model fitting in the *Kepler* SOC pipeline, Figure 1 shows the flux time series of the target star *Kepler*-11 from Q1 to Q4. The transits of six planets are marked with the transit epoch time and orbital period determined by the DV transit model fitter. Figure 2 shows the folded averaged whitened flux time series (with blue circles) and the whitened light curve determined from the fitted parameters of the transit model (with red line) for the planet *Kepler*-11g.

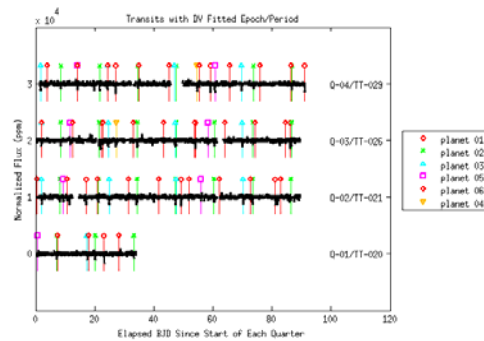


Fig.1 *Kepler*-11 Flux Time Series and Transits with DV Fitted Epoch/Period

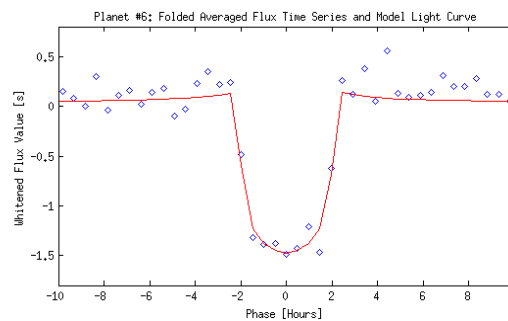


Fig.2 *Kepler*-11g Folded Averaged Whitened Flux Time Series and Whittened Fitted Model Light Curve

Funding for the *Kepler* Mission has been provided by the NASA Science Mission Directorate.

References:

- [1] Jenkins, J. M. et al. (2010) *Proc. SPIE 7740*, 77400D 1-11. [2] Wu, H. et al. (2010) *Proc. SPIE 7740*, 774019 1-12. [3] Tenenbaum, P. et al. (2010) *Proc. SPIE 7740*, 77400J 1-12. [4] Prsa, A. (2011) <http://keplerEBs.villanova.edu/LD>.

To Be or Not To Be (a Planet)? Lucky-Imaging for Kepler Host Candidates.

J. Lillo-Box¹ and D. Barrado², ¹Astrobiology Center, INTA-CSIC (LAEFF, PO Box 78, E-28691 Villanueva de la Cañada, Madrid, Spain, jlillo@cab.inta-csic.es), ²Calar Alto Observatory (barrado@caha.es).

Introduction: The huge planet host candidates' catalog provided by the Kepler Space Telescope is causing a revolution in the exoplanet search. To date, 21 planets (out of the 1235 candidates) have been confirmed from the Q0+Q1+Q2 releases. This clearly shows the great effort that the scientific community have to perform in a follow-up program of the candidates in order to confirm them as real planets and characterize their properties. In that sense, several ground-based observing techniques have been used (see, for example, [1]).

However, after the candidates selection, there is a mandatory step to reject false positives, since the Kepler point-spread function is very large (6''-10'', depending on the particular target), and its pixel size is about 4''. There are four configurations which mimic an exoplanet transit: a./ a small stellar or substellar object (the smallest stars and brown dwarfs have the same size as Jupiter), b./ a grazing binary (which has not been ruled out by additional photometry), c./ a stellar binary blended with a background star, d./ a long-term spot. While cases a./ and b./ are well rejected by the Kepler pipeline for images reduction and individual studies of the lightcurves by the Kepler team, case c./ is the main source of false positives in the sample of exoplanet candidates. Due to the Kepler long base-line, we expect few or no case d./.

In [2], the authors have reported an estimation of the false positive probability (FPP) of Kepler targets (see Fig. 3). Under some assumptions, they conclude that the fainter the target and the shallower the depth of the transit, the greater the FPP, achieving a 40% of FPP for planets with 1.1 R_{Earth} transiting stars as faint as 15 magnitudes in the Kepler band. They also calculate that restricting the blended radius to 2'' with a high resolution image, this probability would decrease ten times until 3-4% for the same conditions.

Hence, an accurate high-resolution imaging follow-up is crucial to confirm the planetary nature of the Kepler candidates.

Our results: We have performed an extensive follow-up program by observing 111 KOIs with the Lucky-Imaging technique. It allows us to go as close to the star as 0.1''. Our preliminar results show that only 25 KOIs (22.5%) were completely isolated (Group 1). Instead, we found clear detections of stellar companions (either bounded or visual) for 77 KOIs at 3''-10'' (Group 3). Finally, 16 KOIs present at least one object closer than 3'' (Group 2). In Fig. 1 we summarize the results of our observations.

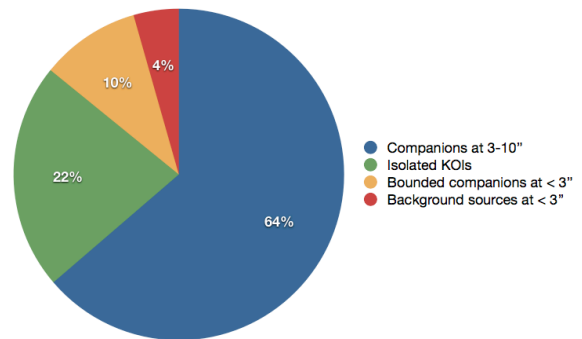


Figure 1: Results of our Lucky-Imaging program with the AstraLux instrument at CAHA. The diagram shows the number of KOIs with stellar (visual?) companions at different distances.

A great variety of scientific analysis can be done with this data. Firstly, KOIs from Group 1 become the best targets for a subsequent radial velocity follow-up to characterize the planet properties. Secondly, stellar companions of objects from Groups 2 and 3 are potential false positives due to case c./ Furthermore, even if the planetary system is actually real, the presence of a blended background source modifies the planet properties as they depend on the host star's luminosity. Finally, close objects to KOIs in Group 2 could be bounded, forming a binary system suitable for a multiplicity study in planetary systems. Some of our companions to KOIs have (i-z) colors typical for brown dwarfs.

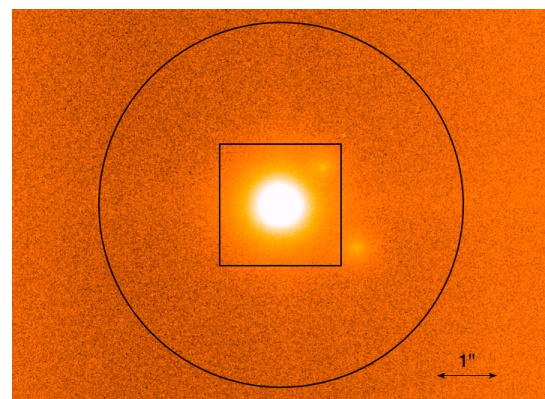


Figure 2: AstraLux image of one KOI. A clear detection of a close companion at less than 1.8'' compared with the pixel size of the Kepler telescope (black square of 4'') and its PSF of 6'' (black open circle). Another object is also detected at 2.8''.

References: [1] Muirhead P. et al., 2011, arXiv, 1109.1819v1 [2] Timothy et al. 2011, ApJ, submitted.

P0120. POSTER SESSION I

EXTRACTION OF LOW-SNR SIGNALS FROM KEPLER LIGHT CURVES BY VIRTUE OF THE KLT

C. Maccone, International Academy of Astronautics, Via Martorelli 43, I-10155 Torino (Turin), Italy,
E-mail: clmaccon@libero.it

The KLT (acronym for Karhunen-Loève Transform) is a mathematical algorithm superior to the classical FFT in many regards:

- 1) The KLT can filter signals out of the background noise over both wide and narrow bands. That is in sharp contrast to the FFT that rigorously applies to narrow-band signals only.
- 2) The KLT can be applied to random functions that are non-stationary in time, i.e. whose autocorrelation is a function of the two independent variables t_1 and t_2 separately. Again, this is a sheer advantage of the KLT over the FFT, inasmuch as the FFT rigorously applies to stationary processes only, i.e. processes whose autocorrelation is a function of the absolute value of the difference of t_1 and t_2 only.
- 3) The KLT can detect signals embedded in noise to unbelievably small values of the Signal-to-Noise Ratio (SNR), like 10^{-3} or so. This feature of the KLT appears to be particularly useful to detect an Earth-transiting signal in the noisy data of its own central star, as it is just the case with the new 1235 planetary candidates discovered by the Kepler mission.
- 4) An excellent filtering algorithm like the KLT, however, comes with a cost that one must be ready to pay for: its computational burden is much higher than for the FFT. In fact, for an autocorrelation matrix of size N , the calculations must be of the order of N^2 , rather than $N \cdot \log(N)$. Nevertheless, in the case of extracting Earth-sized transits from this noise, computational time would not be a limitation as many people on the Kepler project already use the supercomputing center at NASA Ames.

Because of all these reasons, we suggest that the KLT should be considered as a superior algorithm enabling the detection of Earth-sized planets found by Kepler.

REFERENCES

- 1) Claudio Maccone, “The KLT (Karhunen-Loève Transform) to extend SETI searches to broad-band and extremely feeble signals”, *Acta Astronautica*, Vol. 67 (2010), pages 1427–1439. This is the key paper about both the classical KLT and the BAM-KLT that was later used by the following author to apply them to Global Navigation Satellite Systems.
- 2) Arkadiusz Szumski, “Finding the Interference – the Karhunen-Loève Transform as an Instrument to Detect Weak RF Signals”, *InsideGNSS* (“Working Papers” section), May-June 2011 issue, pages 56-63.

THEY MIGHT BE GIANTS: the luminosity class of late-type *Kepler* targets. A. Mann¹, E. Gaidos², and S. Lépine³, ¹Institute for Astronomy (amann@ifh.hawaii.edu) and ²Dept. of Geology & Geophysics, University of Hawaii at Manoa, Honolulu, HI 96822 (gaidos@hawaii.edu), ³Dept. of Astrophysics, American Museum of Natural History, New York, NY 10024 (lepine@amnh.org).

We determine the properties of *Kepler* target stars with $K_p\text{-}J > 2$ (late K and M spectral type) to better determine the frequency and properties of their planets. Planets around cool stars (late K to and M spectral type) are critical tests of planet formation models [1,2], and *Kepler* results have been used to determine the frequency of short-period planets around stars as late as M0 [3], and to extend the well-established correlation between stellar metallicity/mass and giant planet frequency [4,5] to small-radius planets around late-type stars [6].

Studies such as these depend heavily on the properties of the target stars of the *Kepler* sample. There is significant evidence that late-type *Kepler* targets include a large number of interloping giant stars [7]. Inclusion or improper removal of these giant stars from the sample will result in an inaccurate planet frequency and planet-metallicity correlation [6].

We determine the fraction of late-type giant stars in the *Kepler* field using moderate resolution optical spectra for a sample of *Kepler* target stars with $K_p\text{-}J > 2.0$ (~K5 spectral type or later). We use CaH, TiO, K I, CaT and NaI as indicators of gravity and spectral type (Fig. 1). For bright ($K_p < 14$) targets, we find that giant stars make up $98.8 \pm 0.6\%$ of late-type *Kepler* targets, while for dimmer ($K_p > 14$) targets, giants constitute only $5 \pm 1\%$ of targets. The fraction of giant stars does not significantly decrease for these subsamples when we only consider stars with $\log(g) > 4$ as determined by the *Kepler* Input Catalog [8-9].

We use a corrected giant star fraction to calculate the frequency of planets around late-type as well as the metallicity difference between *Kepler* exoplanet hosts and non-hosts [6] (Figure 2). We show that the results are significantly different than when we rely solely on KIC $\log(g)$ values to remove giant stars (Fig. 2).

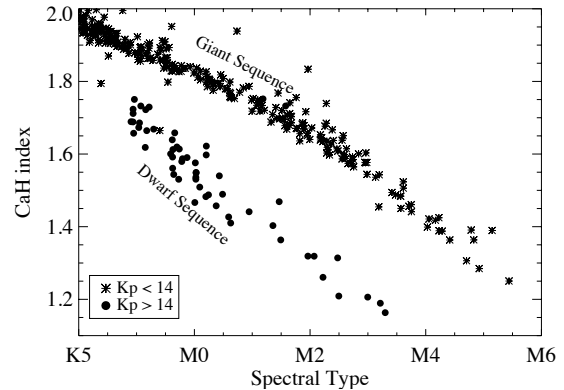


Figure 1. CaH index as defined by [10] shows a clear separation of giants and dwarfs with spectral type for robust giant/dwarf discrimination.

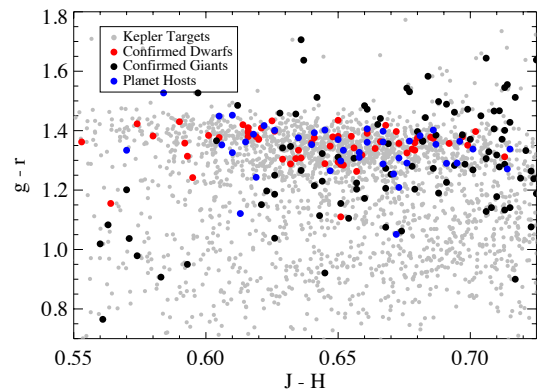


Figure 2. *Kepler* planet hosting stars show a large color offset from the general population of field stars, suggesting planet hosts are significantly more metal rich. When comparing planet hosts to just confirmed dwarfs, the two $g-r$ distributions are not significantly different based on K-S and Welch t tests (70% of having consistent $g-r$ color means/distributions).

References: [1] Laughlin G. et al. (2004) *ApJL* 612 L73. [2] Kennedy G. M. and Kenyon S. J. (2008) *ApJ* 673 502. [3] Howard et al. (2011) arXiv1103.2541. [4] Fischer D. A. and Valenti J. (2005) *ApJ* 622 1102. [5] Johnson J. A. et al. (2010) *PASP* 122 905. [6] Schlaufman K. C. and Laughlin G. (2011) *ApJ* 738 177. [7] Gaidos E. et al (2011) arXiv1108.5686G. [8] Brown T. M. et al. (2011) *AJ* 142, 112. [9] Batalha N. M. (2010) *ApJL* 713 L109. [10] Lepine et al (2007) *AJ* 669 1235.

P0122. POSTER SESSION I

Exploiting the accuracy of Kepler : Discovery of the hottest and largest exoplanet. D. Mislis and S. Hodgkin, Institute of Astronomy, University of Cambridge, UK, mislisdim@ast.cam.ac.uk, sth@ast.cam.ac.uk

Introduction: We present a new approach to determine the parameters of transiting extrasolar planetary systems using photometric light curves (LCs). An analysis that combines a treatment of various phenomena in high-accuracy LCs allows a derivation of orbital and physical parameters. Our method considers the primary transit, the secondary eclipses, and the overall phase shape of a LC between the occultations. Phase variations are induced by reflected and thermally emitted light from the planet. Moreover, the ellipsoidal shape of the star due to the gravitational pull from the planet induce phase variations. As we find, the complete decipherment of LCs yields information about the planetary mass, orbital eccentricity, orientation of periastron, and the planet's albedo. Furthermore, we present the analysis of a Kepler candidate exoplanet system. Using the LC from Kepler mission, we have found ellipsoidal variations due to tidal forces (star-planet), thermal emission from the planet and possible signature due to planetary reflected light. The analysis has shown that the system is a hot Jupiter with mass $M_p = 1.20M_J$. Because the high temperature of the host star (SP = A0V, $T_{\text{eff}} = 8848\text{oK}$), the exoplanet becomes one of the hottest exoplanets, with strong thermal emission ($T_p = 3341.5\text{o K}$). Except ellipsoidal variations and thermal emission, a weak reflected light component is also present in the LC.

DETECTION AND CORRECTION OF STEP DISCONTINUITIES IN KEPLER LIGHT CURVES.

R. L. Morris^{1,*}, J. J. Kolodziejczak², T. Barclay³, M. N. Fanelli³, J. M. Jenkins¹, Jeffrey C. Smith¹, Martin C. Stumpe¹, J. Twicken¹, J. Van Cleve¹. ¹SETI Institute/NASA Ames Research Center, MS 244-30, Moffett Field, CA 94035, USA, ²NASA Marshall Space Flight Center, ³Bay Area Environmental Research Institute.

* robert.l.morris@nasa.gov

Introduction: Approximately one in 30 raw light curves in a typical quarter of Kepler data contains one or more noticeable downward step discontinuities. The vast majority of such discontinuities are the result of cosmic rays or solar energetic particles striking the photometer and causing permanent local changes (typically -0.5%) in quantum efficiency, though a partial exponential recovery is often observed [1]. Since these features, dubbed Sudden Pixel Sensitivity Drop-outs (SPSDs), are not correlated systematics, they cannot be removed by the systematic error correction algorithm in the Presearch Data Conditioning (PDC) module of the Kepler data analysis pipeline. Correction of SPSD signatures prior to removing systematics not only rectifies the light curves of affected targets, but can improve the overall performance of PDC.

We present a new algorithm for detecting and correcting SPSD signatures in long-cadence Kepler data. The algorithm consists of three components: filter design, detection, and correction. The design of the linear shift-invariant detection filter is based on the method of Savitzky and Golay [2] with an added multi-scale analysis step to improve localization of the peak response. Detection and correction are performed iteratively on all targets of a given channel until no remaining SPSD signatures are identified.

The detection step begins with preconditioning of each time series by filling gaps and padding endpoints. Conditioned time series are then convolved with the detection filter and responses are normalized over all targets on the current channel. The maximum normalized detector response for each target is evaluated in the context of its light curve to decide first whether it is likely to be the leading edge of a transit or other transient stellar phenomenon, and second whether it indicates an SPSD event.

Correction is a two-stage process. The first stage estimates a persistent step height from analysis of the entire flux time series, excluding a short recovery window following the SPSD, which typically contains a transient signal. The second stage models the recovery window using a series of exponentials of varying time constant. The algorithm also detects and preserves sinusoids in the signal while removing only the step and recovery transient components.

The algorithm has been tested both on unaltered flight data containing signatures of real SPSD events, and on flight data with SPSD-affected targets removed

and simulated SPSDs injected. Examples of correction results for both cases are shown in figures 1 and 2. Figure 2 illustrates the quality of a typical correction by comparing corrected and uncorrected light curves to ground truth.

References: [1] J. M. Jenkins, et al. (2010) *ApJ*, 713, L87. [2] A. Savitzky and M. Golay (1964) *Analytical Chem.*, 36 (8), 1627-1639.

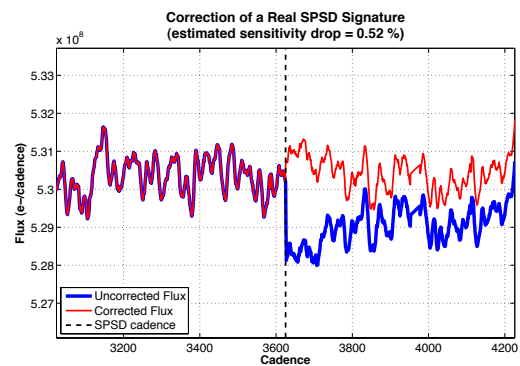


Figure 1. Correction of an actual SPSD event in Kepler flight data (channel 13.1, quarter 7). In this case, the amplitude of the signal's intrinsic variability is comparable to that of the downward step.

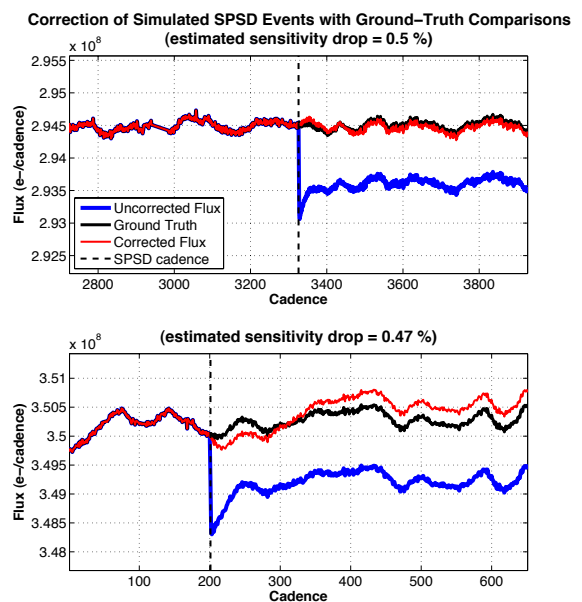


Figure 2. Simulation testing indicates a significant reduction in residual errors.

P0124. POSTER SESSION I

INVESTIGATING THE PLANET-METALLICITY CORRELATION WITH KEPLER

Morton, T.D., Caltech, tdm@astro.caltech.edu

One of the most striking results from the early days of exoplanet science is the strong correlation between a star's metallicity and the probability of it hosting a giant planet. This planet-metallicity correlation is predicted to be weaker for smaller planets but remains unmeasured for Neptune- and Earth-sized planets. The planet detections from the Kepler mission provide an enticing opportunity to test the planet-metallicity relationship for small planets, but the host stars in the Kepler field have unknown metallicities. To this end, we present preliminary results from the California Kepler Survey (CKS), which is designed to measure the stellar properties of Kepler Objects of Interest, as well as characterizing the metallicity distribution of parent sample of Kepler target stars.

P0125. POSTER SESSION I

Planet Frequency as a Function of Stellar Mass in a Quiescent-disk Planet Formation Model. I. Mosqueira¹ and P. R. Estrada¹, ¹SETI Institute, 515 N. Whisman Rd., Mountain View, CA 94043; imosqueira@seti.org

Kepler has measured the planet frequency over stellar spectral types ranging from M0 to F2 dwarves. Over this range, the occurrence of 2-4 Earth-radius planets has been found to increase with decreasing stellar mass [1]. On the other hand, the California Planet Survey finds that the giant planet frequency increases with increasing stellar mass from M dwarves to A stars at fixed metallicity [2].

These contrasting results can be naturally reconciled within a quiescent-disk core accretion model of planet formation. In such a model higher disk masses lead to the formation of larger cores but also to the loss of smaller objects by Type I migration. While Type I migration is faster for larger objects, sufficiently large planetary cores (with mass ratio to the central object $\sim 10^{-4}$) can stall, open a gap in the disk and survive [3, 4], whereas smaller objects can be lost. It should be noted, however, that even if a planet is too small to survive in isolation, it is still possible that it will survive in the presence of planetary companions, albeit with a lower survival probability.

At the other end of the mass spectrum, the formation of giant planets is modulated by the depletion of gas in the planet's feeding-zone. Assuming the formation of a critical core large enough to rapidly accrete gas from the nebula, the question arises whether it can grow into a Jovian-sized giant planet. In the limit that the core accretes all the gas in its feeding zone, the final mass of the planet (in a weakly turbulent disk) is given by the gaseous isolation mass. In general, however, there is a competition between the disk clearing due to the planet's tidal torque and that resulting from gas accretion [5, 6]. Although, the presence of companions can play a role in setting the final masses of non-isolated planets, the frequency of giant planet formation is expected to increase with increasing disk mass (and stellar mass).

The Kepler results concern the planet occurrence within 0.25 AU of solar-type stars. One of the main issues facing the in-situ accretion of a core mass close-in is that the isolation mass generally decreases with semimajor axis [7]. Numerous migration mechanisms have been suggested. In the present context, it is possible to grow a core large and fast enough to survive Type I migration, taking place in a timescale of $\sim 10^5$ - 10^6 years [8], provided that the solids in the planet forming region are enhanced with respect to cosmic mixtures. Furthermore, a core that stalls close-in may continue to grow as a result of the capture of smaller inwardly migrating cores (a related mechanism is discussed in [9]). Therefore, super-Earths can originate

further out in the disk or coalesce with other passing objects.

Here we investigate the interplay of these effects in the context of a simple quiescent-disk model enhanced in solids with respect to solar compositions [6], and discuss the implications for recent observations of planetary frequency as a function of stellar mass.

References: [1] Howard A. W., et al. (2011) *astro-ph*. [2] Johnson, J. A., et al. (2010) *ApJ*, 721, L153. [3] Rafikov, R. R., (2002) *ApJ*, 572, 566. [4] Li, H., Lubow, S. H., Li, S., and Lin, D. N. C., (2009) *ApJ*, 690, L52. [5] Estrada, P. R., and Mosqueira, I., (2004) *LPS XXXV*, Abstract #1854. [6] Estrada, P. R., and Mosqueira, I., this conference. [7] Kokubo, E., and Ida, S., (1998) *Icarus*, 131, 171. [8] Bate, M. R., et al. (2003) *MNRAS*, 341, 213. [9] Ward, W., (1997) *ApJ*, 482, L211.

P0126. POSTER SESSION I

A REVISED EFFECTIVE TEMPERATURE SCALE FOR THE KEPLER INPUT CATALOG. M.H Pinsonneault¹, D. An², H. Bruntt³, J. Molenda-Zakowicz⁴, T.S. Metcalfe⁵ and W.J. Chaplin⁶, ¹Ohio State University, Dept. of Astronomy, 140 W. 18th Ave. Columbus, OH 43210 pinsonneault.1@osu.edu, ²Ewha Womans University, Korea deokkeun@ewha.ac.kr, ³Aarhus University, Denmark bruntt@gmail.com, ⁴University of Wroclaw, Poland molenda@astro.uni.wroc.pl, ⁵High Altitude Observatory, USA travis@ucar.edu, ⁶ University of Birmingham, UK wjc@bison.ph.bham.ac.uk

Introduction: We present a revised effective temperature scale for stars in the Kepler Input Catalog (KIC). Two independent photometric temperature scales (griz and JK) are in agreement with one another, but predict systematically hotter temperatures than those in the KIC by about 200 K. We trace the origin of these differences, and present a revised catalog consistent with the photometric fundamental scale. Corrections for binaries, metallicity, and surface gravity are included. The consequences for stellar and planetary properties are briefly discussed.

P0127. POSTER SESSION I

Empirical Constraints on Planet Migration Halting Mechanisms. P. Plavchan¹ and C. Bilinski², ¹NASA Exoplanet Science Institute, Caltech, M/C 100-22, 770 S Wilson Ave, Pasadena, CA 91125, plavchan@ipac.caltech.edu, ²University of Arizona, cgbilinsk@gmail.com.

Abstract The discovery of "hot Jupiters" very close to their parent stars confirmed that Jovian planets migrate inward via several potential mechanisms. We present empirical constraints on planet migration halting mechanisms. We compute theoretical distributions of planets in the semi-major axis - stellar mass plane for planet migration that is halted at the interior 2:1 resonance with the magnetospheric truncation radius, the interior 2:1 resonance with the dust sublimation radius, and the tidal disruption radius. We also compute theoretical distributions with a planet halting distance that has no dependence on stellar mass, and a distribution that is uniform random in the semi-major axis - stellar mass plane. We fit these distributions to empirical distributions of known exoplanets and Kepler candidates at semi-major axes of less than 0.1 AU. We find that the magnetospheric truncation radius provides the best fit to the empirical distributions. We can rule out migration halting at the tidal disruption and 2:1 resonant dust sublimation radii. Our results favor a weak dependence of the halting distance with stellar mass.

P0128. POSTER SESSION I

Calibration in the Kepler Science Operations Pipeline. E. V. Quintana¹, J. L. Christiansen¹, J. M. Jenkins¹, B. D. Clarke¹, D. A. Caldwell¹, J. Kolodziejczak², H. Chandrasekaran³, J. D. Twicken¹, S. D. McCauliff⁴, M. T. Cote⁵, T. C. Klaus⁴, C. Allen⁴, S. T. Bryson⁵. ¹SETI Institute/NASA Ames Research Center, M/S 244-30, NASA Ames Research Center, Moffett Field, CA, 94035; jessie.l.christiansen@nasa.gov; ²NASA Marshall Space Flight Center; ³Lawrence Livermore National Laboratory; ⁴Orbital Sciences Corporation; ⁵NASA Ames Research Center

Introduction: We present an overview of the Calibration (CAL) software component and its context in the *Kepler* Science Operations Center (SOC) Science Processing Pipeline. CAL operates on original spacecraft data to remove instrument effects and other artifacts that affect the data. Figure 1 shows the CCD architecture, including the location of the collateral data used for calibration. Traditional CCD data reduction is performed, including: (1) removal of the static 2D black (bias) and a dynamic 1D black (see Figure 2); (2) gain and non-linearity correction; (3) correction for distortions induced by the local detector electronics (LDE) (see Figure 3); (4) cosmic ray correction; (5) correction for bleeding charge in the collateral regions due to saturated targets near the edge of the CCD; (6) dark current correction; (7) removal of smear signals that result from the lack of a shutter on the photometer (see Figure 3); (8) flat field correction for variation in pixel sensitivity; and (9) additional operations that are needed due to the complexity and large volume of flight data. CAL also propagates the uncertainty values on the calibrated pixels. CAL operates on long cadence (~30 min) and short cadence (~1 min) sampled data, as well as full-frame images (FFIs), and produces calibrated pixel flux time series, uncertainties, and other metrics that are used in subsequent Pipeline modules. The raw and calibrated data are also archived in the Multi-mission Archive at Space Telescope [Science Institute] (MAST) for use by the community.

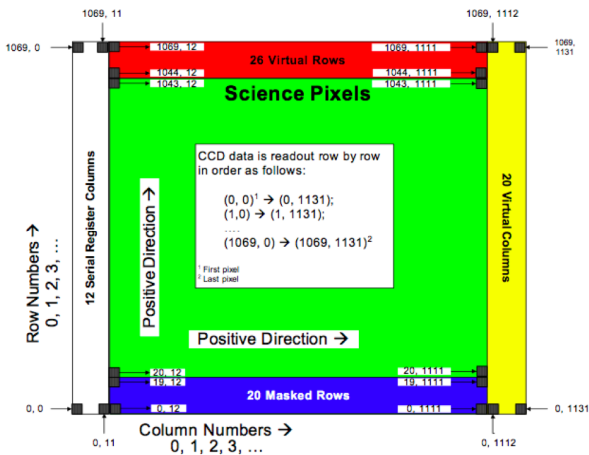


Figure 1: A schematic of the CCD module/outputs, of which Kepler has 84, consisting of a 1070x1132 pixel array that includes science (photometric) pixels and collateral data collected for calibration.

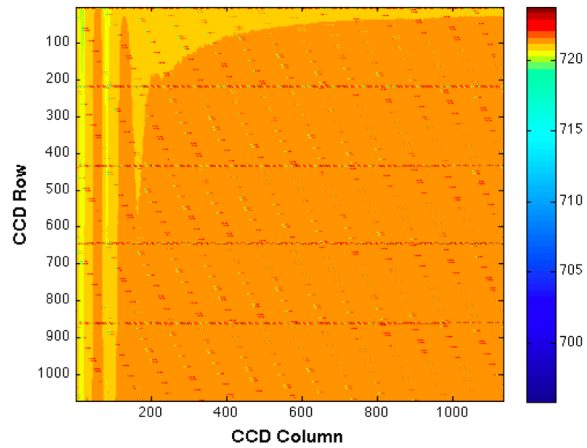


Figure 2: The static 2D black for one of the Kepler CCDs. The structure includes image artifacts due to heating of the readout electronics, start-of-line transients, parallel frame transfer signals, and fine guidance sensor crosstalk clocking signals that are injected into the photometric region as the image is read out [1].

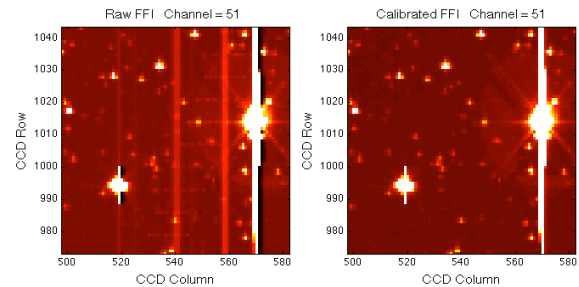


Figure 3: A small section of a Kepler CCD, before (left) and after (right) calibration. Two saturated stars create undershoot (a decrease in the measured flux, shown in black) in the downstream pixels. The fainter vertical lines are smeared starlight from stars on those columns closer to the readout.

Funding for the *Kepler Mission* has been provided by the NASA Science Mission Directorate.

References:

- [1] Caldwell, D.A. et al. (2010), ApJL, 713, L92

SOPHIE velocimetry and independent establishment of *Kepler* transit candidates

A. Santerne^{1,3}, C. Moutou¹, F. Bouchy^{2,3}, G. Hébrard^{2,3}, R. F. Díaz^{2,3}, M. Deleuil¹, A. Bonomo¹ and J.-M. Almenara¹
¹Laboratoire d'Astrophysique de Marseille, Université d'Aix-Marseille & CNRS, 38 rue Frédéric Joliot-Curie, 13388 Marseille cedex 13, France (alexandre.santerne@oamp.fr; claire.moutou@oamp.fr; magali.deleuil@oamp.fr; aldo.bonomo@oamp.fr; josemanuel.almenara@oamp.fr)

²Institut d'Astrophysique de Paris, UMR7095 CNRS, Université Pierre & Marie Curie, 98bis boulevard Arago, 75014 Paris, France (bouchy@iap.fr; hebrard@iap.fr; diaz@iap.fr)

³Observatoire de Haute-Provence, Université d'Aix-Marseille & CNRS, 04870 Saint-Michel-l'Observatoire, France

Introduction: As *CoRoT*, the *Kepler* space mission found a large amount of planetary transit candidates for which radial velocity follow-up is necessary in order to secure the planetary nature and then, to characterize the systems (planetary mass, orbital eccentricity, stellar parameters...). We performed follow-up observations of *Kepler* transit candidates using the SOPHIE spectrograph [2], [6] mounted on the 1.93-m telescope in Observatoire de Haute-Provence (France). SOPHIE is a key instrument of the follow-up of CoRoT [1] and SuperWASP [4] transit candidates since end of 2006 and was used to characterize ~50% of the northern transiting planets.

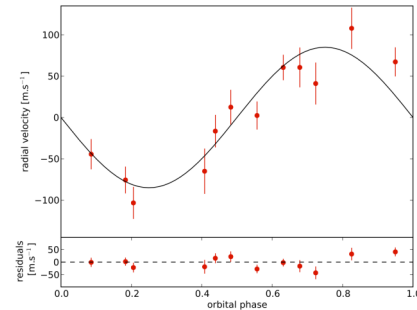
Candidates selection: Using the experience of about 5 years of *CoRoT*, Super-WASP and HAT radial velocity follow-up, we select a subsample of about 30 transiting candidates, out of the 1235 *Kepler* candidates released in February 2011. This subsample was defined using several criteria: the orbital period, the shape, duration and depth of the transits compared with the estimated parameters of their host stars, and finally their expected radial velocity semi-amplitude compared with the expected photon noise of SOPHIE. In this talk, we will report on this candidates selection.

Follow-up results: We performed 2 observationnal campaigns in 2010 and 2011 during which we followed up these *Kepler* candidates with the SOPHIE spectrograph. We identified several planets and find a few false positives that we will highlight during this talk:

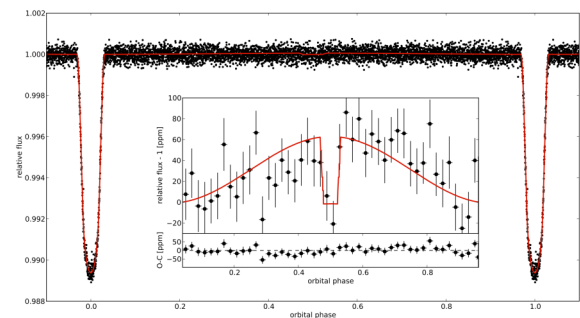
1) Planet characterization: The new planets were fully characterized by combining the publicly-available *Kepler* light-curves and SOPHIE velocimetry, e.g. KOI-428b [7], KOI-423b [3], KOI-196b [8]. Star's typing were determined using SOPHIE spectra. Several new planets will be presented during this conference.

2) False positives : In our candidates selection, we found several high-priority candidates that turned down to be false positives (eclipsing binaries, triple system, ...). We will briefly report on these false positives and present our estimation of the *Kepler* false

positive probability (FPP) and how it compares with other FPP estimations (e.g. [3]).



Phase-folded radial velocity curve of KOI-196 obtained with SOPHIE. With a $K_p=14.5$, KOI-196 hosts a planetary companion with a period of ~ 1.85 d and a mass of $\sim 0.5M_{Jup}$.



Kepler phase-folded light-curve of KOI-196 showing the primary and secondary transits as well as the phase-variation of the planet.

References:

- [1] Barge, P. et al. (2008) A&A, 482, L17
- [2] Bouchy F. et al. (2009) A&A, 505, 853
- [3] Bouchy F. et al. (2011) A&A, 533, A83.
- [4] Cameron, A. C. et al. (2007) MNRAS, 375, 951
- [5] Morton, T. D., & Johnson, J. A. 2011, ApJ, 738, 170
- [6] Perruchot, S. et al. (2008) proc. SPIE, 7014
- [7] Santerne A. et al. (2011a) A&A, 528, A63.
- [8] Santerne A. et al. (2011b) arXiv:1108.0550.

P0130. POSTER SESSION I

A ROBUST DETECTION STATISTIC AND ITS IMPLEMENTATION IN THE TRANSITING PLANET SEARCH SOFTWARE. S. Seader¹, J. M. Jenkins², and P. Tenenbaum³, ¹SETI Institute, NASA Ames Research Center, Mail Stop 244-30, Building N244 R113B, Moffett Field, CA 94035; shawn.seader@nasa.gov. ²SETI Institute, jon.jenkins@nasa.gov. ³SETI Institute, peter.tenenbaum@nasa.gov.

Introduction: The Transiting Planet Search (TPS) software computes a Multiple Event Statistic (MES) at each discrete point of three-dimensional parameter space in period, epoch, and transit duration. The MES values are compared to a threshold to separate the Threshold Crossing Events (TCEs) from background. The false alarm rate of the MES is larger than what Gaussian statistics predicts, largely due to artifacts and noise events in the data that can masquerade as transits. To lend further credibility to the MES and more strictly discriminate against cases where transit depths are not consistent, a Robust Detection Statistic (RDS) is employed algorithmically. A description of how the RDS is calculated and how it is currently implemented in the Kepler analysis pipeline is given. Several deficiencies are pointed out and some recent results are given.

RDS Algorithm:

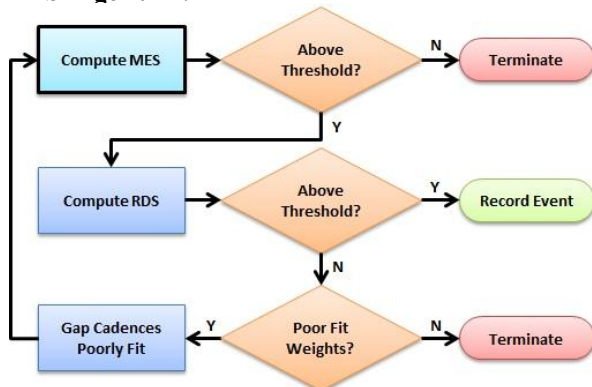


Figure 1: RDS Algorithm Flowchart

The first step in the RDS algorithm is to compute the MES [1,2]. If the MES is below threshold then the search is terminated, otherwise, the RDS is computed. The period, epoch, and trial pulse duration corresponding to the maximum MES are used to construct a model pulse train of square waves. The data and the model are then whitened using a whitener computed from the data. Since the square pulses of the model do not match a true planetary transit signature, we window the data and model using a simple rectangular window centered around each transit and of equal length to the transit duration plus one extra cadence on each side to permit the highest energy term in the tail to contribute. The windowing is necessary to prevent the fitter from fitting the more numerous out-of-transit cadences to noise, thereby driving the robust weights of in-transit cadences toward zero. The RDS is then computed as follows:

$$RDS = \frac{\tilde{s}^T W \tilde{x}}{\sqrt{\tilde{s}^T W \tilde{s}}}$$

where s is a model transit pulse train, x is the data used to form the MES, W is a diagonal matrix of robust fit weights, T denotes the transpose of a vector, and \sim denotes a whitened vector.

The RDS is compared to a threshold to determine whether a robust detection has been made. If the RDS is below threshold, then we gap cadences that had poor robust fit weights and start over with the computation of the MES. Otherwise, if the fit weights are all above some threshold then we terminate and fail to make a robust detection. To prevent costly looping through the folder, the change in fit depth is monitored and convergence is claimed when the fit depth fails to change by some fraction of the error in the depth. We also prevent the case where we might be fitting only one transit worth of cadences when many of the cadences have fit weights of zero.

Improvements: Currently we know of three minor and one major improvement in the RDS algorithm. The data anomaly deemphasis weights are applied now by simply ignoring cadences with weights less than one. Instead, the dot product of the weights with the whitened model and data will be formed prior to the fit. These deemphasized vectors will be used in the RDS calculation. The current handling of the deemphasis weights can lead to situations where we are fitting less than one transit duration of cadences and still achieving an RDS above threshold. With the proposed change however, we can instead just prevent the fitting of a single transit, which is inline with what is done in the MES calculation. The convergence criteria on the change in the fitted depth will also be modified so that it is only applied when the period and epoch returned from the folder are also changing very little between iterations. The major improvement being worked out now is that the algorithm only operates on the maximum MES. If we fail to make a robust detection for the maximum MES then we should fall back to the next largest MES that is above threshold (if one exists), and try again to make a robust detection. The computational burden of such a search warrants further study, which is currently being undertaken.

References: [1] Jenkins, J.M. (2002) *ApJ*, 575, 493-505. [2] P. Tenenbaum et al, these proceedings (2011).

P0131. POSTER SESSION I

Studying orbital photometry of Kepler objects of interest. Avi Shporer^{1,2}, Benjamin J. Fulton¹, and the Kepler team, ¹Las Cumbres Observaory Global Telescope Network, 6740 Cortona Dr., Suite 102, Goleta, CA 93117, USA, ²Department of Physics, Broida Hall, University of California, Santa Barbara, CA 93106, USA, ashporer@lcogt.net

Kepler high precision measurements allow the detection of the minute photometric modulations correlated with the orbit, induced by low-mass companions down to the planetary mass range. Those modulations include the beaming effect, tidal ellipsoidal distortion, and reflection or heating of the companion. They represent an opportunity to study these systems in detail using Kepler photometry alone. For transiting systems the known ephemeris allows a more accurate measurement of the orbital modulations amplitude. We will present results from a search for the photometric orbital signal, including the beaming effect, in short-period Jupiter-mass transiting planets.

P0132. POSTER SESSION I

Wavelet-Based Band Splitting for Improved Systematic Error Correction and Noise Reduction in Kepler Light Curves

Martin C. Stumpe^{1,*}, T. Barclay², M. N. Fanelli², J. M. Jenkins¹, J. Kolodziejczak³, R. Morris¹, Jeffrey C. Smith¹, J. Twicken¹, J. Van Cleve¹. ¹SETI Institute/NASA Ames Research Center, MS 244-30, Moffett Field, CA 94035, USA, ²Bay Area Environmental Research Institute, ³NASA Marshall Space Flight Center.
 *martin.stumpe@nasa.gov

Kepler photometric data contain significant systematic and stochastic errors as they come from the Kepler Spacecraft. The main cause for the systematic errors are changes in the focus of the photometer due to intrinsic and extrinsic thermal changes in the instrument, and also residual spacecraft pointing errors. It is the main purpose of the Presearch-Data-Conditioning (PDC) module of the Kepler Science processing pipeline to remove these systematic errors from the light curves. While PDC has recently seen a dramatic performance improvement by means of a Bayesian approach to systematic error correction (see companion poster by J. C. Smith et al.) and improved discontinuity correction (see poster by R. L. Morris et al.), there is still room for improvement.

One problem of the current (Kepler 8.0) implementation of PDC is that injection of high frequency noise can be observed in a few cases (see Figure 1). Although this high frequency noise does not negatively impact the general co-trending, an increased noise level can make detection of planet transits or other astrophysical signals more difficult.

effect to removing the trends, co-trending with these basis vectors can then also mistakenly introduce these small scale features into the light curves.

A solution to this problem is to perform a separation of scales, such that small scale features and low frequency trends are described by different basis vectors. We present our investigation of a wavelet-based band splitting approach to separate small scale from large scale features in the light curves. The PDC Bayesian co-trending can then be performed on each band individually, such that low frequency trends and high frequency features will be contained in independent basis vectors (see Figure 2).

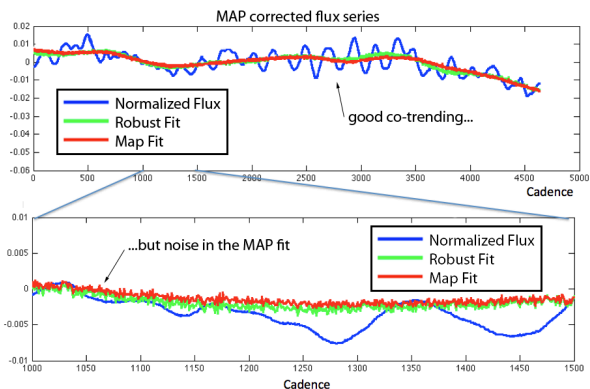


Figure 1: Injection of high frequency noise into corrected light curves. While the co-trending itself is very good (upper panel), the MAP fit (red curve) has a higher noise level than the Normalized Flux (blue curve).

The origin of this noise-injection is that high frequency components of light curves sometimes get included into co-trending basis vectors characterizing long term trends. Similarly, small scale features like edges can sometimes get included in basis vectors which otherwise describe low frequency trends. As a side

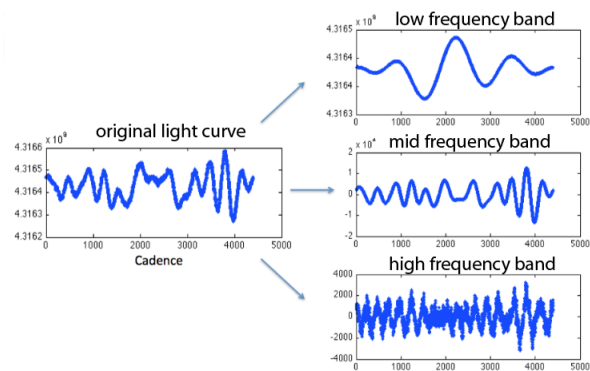


Figure 2: Band splitting of the light curves leads to a decomposition of small scale and large scale features.

Aside from eliminating the problems of noise and small scale feature injection, this wavelet-based scale decomposition will also allow an investigation of characteristic scales and amplitudes of systematic errors, which may lead to further improvements in the systematic error correction.

Funding for this work is provided by the NASA Science Mission Directorate.

P0133. POSTER SESSION I

Kepler: An Astrometric Mission to Detect Giant Planets and Brown Dwarfs around Nearby Stars? A. M. Tanner¹ and D. Monet², ¹Mississippi State University, 235 Hilbun Hall, MSU, MS 39762, angelle.tanner@gmail.com, ²USNO, dgm@nofs.navy.mil

Introduction: While the primary science goal for the Kepler mission is the characterization of terrestrial and giant exoplanets through ultra-precise photometry, the telescope is capable of collecting astrometric data at 0.001 pixel precision or better (see Figure 1). These data have been used to rule out false positives due to blends with eclipsing binaries and could be used to derive trigonometric parallaxes and proper motions, as well as search for 10-40 Jupiter-mass companions around a subset of high priority Kepler targets (see Figure 2). Alas, precise Kepler astrometry remains an elusive goal. The astrometric accuracy is compromised by as yet un-modeled "wiggles" (i.e., slow drifts in the stellar positions). Many numerical experiments have been devoted to understanding these apparent motions, but a predictive model has yet to be found. These motions are at the level of 0.01 pixel and preclude the measurement of proper motion, parallax, and perturbations. The current status of efforts to model these drifts will be reviewed as well as the full impact of the science that will be gained from this unique data set.

References:

- [1] Monet, D. et al. (2010) arXiv:1001.0305

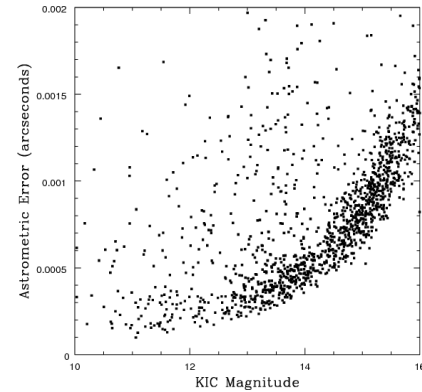


Figure 1: Plot of initial estimates of the astrometric errors from 30 minute (LC) observations as a function of Kepler magnitude¹. There is a substantial portion of the Kepler catalog that achieves milli-arcsecond precision or better sufficient to detect brown dwarf and low mass companions to many Kepler targets and Jupiter-mass companion for the closest members.

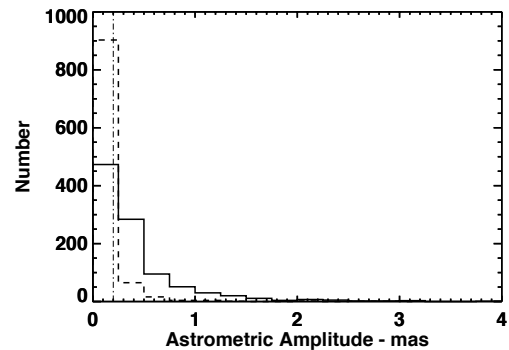


Figure 2: Histogram of the astrometric amplitude of 10 M_J (dashed) and 40 M_J (solid) companions in a 3.5 year orbit around the ~ 1000 Kepler targets with planetary transit candidates (Borucki et al. 2011). Also plotted (dash-dot) is the 0.2 mas astrometric detection limit that results from assuming a S/N of 5, single measurement precision of 4 mas and 22k observations over the lifetime of the mission.

P0134. POSTER SESSION I

DETECTION OF THRESHOLD CROSSING EVENTS IN THE FIRST THREE QUARTERS OF KEPLER DATA. P. Tenenbaum¹, J.M. Jenkins² and J.F. Rowe³, ¹SETI Institute, NASA Ames Research Center, Mail Stop 244-30, Building N244 R301, Moffett Field, CA 94035; peter.tenenbaum@nasa.gov. ²SETI Institute, jon.jenkins@nasa.gov. ³SETI Institute, jason.rowe-1@nasa.gov.

Introduction: The Transiting Planet Search (TPS) module is the SOC Pipeline software which performs automated searches for periodic reductions in light from target stars which are consistent with the signature of a transiting planet (Threshold Crossing Events, or “TCEs”) [1]. We used TPS to search for TCEs in all of the data collected in the first 3 quarters of Kepler science operations.

The Data: The first 3 “quarters” span 218 days from the start of May 12, 2009 to the end of December 17, 2009. Data is acquired at 29.4 minute intervals (“long cadence” data). When taking account of gaps in the observations necessary for downlinking data, spacecraft operations, safe mode events, and other interruptions, a total of 9,853 long cadence integrations were acquired.

A total of 170,854 stars were observed in the first 3 quarters. The vast majority, 151,722, are observed in all 3 quarters. Other targets were observed in a subset of quarters due to positioning (stars which fall on a CCD only in some orientations of the spacecraft) or improvements in target selection: 2,659 stars were observed only in Q1, 1,723 only in Q2, 1,394 only in Q3; 1,085 in Q1 and Q2, 11,671 in Q2 and Q3, 690 in Q1 and Q3.

The Cuts: The threshold for a TCE adopted by the *Kepler* Mission is a Multiple Event Statistic of 7.1 sigmas. A total of 66,593 stars are passed by this cut.

In addition, TPS requires that the ratio between the Multiple Event Statistic and the largest Single Event Statistic in a TCE exceed 1.4142. This cut eliminates cases in which a single large event is combined with a significantly smaller event to yield a TCE, since such detections are most likely false positives. A total of 5,392 stars are passed by the combination of this cut and the cut on Multiple Event Statistic.

The Results: Figure 1 shows the distribution of detected period in days vs detected epoch in Kepler-modified Julian Date (KJD, defined as JD-2454833). Note that the figure is dominated by short-period detections, but that there are no strong “bands” in the plane which would indicate an event which causes large numbers of false positives. The “dead zones” are combinations of period and epoch which are ruled out by the timing and duration of interruptions in data acquisition.

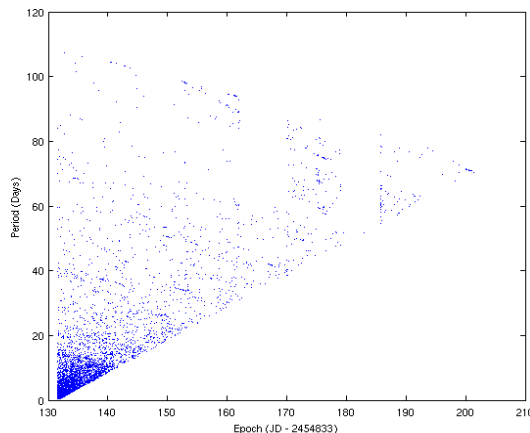


Figure 1 Epoch and period of TPS TCEs in Q1-Q3 data.

Figure 2 shows the distribution of transit depths in the TPS detections.

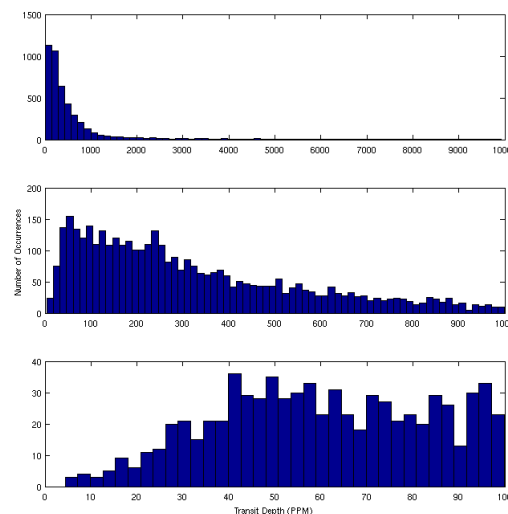


Figure 2 Distribution of transit depths of TPS TCEs in Q1-Q3 data.

Acknowledgements: Funding for the Kepler Mission is provided by the National Aeronautics and Space Administration (NASA) Science Mission Directorate.

References: [1] P. Tenenbaum et al, these proceedings (2011).

P0135. POSTER SESSION I

APPLICATION OF WAVELET-BASED ANALYSIS IN THE TRANSITING PLANET SEARCH ALGORITHM. P. Tenenbaum¹, J.M. Jenkins² and S. Seader³, ¹SETI Institute, NASA Ames Research Center, Mail Stop 244-30, Building N244 R301, Moffett Field, CA 94035; peter.tenenbaum@nasa.gov. ²SETI Institute, jon.jenkins@nasa.gov. ³SETI Institute, scott.seader@nasa.gov.

Introduction: Detection of signals of transiting planets in *Kepler* data requires the ability to detect reductions in the stellar flux as small as 84 parts per million (PPM) which last for a few hours and repeat on time scales of hours to years. This detection must take place against a background due to stellar variability. Stellar variability can be much larger than 100 PPM, but has a time signature which is extremely different from that of a transit [2]. Each star has a unique pattern of flux variations, and these patterns are typically non-white and non-stationary (ie, varying with time). A wavelet-based matched filter is used to extract the transit signal from the background of stellar variability.

Data Conditioning: Each flux time series must be free of data gaps, sampled uniformly in time, and contain a sample count which is a power of 2. Gap filling and flux extension are applied to each flux time series to achieve these requirements.

Filter Bank: The 12-tap Daubechies low-pass filter and the corresponding high-pass filter are used [1]. The filters are used to construct a set of band-pass filters with 1 octave bandwidth. These filters are then applied to the flux time series x , yielding a set of time series (1 per filter) x_i , each of which contains 1 octave of the original time series.

Whitener: For each x_i , the time-dependent in-band power σ_i is estimated by computing a moving RMS of the filtered time series. The window of the RMS must be long compared to the duration of the transits which are being searched for, and also must be long compared to the period of signals in each band. Vector division of x_i by σ_i has the effect of *whitening* the time series.

Sensitivity to Transits: We can now take the trial transit waveform (a square pulse with a selected duration and unit depth), s , and decompose it into a set of single-octave time series s_i , using the filter bank which performed the decomposition on the flux time series. The whitening filter at a time t can be applied to this set of time series by offsetting the σ_i time series and vector-dividing ($s_i(\tau) ./ \sigma_i(\tau-t)$). This shows how a square pulse in the data would be distorted by the whitener at each time t in the time series. It also shows what the in-band signal-to-noise ratio (SNR) is for detection of a unit-depth square pulse at each time in the time series.

The overall SNR as a function of time can be obtained by combining in inverse quadrature the band-by-band SNRs computed as described above. The reciprocal of this overall SNR is the smallest square pulse transit which can be detected with 1σ significance, the Combined Differential Photometric Precision (CDPP). The CDPP is a time series, since the non-stationary noise implies that the detectability of a transit pulse varies with time.

Detection Statistic: The detection statistic as a function of time (qualitatively, “How much does the data look like a transit at each location?”) can be determined by doing a band-by-band correlation of the whitened data with the whitened transit pulse (or equivalently, the doubly-whitened data and the unwhitened transit pulse), summing those correlations to combine the signals from each band, and dividing by the overall SNR as a function of time, computed above.

Whitened Flux Time Series: The wavelet filter bank used to divide the flux time series into single-octave time series can be reversed, which allows the time series to be synthesized back into the original signal. More usefully, the whitened band-by-band time series can be recombined. The resulting time series is a whitened flux time series, in which all of the non-stationary, non-white noise on time scales long compared to a transit has been removed, yielding a time series which is dominated by (approximately) white (approximately) Gaussian noise, and which contains transit signatures which are distorted by the local noise characteristics.

Acknowledgements: Funding for the Kepler Mission is provided by the National Aeronautics and Space Administration (NASA) Science Mission Directorate.

References: [1] Daubechies, I. (1988) *Commun.Pure Appl.Math.* 41,909. [2] Jenkins, J.M. (2002) *ApJ* 575, 493.

P0136. POSTER SESSION I

Terrestrial, Habitable-Zone Exoplanet Frequency from Kepler. W. A. Traub, Jet Propulsion Laboratory, California Institute of Technology, 4800 Oak Grove Dr., M/S 301-355, Pasadena, CA 91109, wtraub@jpl.nasa.gov

Introduction: Data from Kepler's first 136 days of operation are analyzed to determine the distribution of exoplanets with respect to radius, period, and host-star spectral type [1]. The analysis is extrapolated to estimate the percentage of terrestrial, habitable-zone exoplanets. The Kepler census is assumed to be complete for bright stars (magnitude <14.0) having transiting planets >0.5 Earth radius and periods <42 days. It is also assumed that the size distribution of planets is independent of orbital period, and that there are no hidden biases in the data.

Results: I find six significant statistical results:

- (1) there is a paucity of small planet detections around faint target stars, probably an instrumental effect;
- (2) the frequency of mid-size planet detections is independent of whether the host star is bright or faint;
- (3) there are significantly fewer planets detected with periods <3 days, compared to longer periods, almost certainly an astrophysical effect;
- (4) the frequency of all planets in the population with periods <42 days is 29%, broken down as terrestrials ($r/r_{\oplus} \leq 2$) 9%, ice giants ($2 < r/r_{\oplus} \leq 8$) 18%, and gas giants ($8 < r/r_{\oplus}$) 3%;
- (5) the population has a planet frequency with respect to period following a power-law relation $dN/dP \sim P^{\beta-1}$, with $\beta \sim 0.71 \pm 0.08$.

Implication: Extrapolating the power law to longer periods gives the frequency of terrestrial planets in the habitable zones of FGK stars as $\eta_{\oplus} \equiv (34 \pm 14)\%$.

(6) Thus about one-third of FGK stars are predicted to have at least one terrestrial, habitable-zone planet.

Reference: [1] W. A. Traub (2011) ApJ, Nov. issue.

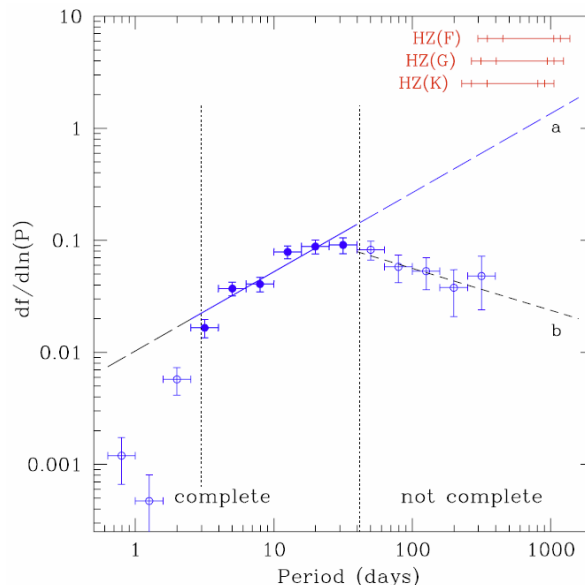


Figure. Distribution of planets in the population is shown as a function of period. The distribution is based on a projection from bright stars in the sample database, using the probability of transit as a projection factor for each planet. The data are fit by a power law $dN/d \ln P \sim P^{\beta}$ with $\beta = 0.71 \pm 0.08$ (thick line), and extrapolated to longer periods, along the upper dashed line, labeled “a”. The habitable zone ranges for FGK stars are indicated. The integrated number of planets in these ranges, multiplied by the fraction of terrestrial planets, gives the estimated value of η_{\oplus} . The lower dashed line, labeled “b,” is a fit to the data with periods >42 days, however these data are not complete, so the projection is not expected to be a true representation of the distribution in the population.

P0137. POSTER SESSION I

DIFFERENCE IMAGING FOR AUTOMATED VALIDATION OF PLANET CANDIDATES IN THE KEPLER SCIENCE OPERATIONS CENTER PIPELINE. J. D. Twicken¹ (joseph.twicken@nasa.gov), S. T. Bryson² (stephen.t.bryson@nasa.gov), R. L. Gilliland³ (gillil@stsci.edu), J. M. Jenkins¹ (jon.jenkins@nasa.gov), ¹SETI Institute/NASA Ames Research Center, MS 244-30, Moffett Field, CA, 94035, USA, ²NASA Ames Research Center, ³Space Telescope Science Institute.

Long cadence targets for which a Threshold Crossing Event (TCE) is generated in the Science Operations Center (SOC) Transiting Planet Search module are then processed in the Data Validation (DV) component [1], [2] of the SOC Pipeline. A transiting planet model is fitted to the light curve for each target, and a search for additional planets is conducted by repeating the transit search on the residual light curve after the model flux has been removed. The process is repeated until all planet candidates have been identified.

A suite of automated tests is performed on all planet candidates in DV for the purpose of aiding in the discrimination between true planets and false positives. The validation tests that were implemented in the initial release of DV have been documented in [1]. In subsequent releases, a difference imaging technique has been implemented to enhance the validation process for planet candidates. This technique aims to locate the source of a transit signature in the photometric mask for the given target, and to estimate the offset between the transit source and the target itself.

Difference imaging is proving to be a powerful diagnostic for identifying astrophysical false positive detections due to background eclipsing binaries. It is also proving to be valuable for identifying the true transit source in crowded apertures. Difference images, centroids and offsets are computed on a quarterly basis for each planet candidate due to the quarterly roll of the spacecraft. The offsets may be averaged, however, over multiple quarters to improve the sensitivity of this difference image diagnostic.

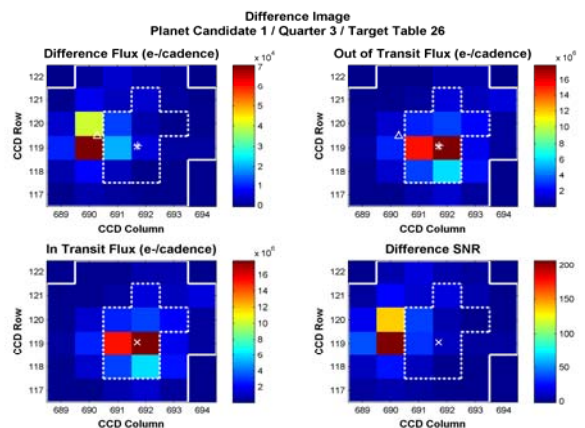
For each planet candidate, mean in- and out-of-transit images are constructed by averaging the flux in and near each transit on a per pixel basis, and then by averaging over all transits for the given observing quarter. In- and out-of-transit cadences are identified through the transiting planet model that is fitted to the target light curve. A difference image is then generated by subtracting the mean in-transit flux for each pixel from the mean out-of-transit flux.

Transits are excluded from the respective images if the associated in- or out-of-transit cadences overlap (1) the transit of another planet candidate for the given target, (2) a known spacecraft anomaly (e.g. Earth-point for data downlink, safe mode, attitude tweak, and multiple-cadence loss of fine point), or (3) the start or end of the given quarter.

The photocenters of the out-of-transit and difference images are computed by fitting the appropriate Pixel Response Function (PRF) for the given channel. The out-of-transit centroid locates the target itself, subject to aperture crowding. The difference image centroid precisely locates the source of the transit signature (which may or may not be the given target). The offset between difference and out-of-transit image centroids provides both absolute and statistical measures of the separation between target and transit source.

The offset is also computed per planet candidate and observing quarter between the difference image centroid and the target location specified by its Kepler Input Catalog (KIC) celestial coordinates. The offset from the KIC reference position is not subject to aperture crowding but is subject to centroid bias.

A difference image for KOI 140 in quarter 3 is shown in the figure below. This KOI has been identified as an astrophysical false positive. The mean out-of-transit image is shown in the upper right panel and the mean in-transit image is shown in the lower left. The difference image in the upper left panel indicates that the “transit” source is offset by 1.5 pixels (5.9 arcseconds) from the target which is marked by the out-of-transit image centroid and the KIC reference position.



Funding for the *Kepler* Mission has been provided by the NASA Science Mission Directorate.

References:

- [1] Wu, H. et al. (2010) *Proc. SPIE 7740*, 774019 1-12.
- [2] Tenenbaum, P. et al. (2010) *Proc. SPIE 7740*, 77400J 1-12.

P0138. POSTER SESSION I

NEW DIRECTIONS IN KEPLER CORRECTIONS

J. Van Cleve^{*1}, T. Barclay², M. N. Fanelli², J. M. Jenkins¹, J. Kolodziejczak³, R. Morris¹, J. C. Smith¹, M. C. Stumpe¹, J. Twicken¹

^{*}jeffrey.vancleve@nasa.gov, ¹SETI Institute/NASA Ames Research Center, MS 244-30, Moffett Field, CA 94035, USA, ²Bay Area Environmental Research Institute, ³NASA Marshall Space Flight Center,

Introduction: The Presearch Data Conditioning (PDC) module of the Kepler science data analysis Pipeline does well at the task for which it was originally designed: removing systematic errors from flux time series while preserving transit signals for the >70% of planetary search target stars which are not intrinsically variable. However, astrophysically interesting signals from variable stars were often distorted or destroyed by the versions of PDC used on data released before 10/1/2011. A companion poster by Smith et al. describes the great progress made in PDC 8.0 towards preserving astrophysical signals while maintaining sensitivity to transits, using an empirical Bayesian approach [1,2]. In a nutshell, this approach uses the distribution of least-squares fit parameters in a reference ensemble of light curves as prior information to moderate the values of the coefficients for each target. An obvious area of further progress is to decouple low and high frequency systematic noise, using wavelet-based band splitting as described in the companion poster by Stumpe et al. Detection and repair of single-pixel sensitivity dropouts (SPSDs), while not systematic errors in themselves, are an integral part of PDC and the current algorithms and improvements are described in a companion poster by Morris and Kolodziejczak.

Current Investigations: In this poster, we describe other ongoing efforts to further improve systematic error correction in PDC after Release 8.0, which include

1. Development of a goodness metric which detects noise injection, signal distortion, and residual correlations between corrected light curves, as a guide to progress in items below.
2. Improved reference light curve ensemble selection and resulting cotrending basis vector (CBV) set generation.
3. Adaptive selection of the number of CBVs used to fit and remove systematic errors
4. Improvement of the prior distribution, by
 - a) generalizing the coefficient distribution space to dimensions beyond the currently-used RA, DEC, and Kepler magnitude
 - b) Using cluster analysis to identify groups of stars with similar systematic errors and generating cluster-specific CBVs

5. Joint fitting of CBVs, cosmic-ray induced single-pixel sensitivity dropouts (SPSDs), and low-frequency astrophysical signals represented by polynomials.

Funding for this work is provided by the NASA Science Mission Directorate.

References:

[1] Jenkins, J.M., J.C. Smith, P. Tenenbaum, J. D. Twicken, and J. Van Cleve, "Planet Detection: The Kepler Mission," in *Advances in Machine Learning and Data Mining for Astronomy* (eds. M. Way, J. Scargle, K. Ali, A. Srivastava), Chapman and Hall/CRC Press, 2011.

[2] S. M. Kay. *Fundamentals of Statistical Signal Processing: Estimation Theory*. New Jersey: Prentice Hall PTR, 1993



How Close are Kepler Systems to Being Dynamically Packed? (And Implications for η_{Earth})

R. Belikov¹ and M. J. Kuchner²

¹NASA Ames Research Center, M/S 245-6, P.O.Box 1, Moffett Field, CA94035, Ruslan.Belikov@nasa.gov,

²NASA Goddard Space Flight Center, marc.j.kuchner@nasa.gov

The release of data on Kepler planet candidates [1] was shortly followed by several papers analyzing planet frequency statistics (e.g. [2], [3]) as well as ones that attempt to extrapolate the data to Earth-like planet sizes and distances from the star (e.g. [4], [5]). Even though these papers took care to compensate for incompleteness and observational biases, results for η_{Earth} based on different extapolations vary by two orders of magnitude, from about 1% to 50%. It would seem that at present the Kepler statistics alone may not be complete enough yet to get a firm handle on η_{Earth} .

However, certain firm conclusions can nevertheless be drawn when considering the Kepler data not by itself, but in combination with the requirement that stable planetary systems must not have more planets than allowed by full dynamical packing.

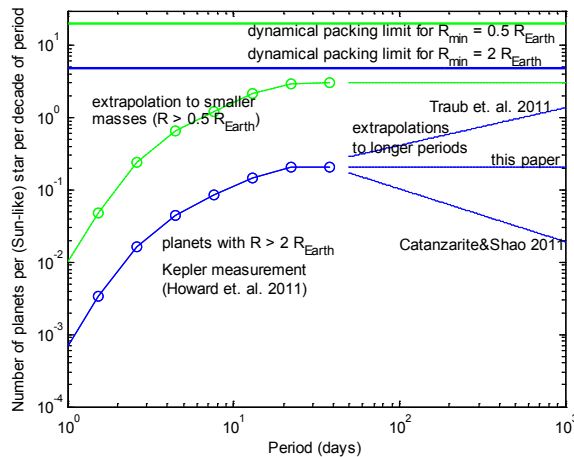


Figure 1. Planet distribution functions in log period. The dynamical packing hypothesis explains the asymptoting behavior of the data and motivates an extrapolation to longer periods that does not rely on incomplete statistics.

Figure 1 illustrates this idea, which shows several planet frequency distributions as a function of log-period for Sun-like stars. The blue lines represent planets with radii down to $2 R_{\text{Earth}}$ and green lines represent planets with radii down to $0.5 R_{\text{Earth}}$. The blue curved line out to period of ~ 40 days represents the expected frequency measured by the Kepler science team based on relatively complete debiased data [2]. The horizontal lines on the top show the limits on the frequency of planets imposed by dynamical packing

(i.e. any more planets and the system will become unstable). These limits were calculated based on the work in [6] and planet masses were converted to radii based on the mass-radius relationships predicted in [7].

It has been hypothesized that most planetary systems may be close to being dynamically packed [8]. Figure 1 shows that this is indeed the case at least in the vicinity of 20-40-day periods, where the frequency of planets down to $0.5 R_{\text{Earth}}$ are within an order of magnitude (21%) of the dynamical packing limit. The 21% number assumes conservatively that there are no planets or other objects smaller than $0.5 R_{\text{Earth}}$ around any Kepler stars (where there is very little Kepler data). Should the observed Kepler planet size power law hold down to $\sim 0.1 R_{\text{Earth}}$, then all systems would be fully dynamically packed, and if any objects exist that are smaller than $0.1 R_{\text{Earth}}$, they would not be on stable isolated orbits. Notably, this is exactly the case with the Solar System, where objects smaller than $\sim 0.1 R_{\text{Earth}}$, e.g. asteroids, tend to exist in a dynamic belt.

This suggests an explanation for why the measured planet frequencies on Figure 1 are starting to level off beyond 10-day periods: they are asymptoting to the dynamical packing limit. If this is so, we would expect the planet frequency to remain flat beyond 40 day periods, as shown by the dashed line in Figure 1. Such a curve would imply that η_{Earth} is 23% and 89% for planets between 1 and $2 R_{\text{Earth}}$, and 0.5 and $2 R_{\text{Earth}}$, respectively (using the more conservative definition of the habitable zone as having a semi-major axis between 0.95 and $1.37 (L/L_{\text{Sun}})^{1/2}$ a.u.)

The combination of the dynamical packing hypothesis and Kepler statistics also allows us to predict the distribution of planet distribution around many other parameters, such as star mass, and we perform a general analysis of this in our paper.

References:

- [1] Borucki, W. J., et. al. 2011, ApJ, 736, 19B.
- [2] Howard, A. W., et. al., 2011, ApJ submitted.
- [3] Youdin, A. N., et. al., 2011, ApJ submitted.
- [4] Catanzarite, J., Shao, M., 2011, ApJ, 738, 151C
- [5] Traub, W. A., 2011, ApJ submitted.
- [6] Chambers, J.E., et. al., 1996, Icarus 119, 261.
- [7] Seager, S., 2007, ApJ 669, 1279.
- [8] Barnes, R., Raymond, S.N 2004, ApJ, 617,569.

P0202. POSTER SESSION I

THE OCCURRENCE RATE OF EARTH ANALOG PLANETS ORBITING SUN-LIKE STARS. J. Catanzarite, Affiliation: Jet Propulsion Laboratory / California Institute of Technology, 4800 Oak Grove Drive, M/S 302-355, Pasadena, CA 91109, Joseph.H.Catanzarite@jpl.nasa.gov

Kepler is a space telescope that searches Sun-like stars for planets. Its major goal is to determine η_{Earth} , the fraction of Sun-like stars that have planets like Earth. When a planet “transits” or moves in front of a star, *Kepler* can measure the concomitant dimming of the starlight. From analysis of the first four months of those measurements for over 150,000 stars, *Kepler*’s Science Team has determined sizes, surface temperatures, orbit sizes, and periods for over a thousand new planet candidates. In this paper, we characterize the probability distribution function of the orbit periods of the super-Earth and Neptune planet candidates with periods up to 132 days, finding three distinct period regimes. For candidates with periods below 3 days, the density increases sharply with increasing period; for periods between 3 and 30 days, the density rises more gradually with increasing period, and for periods longer than 30 days, the density drops gradually with increasing period. We estimate that 1% to 3% of stars like the Sun are expected to have Earth analog planets, based on the *Kepler* data release of 2011 February. This estimate of η_{Earth} is based on extrapolation from a fiducial subsample of the *Kepler* planet candidates that we chose to be nearly “complete” (i.e., no missed detections) to the realm of the Earth-like planets, by means of simple power-law models. The accuracy of the extrapolation will improve as new from the *Kepler* mission are folded in. Accurate knowledge of η_{Earth} is essential for the planning of future missions that will image and take spectra of Earth-like planets. Our result that Earths are relatively scarce means that a substantial effort will be needed to identify suitable target stars prior to these future missions.

P0203. POSTER SESSION I

Searching for evidence of a magnetic field in the exotic super-Earth 55 Cancri e, D. Dragomir¹ and Jaymie M. Matthews¹, ¹Department of Physics and Astronomy, University of British Columbia, 6224 Agricultural road, Vancouver, BC, V6T 1Z1 Canada; diana@phas.ubc.ca, matthews@astro.ubc.ca

Observations of star-exoplanet interactions are the only way at present to investigate the magnetic fields of exoplanets. The category of super-Earth exoplanets (with masses about 2 - 10 times that of Earth, metallic cores and rocky mantles) represents an exciting new hunting ground to study planetary magnetism. 55 Cancri e is a transiting superEarth with two notable distinctions: (1) It orbits the brightest star ($V = 6$) known to have a transiting planet, and (2) it has the shortest orbital period (about 18 hours) of any known planet.

We propose to obtain ESPaDOnS spectropolarimetry of the 55 Cnc system to measure the star's magnetic field and to search for evidence of interactions between it and the exoplanet's magnetosphere (if it has one). There is circumstantial evidence for such an interaction in MOST space telescope photometry of 55 Cnc: Subtle modulation in the system brightness phased with the planet's orbital period, too large to be explained solely by reflected light from the planet. The modulation may be due to a concentration of starspots and/or a different granulation pattern on the planet-facing hemisphere of the star, as seen already in MOST and ESPaDOnS data for the 'hot Jupiter' system tau Bootis.

Evidence of star-exoplanet interaction in the 55 Cnc system would be the first (indirect) detection of a magnetic field in a super-Earth.

P0204. POSTER SESSION I

SPITZER EVIDENCE FOR A PLANET DRIVEN LATE HEAVY BOMBARDMENT IN η CORVI AT ~ 1 GYR. C.M. Lisse¹, ¹Johns Hopkins University Applied Physics Laboratory, 11100 Johns Hopkins Road, Laurel, MD 20723; carey.lisse@jhuapl.edu

Abstract. We have analyzed *Spitzer* and NASA/IRTF 2 – 35 μm spectra of the warm, ~ 350 K circumstellar dust around the nearby MS star η *Corvi* (F2V, 1.4 ± 0.3 Gyr). The spectra show clear evidence for warm, water- and carbon-rich dust at ~ 3 AU from the central star, in the system's Terrestrial Habitability Zone. Spectral features due to ultra-primitive cometary material were found, in addition to features due to impact produced silica and high temperature carbonaceous phases. At least 9×10^{18} kg of 0.1 – 100 μm warm dust is present in a collisional equilibrium distribution with $dn/da \sim a^{-3.5}$, the equivalent of a 130 km radius KBO of 1.0 g/cm^3 density and similar to recent estimates of the mass delivered to the Earth at 0.6 – 0.8 Gyr during the Late Heavy Bombardment. We conclude that the parent body was a Kuiper-Belt body or bodies which captured a large amount of early primitive material in the first Myrs of the system's lifetime and preserved it in deep freeze at ~ 150 AU. At ~ 1.4 Gyr they were prompted by dynamical stirring of the parent Kuiper Belt into spiraling into the inner system, eventually colliding at 5-10 km/sec with a rocky planetary body of mass $\leq M_{\text{Earth}}$ at ~ 3 AU, delivering large amounts of water ($>0.1\%$ of $M_{\text{Earth's Oceans}}$) and carbon-rich material. The *Spitzer* spectrum also closely matches spectra reported for the Ureilite meteorites of the Sudan Almahata Sitta fall in 2008, suggesting that one of the Ureilite parent bodies was a KBO.

Transit Spectroscopy of sub-Neptune-sized Planets GJ1214b and HD97658b with HST WFC3. P. R. McCullough¹, ¹STScI (3700 San Martin Dr., Baltimore MD 21218, pmcc@stsci.edu).

Abstract: We analyze 1.1-1.7 micron spectra of a transit of the super-Earth GJ1214b obtained 2011-4-18 during re-commissioning of a technique for spatially scanning the Hubble Space Telescope (Figure 1). These are the first data of this type obtained with the HST instrument WFC3. Results are directly compared to staring-mode observations with the same instrument of the same target by Berta et al. [1]. Spatial scanning is expected to have some advantages over staring-mode observations with existing HST instruments, especially for very bright stars, i.e. those that intrinsically can provide the highest sensitivity observations. We also describe a case study of the sub-Neptune-sized planet HD 97658b in terms of proposed observations and what they may reveal of that planet. We also summarize publicly-available descriptions of additional HST programs that use the spatial-scanning technique (Table 1).

References:

[1] Berta, Z. K. et al. 2011, submitted to ApJ.

Table 1

| |
|---|
| HST program, Title, Investigators, Scanned Targets |
| 12181 The Atmospheric Structure of Giant Hot Exoplanets, Deming, L. D. et al., HD 209458 and HD 189733 |
| 12325 Photometry with Spatial Scans, MacKenty, J. W., & McCullough, P. R., GJ1214 |
| 12336 Scan Enabled Photometry, MacKenty, J. W., McCullough, P. R., & Deustua, S., Vega and other calibration stars |
| 12449 Atmospheric Composition of the ExoNeptune HAT-P-11, Deming, L. D., et al., HAT-P-11 |
| 12473 An Optical Transmission Spectral Survey of hot-Jupiter Exoplanetary Atmospheres, Sing, D. K. et al., WASP-31, HAT-P-1 |
| 12495 Near-IR Spectroscopy of the Hottest Known Exoplanet, WASP-33b, Deming, L. D. et al., WASP-33 |
| 12679 Luminosity-Distance Standards from Gaia and HST, Riess, A., et al., Milky Way Cepheids |

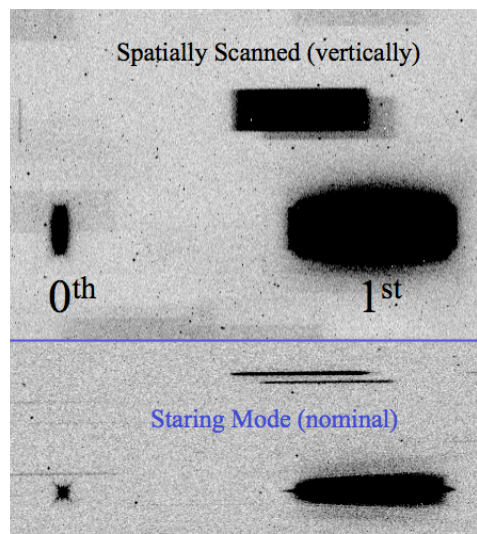


Figure 1: The spatially scanned spectrum of the star GJ1214 is labeled with its 0th and 1st order light and compared to a nominal staring-mode slitless spectrum of the same field (below the blue line). The scan was 40 pixels high (4.8 arcsec).

P0206. POSTER SESSION I

CARMENES: A RADIAL-VELOCITY SURVEY FOR TERRESTRIAL PLANETS IN THE HABITABLE ZONES OF M DWARFS. A. Quirrenbach¹ and the CARMENES Consortium, ¹Landessternwarte, Zentrum für Astronomie der Universität Heidelberg (ZAH), Königstuhl 12, D-69117 Heidelberg, Germany

Introduction: CARMENES (Calar Alto high-Resolution search for M dwarfs with Exo-earths with Near-infrared and optical Echelle Spectrographs) is a next-generation instrument to be built for the 3.5m telescope at the Calar Alto Observatory by a consortium of eleven Spanish and German institutions. Conducting a five-year exoplanet survey targeting ~300 M dwarfs with the completed instrument is an integral part of the project. The CARMENES instrument consists of two separate échelle spectrographs covering the wavelength range from 0.55 to 1.7 μm at a spectral resolution of $R = 85,000$, fed by fibers from the Cassegrain focus of the telescope. The spectrographs are housed in vacuum tanks providing the temperature-stabilized environments necessary to enable a 1m/s radial velocity precision employing a simultaneous calibration with an emission-line lamp.

Science Case: The fundamental scientific objective of CARMENES is to carry out a survey of late-type main sequence stars with the goals of characterizing the population of planets around these stars, and of detecting low-mass planets in their habitable zones (HZs). In the focus of the project are very cool stars later than spectral type M4V and moderately active stars, but the target list will also comprise earlier and therefore brighter M dwarfs. In particular, we aim at being able to detect a $2M_{\oplus}$ planet in the HZs of M5 stars. A long-term radial velocity precision of 1m/s per measurement will permit to attain this goal. For stars later than M4 ($M < 0.25M_{\odot}$), such precision will yield detections of super-Earths of $5M_{\oplus}$ and smaller inside the entire width of the HZ. For a star near the hydrogen-burning limit, a planet with the mass of our own Earth in the HZ could be detected at a precision of 1m/s. In addition, the HZ of all M-type dwarfs can be probed for super-Earths. Thus, a RV precision of 1m/s can trigger a breakthrough in exoplanet research in the spectral range of mid and late M-type stars.

We plan to survey a sample of 300 M-type stars for low-mass planet companions. Besides the detection of the individual planets themselves, the ensemble of objects will provide sufficient statistics to assess the overall distribution of planets around M dwarfs: frequency, masses, and orbital parameters. The survey will confirm or falsify the seemingly low occurrence of Jovian planets around M stars, and the frequency of ice giants and terrestrial planets will be established along with their typical separations, eccentricities, multiplicities, and dynamics. Thus, the CARMENES survey can

provide the first robust statements about planet formation in the low-mass star regime.

Instrument: For late-M spectral types, the wavelength range around 1000 nm (Y band) is the most important wavelength region for RV work. Therefore, the efficiency of CARMENES will be optimized in this range. Since CCDs do not provide high enough efficiency around 1000 nm and no signal at all beyond the Si cutoff at 1100 nm, a near-IR detector is required.

It is thus natural to adopt an instrument concept with two spectrographs, one equipped with a CCD for the range 550-1050 nm, and one with HgCdTe detectors for the range from 0.9-1.7 μm . Each spectrograph will be coupled to the 3.5m telescope with its own optical fiber. The front end will contain a dichroic beam splitter and an atmospheric dispersion corrector, to feed the light into the fibers leading to the spectrographs. Guiding is performed with a separate camera. Additional fibers are available for simultaneous injection of light from emission line lamps for RV calibration.

The spectrographs are mounted on benches inside vacuum tanks located in the coudé laboratory of the 3.5m dome. Each vacuum tank is equipped with a temperature stabilization system capable of keeping the temperature constant to within $\pm 0.01^{\circ}\text{C}$ over 24h. The visible-light spectrograph will be operated near room temperature, the NIR spectrograph will be cooled to -80°C .

The CARMENES instrument passed its preliminary design review in July 2011; completion of the instrument is planned for late 2013. At least 600 useable nights have been allocated at the Calar Alto 3.5m Telescope for the CARMENES survey in the time frame from 2014 to 2018. The instrument is also well-suited for RV follow-up of planet candidates from transit surveys. More details can be found on the project web page and in Quirrenbach et al. (2010).

References:

- <https://carmenes.caha.es/ext/index.html> (CARMENES project public web page)
- Quirrenbach, A., Amado, P.J., Mandel, H., et al. (2010). *CARMENES: Calar Alto high-Resolution search for M dwarfs with Exo-earths with Near-infrared and optical Echelle Spectrographs*. In *Ground-based and airborne instrumentation for astronomy III*. Eds. McLean, I.S., Ramsay, S.K., & Takami, H., SPIE Vol. 7735, 773513, p. 1-14

An astronomical criterion for association of the four fundamental interactions. Murat Zhussupov (24, Buhar-Zhyrau Street, Almaty, Kazakhstan, mjalmata@mail.ru)

Introduction: The whole diversity of nature and life around us is caused by such fundamental phenomena, as gravitation, electromagnetism, strong and weak interaction. Accordingly, researches in all areas of modern science - physics, astronomy, chemistry, biology and other, are compelled to prefer to one of this phenomena. As a result often receive too complicated and inconsistent the picture of the description the nature. Historically sights at these interactions consistently formed to a measure of opening and studying of phenomena accompanying them. Simultaneously, for the purpose of creation of complete and objective picture of physical laws of the Universe, were conducted searches of ways of their association as, for example, it has been successfully carried out in the end of the last century for electromagnetism [1]. At present work on creation of the theory of association of four fundamental interactions has the continuation, mainly, within the frames of the theoretical physics. In this direction the essential contribution can make also the astronomy. The astronomy is the purest for virtual experiment by the tool of research so as all spatial relations of heavenly bodies are defined uniform force of gravitation. Laws of behavior of heavenly bodies are one of main criterion which can to associate the fundamental interaction. Taken together with researches in other areas of science - physics, astrophysics, thermo-dynamics and mineralogy, author discovered the principle of unity of the gravitational, electromagnetic, strong and weak interactions. This principle is based on the fact that the source of all the fundamental relationships in nature is a unified force of Transpressure [2]. This is unknown a previously type of pressure, which exist in "vacuum", penetrates through environment of various substances and influences only fundamental particles. It exists in the nature along with molecular pressure and pressure of light. Numerically pressure is equal $4,775e^{24}$ Pa (round-off). Pressure resembles hydrostatic and probably spread within the Universe everywhere - in vacuum and molecular environments of stars and planets. The pressure operates only a surface of fundamental particles - electrons, nucleons, mesons, etc., and does not influences in space free from these particles, even inside molecules and atoms. Reaction of fundamental particles to pressure, according to Newton's third law, is expressed in occurrence of forces of counteraction. The directions of these forces depend on structural, morphological features of objects which structure includes fundamental particles and symmetry of the environment. The size of transpressure seems an enormous, but live organism does not feel it, because it operates only on an electronic and nucleon lattice of molecules from which these organisms consist. In essence this lattice fastened from this pressure. **Behavior of planet Earth under the influence of transpressure:** Any moving material bodies behave as a wave. They have received the wave name de Broglie. Is

considered, that wave properties of macroscopic objects are not appreciably because of small length of a wave. However in plan of action the transpressure it is no so. In Fig.1 schematically shown movement of the Earth (E) round the Sun (S), where r - radius of the Earth, a - radius of an orbit of its rotation round the Sun. Torus which is

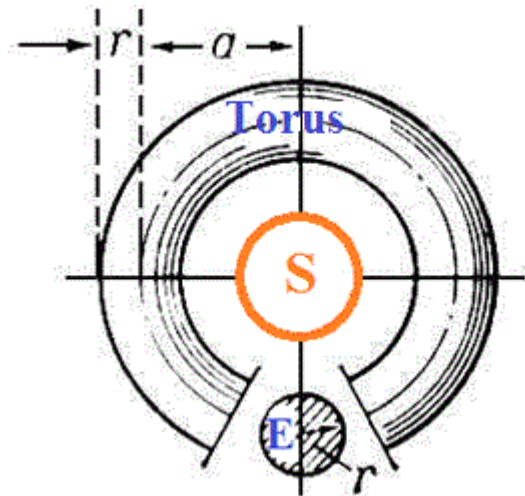


Fig.1. Scheme of rotation of Earth around Sun

formed from moving of planet has volume

$V_T = \pi r^2 2\pi a$. The equation $\frac{\lambda_r}{\lambda_b} = \frac{P_t V_T}{m_s c^2}$, where λ_r length of orbit, λ_b de Broglie wave length for Earth

equal $\lambda_b = \frac{h}{m_E g_E}$, P_t transpressure, m_s mass of

soliton: ($m_s = \frac{\pi m_e}{c^2 \mu_o}$, where m_e - mass of electron, C -

speed of light, μ_o - magnetic constant) - shown what the orbit of Earth around Sun is the wave of de Broglie. Now it is possible to notice that in calculations necessity of use the gravitational constant disappears.

Conclusion: Laws of behavior of heavenly bodies are one of main criterion which can to associate the all four fundamental interaction. Is established unknown a previously type of pressure with action in "vacuum", it penetrates through of various substances and influences only fundamental particles. This pressure is a unique source of forces for gravitational, electromagnetic, the strong and weak interactions. Mutual relations of heavenly bodies depend from their reactions to this pressure and from symmetry of environment. Thus, the orbit of the Earth round the Sun is represented as wave de Broglie generated under the influence of transpressure.

References: [1] Davies P., (1989), NY, 10-15, [2] Zhussupov M. (2011), Thermodynamics2011, Abstract #431, #508

P0301. POSTER SESSION I

Exoplanet Migration and the Distribution of Period Ratios in Multiple Planet Systems Katherine M. Deck¹ and Matthew J. Holman², ¹Massachusetts Institute of Technology, Physics Department, kdeck@mit.edu, ²Harvard-Smithsonian Center for Astrophysics, mholman@cfa.harvard.edu

Capture into resonance is a natural consequence of convergent migration in multiple planet systems [1,2,3,4]. As planets migrate, the ratios of orbital periods within the system slowly change. When they approach a commensurability, there is some probability of capture into resonance. An interesting observational result from the Kepler data is that planets in multiple planet systems found near first order mean motion resonances tend to be grouped outside of the nominal resonance value [5]. If this result holds as more planets are discovered, it could constrain planetary migration theories.

We are studying the process of capture into the 2:1 resonance in particular, as period ratios near two are common among the systems discovered [5]. By numerically evolving a planetary system with two planets, according to the usual Hamiltonian gravitational dynamics as well as a very general migration mechanism, we confirm that capture into the 2:1 resonance can occur and show that period ratios greater than two can be achieved for specific dissipation rates. We are exploring whether or not these rates are physical. In addition, we are also studying the evolution semi-analytically by modeling the system as being governed by an adiabatically changing Hamiltonian. This will allow us to better understand the distribution of period ratios that result from convergent migration, capture into resonance, and subsequent termination of migration.

[1] Goldreich, P. 1965, MNRAS, 130, 159

[2] Lee, M. H., and Peale, S. J., 2002, ApJ, 567, 596.

[3] Lee, M. H., 2004, ApJ, 611, 517

[4] C. Beaugé, S. Ferraz-Mello & T.A. Michtchenko, 2003, ApJ, 593, 1124-1133

[5] JJ Lissauer et al, November 2011, ApJs, & arXiv:1102.0543v4

P0302. POSTER SESSION I

Predicting Planets in *Kepler* Candidate Multi-Planet Systems. J. Fang¹ and J. L. Margot², ¹Department of Physics and Astronomy, 430 Portola Plaza, Box 951547, University of California, Los Angeles, CA 90095, USA, e-mail: fang@astro.ucla.edu, ²University of California, Los Angeles, e-mail: jlm@astro.ucla.edu

Introduction: Early studies of extrasolar planetary systems showed residual velocity trends in Keplerian orbit fits to radial velocity data [1-5], suggesting that these systems may harbor additional, yet-undetected companions. Many of these systems were later discovered to host additional planet(s). In more recent years, the study and prediction of undiscovered planets have been boosted by long-term N-body simulations. These numerical investigations searched for stability zones in multi-planet systems by integrating many test bodies, which were injected into empty regions between known planets [6-10]. In the case of exoplanet HD 74156d [11], this Saturn-mass planet was first predicted through numerical simulations showing a stable region between planets b and c [8], and then later discovered [12]. This successful prediction was motivated by the “packed planetary systems” (PPS) hypothesis.

The PPS hypothesis is the idea that planetary systems are formed “dynamically full” and filled to capacity, and any additional planets will cause the system to be unstable [7-8,13-14]. Consequently, planetary systems with stable stability zones between the innermost and outermost planets are suggestive of additional, yet-undetected planets. The orbital properties of predicted planets can be identified through long-term numerical simulations.

In the present study, we apply the PPS hypothesis to multi-planet candidate systems discovered by the *Kepler* mission [15]. Given the high frequency of packing found in known planetary systems, we seek to test the PPS hypothesis and predict additional planets in *Kepler* candidate multi-planet systems through analytical and numerical methods.

Methods: We use publicly available *Kepler* data covering the first four and a half months of observations [16]. One-third of the planetary candidates in this dataset are hosted in a total of 170 multi-planet systems [17]. Of these systems, we analytically calculate the Hill stability of all adjacent planet pairs to discern the extent of packing in the systems. Fulfillment or over-fulfillment of the Hill stability criterion, implying that the considered planet pair is not on the verge of instability, suggests the presence of additional planets. We find that many of the systems are packed and we focus on <10 two-planet systems that are most likely to harbor additional planet(s).

For these non-packed 2-planet systems, we conduct numerical simulations by placing thousands of test particles in each system to map out their zones of stability. For each system, our simulations include the star

and its two detected planets as well as thousands of test particles placed in between the locations of the inner and outer planets. These test particles are massless, which can be good proxies for terrestrial-class planets. We integrate for 10^7 years and test particles that survive the length of the integration are considered stable test particles. We record the starting orbital elements such as the semi-major axis and eccentricity of all stable and unstable test particles.

Results and Summary: We calculate which *Kepler* candidate multi-planet systems may be capable of harboring additional planet(s) between the inner and outer detected planets. For each non-packed system under consideration, we perform a numerical investigation and map out the regions in parameter space (semi-major axis and eccentricity) that have stable test particles. We quantify the ranges of semi-major axis and eccentricity of these stable regions and predict the existence of additional planet(s) in these stability zones. Additional quarters of *Kepler* data may reveal additional planets in the stable gaps suggested by our simulations.

References: [1] Marcy, G. W. & Butler, R. P. (1998) *ARA&A*, 36, 57. [2] Butler, R. P. et al. (1998) *PASP*, 110, 1389. [3] Marcy, G. W. et al. (1999) *ApJ*, 520, 239. [4] Vogt, S. S. et al. (2000) *ApJ*, 536, 902. [5] Fischer, D. A. et al. (2001) *ApJ*, 551, 1107. [6] Menou, K. & Tabachnik, S. (2003) *ApJ*, 583, 473. [7] Barnes, R. & Raymond, S. N. (2004) *ApJ*, 617, 569. [8] Raymond, S. N. & Barnes, R. (2005) *ApJ*, 619, 549. [9] Rivera, E. & Haghighipour, N. (2007) *MNRAS*, 374, 599. [10] Raymond, S. N. et al. (2008) *ApJ*, 689, 478. [11] Barnes, R. et al. (2008) *ApJ*, 680, L57. [12] Bean, J. L. et al. (2008) *ApJ*, 672, 1202. [13] Raymond, S. N. et al. (2006) *ApJ*, 644, 1223. [14] Barnes, R. & Greenberg, R. (2007) *ApJ*, 665, L67. [15] Borucki, W. J. et al. (2010) *Science*, 327, 977. [16] Borucki, W. J. et al. (2011) *ApJ*, 736, 19. [17] Lissauer J. J. et al. (2011) ArXiv e-prints.

P0303. POSTER SESSION I

A new analysis of WASP-3b

POSTER CONTRIBUTION

September 30, 2011

M. Montalto¹, J. Gregorio³, G. Boué¹, M. Oshagh¹, M. Maturi⁴, N. C. Santos^{1,2}

1. Centro de Astrofísica da Universidade do Porto (CAUP), Rua das Estrelas, 4150-762 Porto, Portugal NIF 502 216 450
2. Departamento de Física e Astronomia, Faculdade de Ciências, Universidade do Porto, Portugal
3. Grupo Atalaia
4. Zentrum fuer Astronomie, ITA, Universitaet Heidelberg, Albert-Ueberle-Str. 2, D-69120, Heidelberg, Germany

Abstract

A battery of new transits of WASP-3b has been observed by our group. In this poster we present our re-analysis of the properties of this planet. In particular we studied the entire sample of transit timing and radial velocity measurements acquired so far, constraining the presence of other perturbing planets in the system.

THE TASTE PROJECT: A GROUND-BASED SEARCH FOR TRANSIT TIME VARIATIONSV. Nascimbeni¹, G. Piotto², L. R. Bedin³, M. Damasso⁴, L. Malavolta⁵, L. Borsato⁶, and A. Cunial¹Dipartimento di Astronomia, Università di Padova (UniPD), Vicolo dell'Osservatorio 3, 35122 Padova, Italy,valerio.nascimbeni@unipd.it, ²UniPD, giampaolo.piotto@unipd.it, ³INAF-OaPD, luigi.bedin@oapd.inaf.it,⁴UniPD, mario.damasso@unipd.it, ⁵UniPD, luca.malavolta@studenti.unipd.it, ⁶UniPD, luca.borsato.2@unipd.it

Introduction: Photometric transits represent a great opportunity to discover and characterize extra-solar planets. They are, for instance, the only direct method to estimate the planetary radius and to constrain other important physical and orbital parameters. A new powerful technique is emerging in this field, able to detect low-mass companions in systems where at least one planet is transiting. In principle, a single planet orbiting the host star in a Keplerian orbit is expected to transit at strictly periodic time intervals, unless it is perturbed by a third body [1]. By performing accurate measurements of the central instant time of a known transiting planet, it is possible to detect deviations from a linear ephemeris, and to infer the parameters of the perturber [2]. Such a search for other bodies via *transit time variations* (TTV) is very sensitive to low-mass planets when they are locked in low-order orbital resonances. In these orbits, even earth-mass perturbers would cause TTVs of the order of a few minutes, i.e. easily detectable with ground-based techniques.

In the past few years, some authors have claimed TTV detections using ground-based facilities, for instance from WASP-3b [3] and HAT-P-13b [4], though none have been independently confirmed so far. In contrast, the Kepler mission found astonishing mutual TTVs for many systems, including five among six planets transiting on Kepler-11 [5]. These works have led to the validation of those planets, as well as a deep characterization of their systems.

The TASTE project. Our group started in 2010 the TASTE project, previously known as The Asiago Search for Transit Timing Variations of Exoplanets [6]. Our goal is to perform an accurate photometric follow-up of a small sample of transiting exoplanets, purposely chosen as suitable targets for a TTV search. We developed an independent pipeline for the data reduction (STARSKY, [6]). STARSKY is optimized to carry out high-precision differential photometry over defocused images. It implements empirical, iterative algorithms to weight a set of reference stars, aiming at minimizing the final photometric scatter. Additional routines analyze the light curve itself to identify, model, and decorrelate any residual systematic error. A transit model is then fitted to the light curve by a modified version of JKTEBOP [7]. The uncertainties over each fitted parameter (including the central instant T_0) are estimated in the most conservative way,

using both resampling and bootstrapping techniques such as the “residual-permutation” algorithm.

TASTE observations started at the Asiago 1.82m telescope in 2010, and are currently ongoing or scheduled at other medium-class facilities around the world: IAC-80, TCS (Observatorio del Teide, Canary Islands), NOT, TNG (ORM, Canary Islands), CTIO-0.9m (Cerro Tololo), REM (La Silla), and others.

First results. On most targets, TASTE is able to achieve a photometric scatter of the order of 0.5 mmag (120s bins) or better. The first light curves, published as test case (HAT-P-3b and HAT-P-14b, [6]) demonstrate a timing accuracy spanning $\Delta T_0=10$ -25 s on typical targets. Recently we published a TTV study that shed some light on the controversial case of HAT-P-13b [7]. New results from the IAC facilities are going to be published.

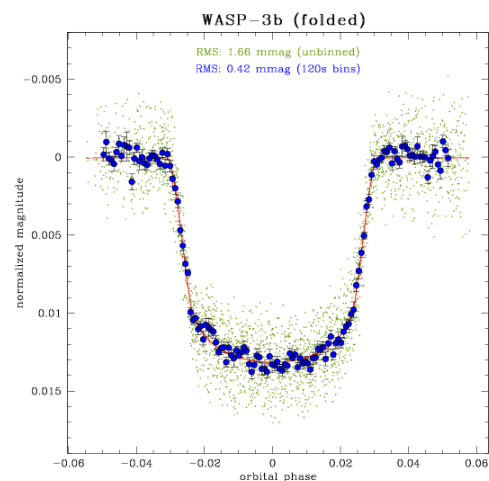


Fig. 1: Folded light curve of two TASTE transits of WASP-3b observed at IAC-80 in 2011.

References: [1] Holman & Murray (2005), *Science*, 307, 1288 [2] Agol et al. (2005), *MNRAS*, 359, 567 [3] Maciejewski et al. (2010), *MNRAS*, 411, 1204 [4] Pal et al. (2011), *MNRAS* 413, L43 [5] Lissauer et al. (2010) *Nature*, 470, 53 [6] Nascimbeni et al. (2011a), *A&A*, 527, A85 [7] Southworth et al. (2004), *MNRAS*, 351, 1277 [8] Nascimbeni et al. (2011b), *A&A* 532, A24.

P0401. POSTER SESSION I

SPIN-ORBIT ALIGNMENT OF TRANSITING PLANETARY SYSTEMS FROM RM EFFECT OBSERVATIONS USING CYCLOPS.

Brett Addison¹, Duncan Wright¹, and Chris Tinney¹, ¹Department of Astrophysics and Optics, University of New South Wales, NSW 2052, Australia. b.addison@student.unsw.edu.au

Introduction: Over 500 extrasolar planets have been discovered over the last decade and a half with many more to be discovered in the next couple of years. In addition to discovering new extrasolar planets, a detailed analysis of their structure, composition, and other bulk properties is also needed in order to gain an understanding of the processes involved in the formation of planets in other systems as well as in our own solar system.

The Exoplanetary Science group at UNSW is commissioning a Cassegrain-fed optical-fiber bundle called CYCLOPS at the Anglo-Australian Telescope (AAT) to carry out Doppler spectroscopy of transiting planet candidate stars arising from Southern Hemisphere transit searches. In addition, our team will carry out measurements of the Rossiter-McLaughlin (RM) effect in transiting exoplanets. The RM effect is a spectroscopic anomaly in the radial velocity curve that arises when a planet occults a small spot on the rotating disk of its host star. This in turn causes asymmetric distortions in the line profiles of a star's spectrum creating the apparent anomaly seen in the radial velocity curve (1). The detection of this effect allows us to estimate the spin-orbit alignment of transiting planetary system which is a critical component in order to study the processes involved in planetary formation and migration.

CYCLOPS: CYCLOPS is an upgrade for the AAT's existing UCLES coude-echelle spectrograph. It replaces the five mirror Coude train, with a Cassegrain-fed optical-fiber bundle, which reformats an area of 4.7 square arcseconds on the sky (formatted as fifteen 0.6" diameter hexagons) into a pseudo-slit of 15 fibers at the entrance of UCLES. Each fibre at the entrance slit has a diameter of 0.61", which delivers a resolution of $\lambda/\Delta\lambda = 70,000$. Commissioning tests demonstrate CYCLOPS delivers 70% more photons to our spectrograph than the old mirror train, and does so at 50% higher resolution (2).

Spin-orbit Alignment of Transiting Exoplanets and the Rossiter-McLaughlin Effect: Observing the RM effect provides an estimate of the alignment of the projected stellar spin axis to the orbital plane of the planet known as "spin-orbit" alignment, measured by the angle (λ). This information is critical in order to place constraints and test different theories on planetary formation and migration (1). Using both CYCLOPS and UCLES, our team will follow up a number of transiting planet candidate stars arising from

the HAT-South transit search with high precision radial velocity both during and out of the transit phase. Our team has also developed a chi squared minimization analysis model called ExOSAM (Exoplanetary Orbital and Simulation Analysis Model) to estimate $v\sin i$ and λ by comparing the observed RM effect data to our theoretical model. We have tested ExOSAM with actual data obtained for Wasp-18 (3). We find that $\lambda = 4^\circ$ and $v\sin i = 11.6$ km/s for this system. Figure 1 shows the RM anomaly in the radial velocity modeled using ExOSAM with Wasp-18 data during transit.

Conclusion: The Exoplanetary Science group at UNSW has commissioned a Cassegrain-fed optical-fibre bundle spectrograph called Cyclops at the AAT to carry out Doppler spectroscopy and measurements of the RM effect of transiting planet candidate stars arising from the HAT South transit survey. This research will allow us to estimate the orbital parameters and mass of transiting exoplanets, critical components needed to study their structure and formation processes as well as their migration history.

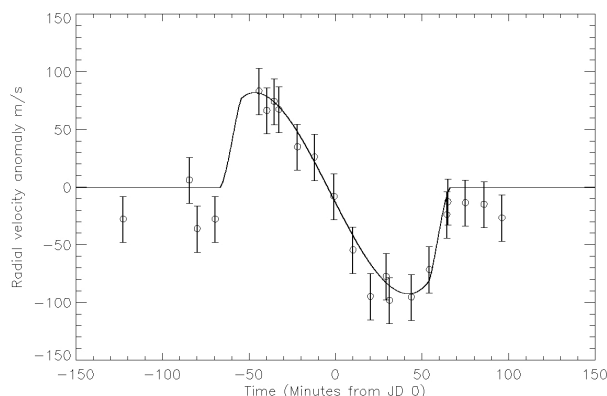


Figure 1 RM anomaly in the radial velocity modeled by ExOSAM with data obtained during the transit of WASP-18 b (Triaud et al. 2010). The underlying Keplerian trend of the star's orbit due to the planet has been removed for clarity.

References: [1] Ohta, Taruya & Suto (2004) *Nat.*, 90, 1151–1154.
 [2] <http://www.phys.unsw.edu.au/~cgt/CYCLOPS/CYCLOPS.html>. [3] Triaud et al. (2010) *A&A*, 524, A25.

ORBITAL MIGRATION MODELS OF EARTHS AND SUPER-EARTHS. G. D'Angelo^{1,2} and U. Gorti^{2,1}, ¹NASA-ARC, MS245-3, Moffett Field, CA 94035 (gennaro.dangelo@nasa.gov), ²SETI Institute, 189 Bernardo Ave., Mountain View, CA 94043 (uma.gorti-1@nasa.gov).

Introduction: Transit data from the Kepler mission indicate that over 10% of solar-type stars may host planets with radii between 2 and 4 R_{\oplus} and orbital periods shorter than 50 days [1]. Radial velocity data show that nearly 20% of solar-type stars may harbor planets with masses smaller than 10 M_{\oplus} and periods less than 50 days [2].

The assembly of a planet of a few Earth masses at 0.25 AU from a solar-mass star requires high surface densities of solid material, on the order of 2000 g/cm^2 or higher. Additionally, a large fraction of it should be icy material. In fact, recent studies, e.g., [1,3], imply that Super-Earths may have a wide range of possible compositions, including ice/water-dominated planets. It appears therefore improbable that all these planets formed at their current locations. More likely, most of them formed at larger orbital distances and afterward moved closer to the star. One mechanism that may explain this long-range mobility is orbital migration driven by tidal torques exerted by a gaseous protoplanetary disk. We present detailed models of such mechanism.

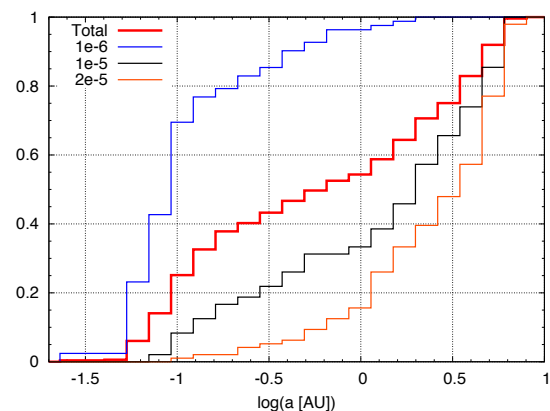
Model Description: We have constructed time-dependent models that describe the orbital evolution of planets in the Earth-to-Super-Earth mass range. These models self-consistently take into account the viscous evolution of the gaseous disk, the photo-evaporation of the gas that originates from Far-Ultraviolet (FUV), Extreme-Ultraviolet (EUV), and X-ray radiation emitted by a solar-mass star, and the gravitational torques that are exchanged between the planet and the disk.

Viscous model. The disk evolution driven by viscous stresses is obtained from the solution of a 1-D equation that governs conservation of angular momentum and accounts for photo-evaporation and tidal torques [4]. The equation is solved numerically using an implicit scheme, allowing us to include disk regions extending very close to the star.

Photo-evaporation model. The rates at which disk gas evaporates are computed by solving the 1+1-D radial-vertical structure of the disk [5]. These rates depend on both radial distance and time, and their calculation is embedded in the disk evolution calculation outlined above.

Tidal torque model. Gravitational perturbations produced by the planet give rise to a torque density distribution that acts on the disk. In response, the disk exerts the same torques on the planet. We use torque density fields derived from 3-D hydrodynamics, high-resolution calculations of disk-planet interactions [6].

Physical Parameters: We have performed simulations of radially extended disks, from 0.02 AU to 1000 AU, surrounding a solar-mass star. The initial surface density follows that derived from [7] for an early Solar Nebula. The X-rays and EUV luminosities are $\sim 10^{-3} L_{\odot}$, whereas FUV luminosities depend on the time-varying accretion rate of the star, but lies in the range from $\sim 10^{-4}$ to $\sim 0.1 L_{\odot}$. We have investigated different viscosity regimes, with characteristic kinematic viscosity $\nu = \nu_1 (R/\text{AU})^{1/2}$, where viscosity ν_1 is between 10^{-6} and 2×10^{-5} in units of $(G M_{\odot} \text{AU})^{1/2}$. The planet mass grows from 0.1 M_{\oplus} to M_{iso} , the isolation mass, over the time T_{iso} . The growth proceeds at an oligarchic rate, $dM/dt \propto M^{2/3}$. The values of M_{iso} and T_{iso} are chosen randomly within the ranges, respectively, from 1 to 10 M_{\oplus} and from 10^4 to 10^5 local orbital periods. The initial orbital radius varies randomly between 1 and 10 AU.



Results: We find that the final orbital distributions are dependent on the applied viscosity regime. When $\nu_1 \sim 10^{-6}$, about 90% of the planets orbit within ~ 0.5 AU, whereas, for $\nu_1 \sim 10^{-5}$, only $\sim 30\%$ have orbital radii smaller than 1 AU. About 50% of the planets settle on orbits beyond ~ 3 AU when $\nu_1 \sim 2 \times 10^{-5}$. The total distribution shows that $\sim 6\%$ of the planets orbit within 0.07 AU and $\sim 50\%$ within 1 AU. No region appears devoid of planets. Cumulative distributions for the total population and for selected values of ν_1 are shown above.

References: [1] Howard A. W. *et al.* (2011) *arXiv:1103.2541*. [2] Wittenmyer R. A. *et al.* (2011) *ApJ*, 738, 81-86. [3] Pont F. *et al.* (2011) *MNRAS*, 411, 1953-1962. [4] D'Angelo G. *et al.* (2010) in *EXOPLANETS*, S. Seager ed., 319-346. [5] Gorti U. *et al.* (2009) *ApJ*, 705, 1237-1251. [6] D'Angelo G. and Lubow S. H. (2010) *ApJ*, 724, 730-747. [7] Davis S. S. (2005) *ApJ*, 627, L153-L155.

P0403. POSTER SESSION I

THERMAL EVOLUTION AND MASS LOSS OF WATER-RICH SUPER-EARTHS. K. Kurosaki¹, M. Ikoma¹, Y. Hori² and S. Ida¹ ¹Department of Earth and Planetary Sciences, Tokyo Institute of Technology, Ookayama, Meguro-ku, Tokyo 152-8551, Japan; kurosaki@geo.titech.ac.jp (K. K.), mikoma@geo.titech.ac.jp (M. I.), ida@geo.titech.ac.jp (S. I.). ²Division of Theoretical Astronomy, National Astronomical Observatory of Japan, Osawa, Mitaka, Tokyo, 181-8588, Japan; yasunori.hori@geo.titech.ac.jp .

Introduction: Recent progresses in transit photometry—especially, operation of the two space-based telescope *Kepler* and *CoRoT*—have enabled us to find relatively small short-period exoplanets with radii of a few to several Earth radii. Combined with planetary masses measured by radial-velocity or transit-timing-variation methods, many of the planets and planetary candidates are inferred to be water-rich objects like Uranus and Neptune. Such objects are often called hot Neptunes. The radii of hot Neptunes are relatively sensitive to their thermal and gravitational energy. Thus, understanding the distribution of hot Neptunes in the mass-radius (or bulk density) diagram gives us great insights into the formation and evolution of the planets which include the histories of accretion, impact/erosion, and loss of energy and mass.

Similarly to gas giants, water-dominated planets are born big in size. Then they shrink or become denser losing their accretion energy into space. Furthermore, since transiting planets orbit close to their host stars, they experience mass loss driven by intense stellar X-ray and UV irradiation (XUV). Thus, interesting questions are how large is the maximum radius (or the minimum bulk density) of a hot Neptune of a given mass that we observe and how large is the minimum mass of a hot Neptune that survives the mass loss.

Previously, the thermal evolution and mass loss of hot-Jupiters were investigated [1,2]. The mass and radius relationships of water-rich planets were calculated for relatively wide ranges of intrinsic and equilibrium temperatures by Rogers et al. (2011) and Valencia et al. (2010); they also estimated the possible amounts of mass loss [3,4]. However, to our knowledge, there is no study that simulates the thermal evolution and mass loss of water-rich planets concurrently.

Methods: In this study, we have simulated the spherically symmetric structure and thermal evolution of planets that are composed mainly of water. The mass loss is assumed to be due to stellar XUV irradiation; the mass loss rate is calculated, based on theory of the energy limited hydrodynamic escape through the Roche lobe of the planet. The structure of the atmosphere is integrated, following Guillot (2010) [5].

Results: The planet gets cold and shrinks by emitting its intrinsic heat. Inside the planet, the boundary between the radiative and convective layers becomes deeper and deeper. This controls the thermal evolution.

On a timescale of 1-10 Gyr, the intrinsic temperature decreases to a few ten Kelvin. At that time, the radii are several to ten Earth radii for 1-10 Earth-mass water-dominated planets, provided the mass loss is ignored. However, if the mass loss is included, the low-mass and large-radius planets evaporate completely. Since the stellar XUV declines and the planetary radius becomes small with time, we have found there are distinct threshold masses beyond which the planet survives the evaporation due to XUV irradiation from the host star. While the threshold mass depends on several properties of the planet and the star, it is found to be around 10 Earth masses.

Conclusions: We have found that the thermal evolution of water-rich planets has a significant impact on their radius and mass loss rate. Besides, there is the lower limit to the mass of the planet that survives the mass loss due to XUV irradiation from the host stars for 10 billion years. These results give constraints to the distribution of water-rich super-Earths on the mass-radius (or bulk density) diagram.

References: [1] Baraffe, I. et al. (2003) *A&A*, 402, 701-712. [2] Yelle, R. (2004) *Icarus*, 170, 167-179. [3] Rogers, L. et al. (2011) *ApJ*, 738, 59. [4] Valencia, D. et al. (2010) *A&A*, 516, A20. [5] Guillot, T. (2010) *A&A*, 520, A27.

P0404. POSTER SESSION I

THE HABITABLE EXOPLANETS CATALOG: AN EXTENSIVE QUANTITATIVE ASSESSMENT OF THE HABITABILITY OF EXOPLANETS. A. Méndez, Planetary Habitability Laboratory, University of Puerto Rico at Arecibo, Arecibo, PR 00613 (abel.mendez@upr.edu).

Introduction: There are many catalogs compiling and describing the nearly 700 exoplanets that have been confirmed such as the *Extrasolar Planets Encyclopaedia* (exoplanet.eu), the *Exoplanet Data Explorer* (exoplanets.org), and The *Visual Exoplanet Catalogue* (exoplanet.hanno-rein.de). New ground and orbital observations with telescopes, like Kepler, is helping to identify and confirm hundreds or thousands of additional exoplanets in the coming years. Catalogs are getting quite large and is becoming more difficult to sort out those habitable exoplanets that are of special interest for the astrobiology field.

The Habitable Exoplanets Catalog (HEC) is a new project by the Planetary Habitability Laboratory (PHL) of the University of Puerto Rico at Arecibo to help identify, compare, and visualize habitable exoplanets from current discoveries [1]. The HEC is using new developments by the PHL on habitability metrics and classifications like the Earth Similarity Index (ESI) [2], the Habitable Zones Distance (HZD), and comparisons with Earth past and present to help quantify the habitability of exoplanets, including potential exomoons.

Habitability Metrics: Habitability metrics can be used to assess and compare the potential for life of exoplanets as a function of many stellar and planetary properties. They provide a system for their identification, ranking, prioritization of observations, and even recognize those probably even more habitable than Earth itself. Most of these metrics requires stellar and planetary properties that are already available for many exoplanets but models can be used otherwise. Four habitability metrics were used as first assessments.

Habitable Zones Distance (HZD). The HZD is a measure of how far a planet is from the center of its parent star habitable zone (HZ) in habitable zone units (HZU). Planets inside the HZ have HZD values between -1 to +1 HZU, with zero being the exact center of the HZ. The negative and positive values correspond to locations closer and farther to the star, respectively. The HZD is a function of the star's luminosity and temperature, and the planet's distance.

Earth Similarity Index (ESI). The ESI or the "easy scale," measures how similar is a planet to Earth in a scale from zero to one, with one being identical [2]. Planets with ESI values between 0.8 and 1.0 are classified as Earth-like because they potentially have a rocky composition that is able to hold a terrestrial atmosphere under temperate conditions. The ESI is a function of the planet's radius, density, escape velocity, and surface temperature.

Global Primary Habitability (GPH). The GPH or "gp-hab," measures the surface suitability of a planetary body for a global biosphere of primary producers in a scale from zero to one, with one being more habitable. The GPH is a function of the star's luminosity, temperature, age, and metallicity, and the planet's albedo, distance, mass and radius. It provides the most complete evaluation of planetary habitability given the information we already know for many exoplanets.

Standard Primary Habitability (SPH). The SPH or 'sp-hab,' measures the thermal-water climate suitability of a planet for land primary producers in a scale from zero to one, with one being more habitable [3]. It is correlated with the distribution of vegetation and net primary productivity (NPP). The SPH is a function of the planet's surface temperature and relative humidity. The SPH was originally developed for terrestrial ecology assessments but it was also extended for exoplanets studies.

Conclusion: The HEC identifies, organizes, and visualizes potential habitable exoplanets, including exomoons, in new ways. All metrics focus on surface habitability and does not consider yet subsurface environments. They are limited to what we can measure today for exoplanets and assume that all the other requirements of life are present. The GPH and the SPH metrics are better indicators of habitability than the HZD and the ESI, but require more information about the exoplanets. So far, there are two potential habitable exoplanets identified and ranked in the catalog and fourteen from Kepler candidates, but more are expected in the near future.

The HEC provides tools for both scientists and educators studying the habitability of exoplanets. We also developed various media and web tools to help understand and visualize the number, diversity, and characteristics of exoplanets. The HEC is an initiative of the PHL at the UPR Arecibo with the collaboration of various international scientists and educators, and it will be freely available on the PHL web site (phl.upr.edu) on December 5, 2011. We expect that input from scientists, educators, and the general public will help improve the catalog, and probably take it in new directions.

References: [1] Méndez A. *et al.* (2011) The Habitable Exoplanets Catalog (in preparation). [2] Schulze-Makuch D. *et al.* (2011) *Astrobiology* (in press). [3] Méndez A. (2010) *AbSciCon 2010*, 5483–5484.

P0405. POSTER SESSION I

PLANET MIGRATION TOWARDS DESTRUCTION: DISTRIBUTION EVOLUTION AND ROCHE LOBE OVERFLOW. S. F. Taylor¹, ¹National Tsing Hua University Institute of Astronomy, No. 101, Section 2, Kuang-Fu Road, Hsinchu, Taiwan 30013, astrostuart@gmail.com .

Introduction: We explore the tidal migration of the hot Jupiter distribution found from Kepler data to show that the three day pile up is consistent with a higher rate of in-migration for the most massive planets (Figure 1). The manner in which the distribution of the most massive planets turns over closer to the star may be due to a population of eccentric planets being rapidly migrated towards the star by processes such as planet scattering and Kozai migration.

We show that planets undergoing Roche lobe overflow may a very long time (Figure 2). Such events may last longer than the 50,000 years which Spezzi et al. [1] (hereafter S11) suggest explains objects they found that appear as overluminous bright brown dwarf-like objects. S11 found nine objects with temperatures more typical of brown dwarfs (BDs) in the massive galactic cluster NGC 3603 but with luminosities much too high. They conclude that planets filling their Roche lobe provide the best explanation for these objects. We also show that planets more massive than Jupiter may observably increase the luminosity of the star, but Jupiter-mass planet might not. We show that a broad range of planet masses will migrate outwards during their overflow mass loss, but once a more dense core starts to overflow, the planet will migrate back in.

Three-day pileup as “pause” in migration: We consider the hypothesis that the three day pileup of “giant planets” may be a region where inward migration due to planetary tides slows but before migration due to stellar tides is strong (where giant planets are considered to be at or above one Jupiter mass, or in Kepler data, 8 earth radii). In Figure 1, we show that such a scenario would allow for a little higher value of tidal friction, represented by a little lower value of the stellar tidal quality factor Q'_s . A Q'_s value of $10^{7.5}$ can be seen to have maintained a reasonable distribution, while a Q'_s value of $10^{6.5}$ can be seen to have unreasonably changed the distribution. A Q'_s value such as shown here for $Q'_s = 10^{7.0}$ need not be excluded even if it requires a pileup, since a pileup does exist. To comprehensively determine what value of tidal friction is indicated by the Kepler distribution will require that the distribution be characterized with a pileup (next section).

Characterization of three-day pileup: The Kepler distribution modeled by [2] did not seek to parameterize the pileup. It is clear from Figures 4 and 7 of [2] that the modified power law found there has not been designed to fit for the pileup. We are preparing a fit to include a pileup, with the goal of finding what value of the tidal friction may explain the location of the cutoff. A comparison with the much

stronger three day pileup seen in radial velocity and previous transit measurements.

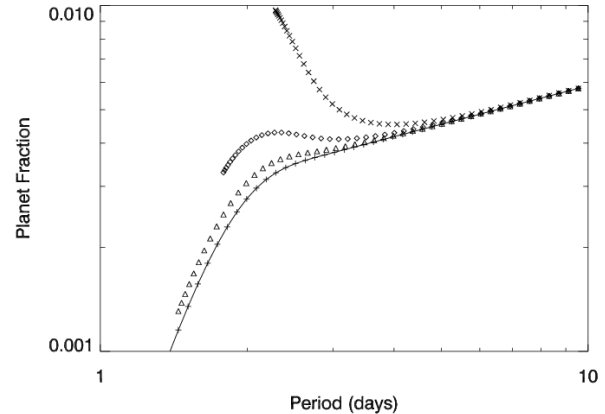


Figure 1. The distribution of giant planets ($\geq 8 R_{\text{Earth}}$) from Kepler, with what distribution this would imply 4.5×10^9 years ago for three different values of the stellar tidal friction Q'_s . The Kepler distribution from [2] is given by the “+” symbols connected by the line, below the other curves. The crosses represent the most tidal friction, or $Q'_s = 10^{7.5}$, the triangles $Q'_s = 10^{7.0}$, and the diamonds the least tidal friction, $Q'_s = 10^{6.5}$.

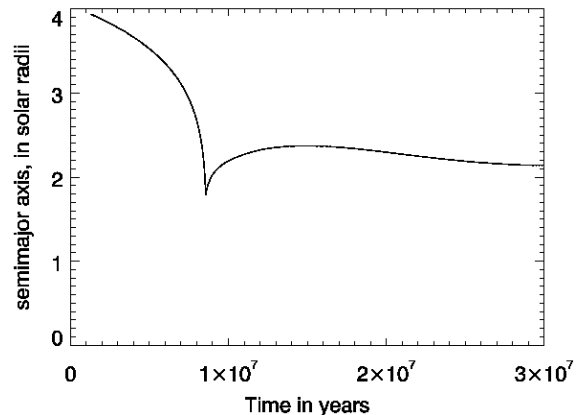


Figure 2. The migration of a $2 M_{\text{Jupiter}}$ planet hosted by a $1 M_{\text{Sun}}$ star from 4 solar radii to the point of Roche lobe overflow and subsequent outward migration, for $Q'_s = 10^{6.0}$.

Rates of planet accretion: We will also address how common systems with Roche lobe accretion or collision planet accretion may be.

References: [1] Spezzi, L. et al., (2011) *ApJ*, 771, id 1. [2] Howard et al., 2011, eprint arXiv:astro-ph:1103.2541.

P0406. POSTER SESSION I**Protoplanetary Disk Resonances and Type I Migration.** D. Tsang¹,

¹Theoretical Astrophysics, California Institute of Technology, 1200 E. California Blvd MC 350-17, Pasadena CA, 91105. dtsang@caltech.edu

Waves reflected by the inner edge of a protoplanetary disk are shown to significantly modify Type I migration, even allowing the trapping of planets near the inner disk edge for small planets in a range of disk parameters. This may inform the distribution planets close to their central stars, as observed recently by the Kepler mission. Implications of this process for multi-planet systems will also be discussed.

P0501. POSTER SESSION I

Kepler-15b: A Hot Jupiter Enriched In Heavy Elements And The First *Kepler* Mission Planet Confirmed With The Hobby-Eberly Telescope

M. Endl¹, P. J. MacQueen¹, W. D. Cochran¹, E. J. Brugamyer², L. A. Buchhave³, J. Rowe⁴, P. Lucas⁵, H. Isaacson⁶, S. Bryson⁷, S. B. Howell⁷, J. J. Fortney⁸, T. Hansen³, W. J. Borucki⁷, D. Caldwell⁷, J. L. Christiansen⁹, D. R. Ciardi¹⁰, B.-O. Demory¹¹, M. Everett¹², E. B. Ford¹³, M. R. Haas⁷, M. J. Holman¹⁴, E. Horch¹⁵, J. M. Jenkins⁹, D. J. Koch⁷, J. J. Lissauer⁷, P. Machalek⁴, M. Still⁷, W. F. Welsh¹⁶, D. T. Sanderfer⁹, S. E. Seader⁹, J. C. Smith⁹, S. E. Thompson⁹, J. D. Twicken⁹

¹McDonald Observatory, University of Texas at Austin, Austin, TX 78712, mike@astro.as.utexas.edu, pjm@astro.as.utexas.edu, wdc@astro.as.utexas.edu, ²Department of Astronomy, University of Texas at Austin, ³Niels Bohr Institute, University of Copenhagen, ⁴SETI Institute, ⁵Centre for Astrophysics Research, University of Hertfordshire, ⁶Department of Astronomy, University of California, Berkeley, ⁷NASA-Ames Research Center, ⁸Department of Astronomy and Astrophysics, University of California, Santa Cruz, ⁹SETI Institute/NASA Ames Research Center, ¹⁰NASA Exoplanet Science Institute/Caltech, ¹¹Department of Earth, Atmospheric and Planetary Sciences, Massachusetts Institute of Technology, ¹²NOAO, Tucson, ¹³Astronomy Department, University of Florida, ¹⁴Harvard-Smithsonian Center for Astrophysics, ¹⁵Southern Connecticut State University, ¹⁶Astronomy Department, San Diego State University

Abstract:

We report the discovery of Kepler-15b (KOI-128), a new transiting exoplanet detected by NASA's *Kepler* mission. The transit signal with a period of 4.94 days was detected in the quarter 1 (Q1) *Kepler* photometry. For the first time, we have used the High-Resolution-Spectrograph (HRS) at the Hobby-Eberly Telescope (HET) to determine the mass of a *Kepler* planet via precise radial velocity (RV) measurements. The 24 HET/HRS radial velocities (RV) and 6 additional measurements from the FIES spectrograph at the Nordic Optical Telescope (NOT) reveal a Doppler signal with the same period and phase as the transit ephemeris. We used one HET/HRS spectrum of Kepler-15 taken without the iodine cell to determine accurate stellar parameters. The host star is a metal-rich ($[Fe/H]=0.36\pm 0.07$) G-type main sequence star with $T_{\text{eff}}=5515\pm 124$ K. The semi-amplitude K of the RV-orbit is $78.7^{+8.5}_{-9.5}$ m s⁻¹ which yields a mass of the planet of $0.66\pm 0.1 M_{\text{Jup}}$. The planet has a radius of $0.96\pm 0.06 R_{\text{Jup}}$ and a mean bulk density of 0.9 ± 0.2 g cm⁻³. The radius of Kepler-15b is smaller than the majority of transiting planets with similar mass and irradiation level. This suggests that the planet is more enriched in heavy elements than most other transiting giant planets. For Kepler-15b we estimate a heavy element mass of 30-40 M_{Earth} .

THE CONNECTION BETWEEN SOLAR- AND EXTRASOLAR- GIANT PLANETS

R. Helled¹, ¹Departement of Geophysics and Planetary Sciences, Tel-Aviv University, Tel-Aviv 69978, Israel (r.helled@gmail.com).

Introduction: The fields of Extrasolar Planets and Planetary Sciences are flourishing. In order to improve our understanding of planet formation and evolution we must study solar and extrasolar planets *simultaneously*. While the number of discovered extrasolar planets is large, their physical properties are not well constrained. On the other hand, we have only a few planets in the solar system but we know much more about them. Often, extrasolar planets are studied by “astro-physicists” while solar-system planets are studied by “planetary scientists”, however, as discussed below, by studying solar and extrasolar planet together a more complete understanding of planetary formation, evolution, and internal structure can be achieved. It is also important to understand the limitations of the available observations. Below we summarize some of the available constraints and measurements for solar and extrasolar giant planets, present the questions that should be asked, and discuss how measurements can be used to improve our understanding of gas giant planets.

Physical Constraints and Observed Properties:

Formation Timescale: In order to discriminate between giant planet formation mechanisms we must know how long it takes for gas giant planets to form. Constraints on the formation timescale are available from observations of protoplanetary disks suggesting that gas is present up to ~ 10 million years. While on one hand giant planets must form fast enough to accrete sufficient amounts of hydrogen and helium, one explanation for the existence of noble gases in Jupiter’s atmosphere is by relatively late formation [1]. *How long does it take for gas giant planets to form?*

Core Mass and Heavy Element Enrichment: Measurements of the gravitational fields of Jupiter and Saturn indicate that the planets consists of a few tens Earth masses of heavy elements and possibly have cores (e.g., [2]). Transiting planets also seem to consist of tens of Earth masses, or more, of heavy elements [3]. While the internal structures of the solar system giant planets can be modeled in detail, for extrasolar planets only constraints on the mean density are available (although in some cases more constraints on the density profile can be derived [4]). Planetary enrichment / internal structure, however, cannot be used to discriminate between formation mechanisms (e.g., [5]). A complication arises from the fact that the current internal structures of the planets can be different from the ones shortly after formation. Different physical processes such as core erosion, grain settling, etc., can change the internal structure over time. *Do all giant*

planets have cores? What are the core masses and enrichments of giant planets, and how large is this range?

Orbital Location: Extrasolar giant planets have been observed in orbits very close to their host stars. Even if this observed feature is caused by a selection effect, the fact that giant planets can reach such small radial distances (or possibly form there) introduces important dynamical constraints. On the other hand, Jupiter and Saturn orbit the Sun at ~ 5.2 and 9.5 AU, respectively, significantly farther. *What determines the final orbital location of giant planets? Do most giant planets have small or large radial distances? Where in the disk can giant planets form?*

Atmospheric Properties: The composition of planetary atmospheres is crucial for our understanding of planetary formation, internal dynamics, and chemical processes. Constraints on the composition and dynamics of the solar-system giant planet are available from different measurements although many open questions remain. Recently, spectroscopy observations of extrasolar planet atmospheres became available and provided constraints on the chemical composition and thermal structure of the observed atmospheres. While Jupiter represents a “cold giant planet” measurements of extrasolar atmospheres are so far limited to “hot Jupiters” which are typically tidally locked to the star, and are strongly irradiated. In addition, measurements of exoplanets’ atmospheres represent only a limited region of the planetary atmosphere. *How can we use the available measurements to better understand planetary atmospheres? What are the data limitations? What is the atmospheric composition of gas giant planets? and how much can it vary? Are giant planets adiabatic? What are the dynamical/chemical processes in the atmosphere?*

Summary: The discovery of planets outside our solar system opens an opportunity to learn about giant planets as a class, and to improve our understanding of the planets in our own solar system. It is important to combine the available physical constraints of extrasolar and solar gas giant planets in order to achieve a more complete picture of the nature of these planets.

References: [1] Guillot, T. and Hueso, R., (2006), *MNRAS*, 367, L47. [2] Saumon, D. and Guillot, T. (2004) *Nat.*, 90, 1151–1154. [3] Miller, N. and Fortney, J. J. (2011) *ApJ*, 32, A74. [4] Ragozzine, D. and Wolf, A. S. (2009) *ApJ*, 698, 1778. [5] Boley, A., Helled, R., and Payne, M. (2011), *ApJ*, 735, 30.

P0503. POSTER SESSION I

NEAR-INFRARED SPECTROSCOPIC VIEW OF GJ1214B.

V.D. Ivanov¹, P. Kabath¹, P. Rojo², C. Caceres³, J. Girard¹, J. Fortney⁴, and E. Miller-Ricci⁴

¹European Southern Observatory, Alonso de Cordova 3107, Vitacura, Santiago 19001, Chile (vivanov, pkabath, jgirard@eso.org); ²Departamento de Astronomia, Universidad de Chile, Santiago, Chile (pato@das.uchile.cl); ³Department of Astronomy and Astrophysics P. Universidad Católica de Chile, Av. Vicuña Mackenna 4860, 7820436 Macul, Santiago, Chile (cccacere@astro.puc.cl); ⁴Department of Astronomy and Astrophysics, University of California, Santa Cruz, CA 95064, USA (jfortney, elizamr@ucolick.org)

Introduction: Th handful of transiting super-Earths known today typically have few Earth masses, and they are very interesting for the further studies because of their potential similarities with our life-bearing planet, Earth. Knowing the composition of their atmospheres is a most critical piece of information.

GJ1214b has an advantage over the rest because it orbits a late-type star, which boosts the planet-to-star ratio, and makes this planet more accessible than the others, orbiting Solar analogs.

Current theoretical models predict that GJ1214b is either water world with thin atmosphere or it has an extensive H/He atmosphere.

Observations: We present 1.5-2.5 micron transmission spectra of the super-Earth GJ1214b, obtained during three different transits with the SofI spectrograph [1] at the ESO NTT on La Silla. An additional parallel Ks-band light curve was obtained with the INT during one of the transits.

Results: Our data agree with the conclusion of [3] that the GJ1214b atmosphere must have a cloud layer.

References: [1] Moorwood, A., Cuby, J.G., Lidman, C. 1998, *The Messenger* 91, 9. [2] Miller-Ricci, E., et al. 2010, *ApJ*, 716, 74. [3] Bean, J. et al., 2011, *ApJ*, submitted (astro-ph/1109.0582).

P0504. POSTER SESSION I

Constraints on Exoplanet Transit Observations Using JWST NIRSpec. D. R. Long, Space Telescope Science Institute (3700 San Martin Drive, Baltimore, MD 21218. drl@stsci.edu)

Introduction: Characterization of exoplanet atmospheres is a high-profile goal of the James Webb Space Telescope [1]. In this poster I describe likely observing strategies using JWST NIRSpec as part of ongoing work so observers may get the best results during the mission's limited lifetime. Constraints imposed by the observatory, instrument, and nature of the targets are discussed. These constraints are examined in light of the Kepler candidates and confirmed planets through Cycle 1 Quarter 3.

References:

- [1] Gardner, J. P. et al. (2006) *Space Sci. Rev.*, 123, 4.

P0505. POSTER SESSION I

The Effect of Exotic Clouds on the Transmission Spectra of Transiting Super-Earths.

C. V. Morley¹, J. J. Fortney², M. S. Marley³, C. Visscher⁴.

¹UC Santa Cruz, 1156 High St, Santa Cruz, CA (cmorley@ucolick.org), ²UC Santa Cruz (jfortney@ucolick.org), NASA Ames Research Center (mark.s.marley@nasa.gov), ⁴Southwest Research Institute, Boulder (visscher@boulder.swri.edu).

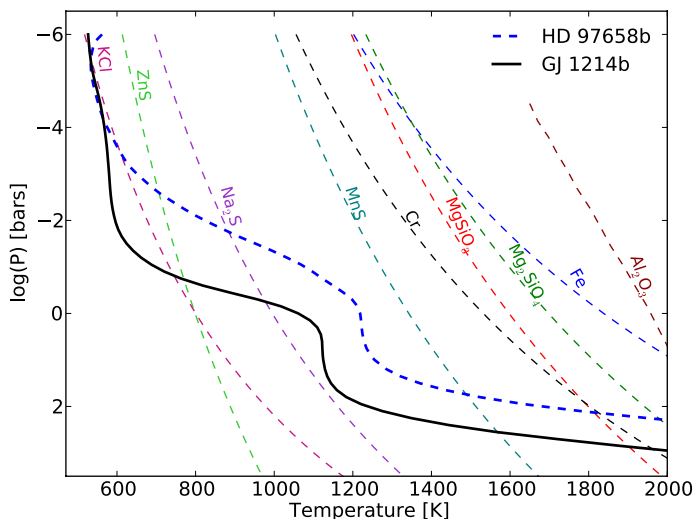
The formation of clouds in exoplanet atmospheres is expected to significantly change the observable spectra. This is widely understood for solar system planets and brown dwarfs. For exoplanets, the gray opacity of hazes or clouds has been invoked as a possible explanation for the observed flat transmission spectrum of transiting super-Earth GJ 1214b [1]. Previous atmosphere models for irradiated planets have included the most important condensates expected to form in brown dwarf and giant planet atmospheres — iron, silicate, and corundum — but have not included the condensates expected to form at colder temperatures.

The most important of these new clouds are sodium sulfide, potassium chloride, and zinc sulfide. These clouds should be most prominent at low surface gravity, strongly super-solar atmospheric abundances, and at the slant viewing geometry appropriate for transits. Hence they could be quite important for affecting the transmission spectra of cool low density super-Earth and Neptune-class planets.

Here, we present results from a series of 1D atmospheric models that include these previously ignored condensates for the transiting super-Earths GJ 1214b and HD 97658b [2]. We vary both the metallicity of the atmosphere and the thickness of the cloud layer, and we determine whether these exotic clouds could be sufficiently optically thick to reproduce observations of GJ 1214b.

[1] Bean et al. (2011) submitted to *ApJ*.

[2] Henry et al. (2011) submitted to *ApJ*.



Pressure-Temperature Profiles with Condensation Curves:

Pressure-Temperature profiles of transiting Super-Earths GJ 1214b and HD 97658b are plotted with the condensation curves of all clouds expected to form. Cloud bases are located at the intersection between profiles and condensation curves. Note that the pressure temperature profiles cross the sodium sulfide, zinc sulfide, and potassium chloride condensation curves; these clouds will form in the upper atmosphere of both planets.

REFRACTION OF LIGHT IN EXOPLANET ATMOSPHERES.

Taishi Nakamoto¹ and Tetsuo Yamamoto², ¹Tokyo Institute of Technology (Meguro, Tokyo 152-8551, Japan, nakamoto@geo.titech.ac.jp), ²Hokkaido University (ty@lowtem.hokudai.ac.jp).

Introduction: Some exoplanet atmospheres have been observed by transit photometry and spectroscopy. Their composition, temperature, and stratified structure have been investigated based on those observations [e.g., 1 and references therein]. In the analyses, paths of light that is emitted from the central star and passes through the atmosphere are assumed to be straight [2]. In general, however, the path of light in the atmosphere would be curved due to the refraction by the atmosphere. In addition, the refraction is generally dependent on the wavelength of light. Thus, the color dependent refraction may affect the observed quantities. If it is the case, we would be able to obtain some information about the exoplanet atmosphere by observing the refraction. The refraction of light by exoplanet atmosphere was studied by [3]. In this study, we derive a higher order analytic formula for the refraction angle, and examine the effect of refraction.

Refraction Angle: We derive an analytic formula for the refraction angle. We assume that the planet including the atmosphere is spherically symmetric, the atmosphere is isothermal, and the atmosphere is in the hydrostatic equilibrium. The refraction angle Θ is then given as,

$$\Theta(b, \omega) \approx \sqrt{\frac{2\pi b}{H}} \Delta(b) \exp\left(-\frac{b-R}{H}\right) \left[1 + \left(\frac{3}{2} - S_0\right) \frac{b\Delta(b)}{H} - \frac{H}{8b}\right],$$

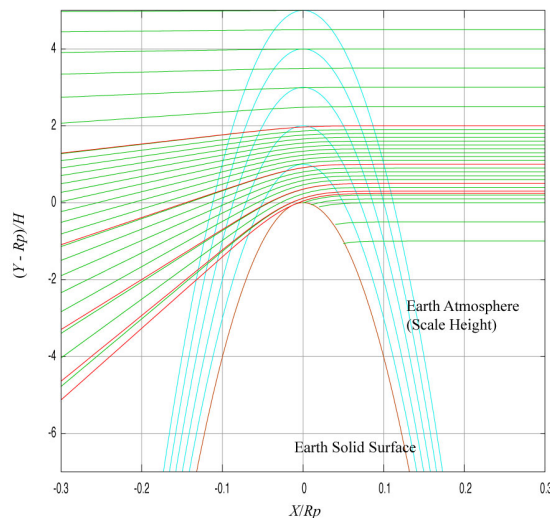


Figure 1: Paths of light passing through the atmosphere. Green and red curves correspond to the light with wavelengths of 500 μm and 800 μm, respectively. Light blue curves show height from the solid surface in unit of the atmospheric scale height.

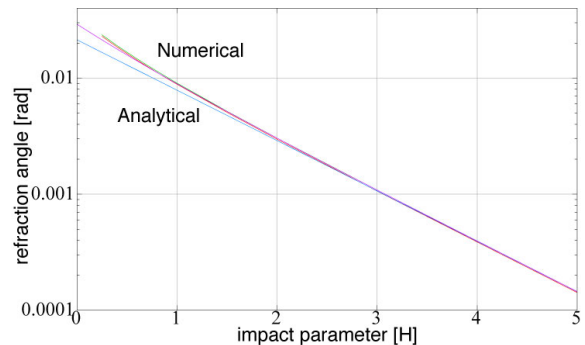
where b is the impact parameter, ω is the frequency of the light, H is the scale height of the atmosphere, R is the radius of the solid part of the planet, $S_0 = 0.0858$ is a constant, and $\Delta(b)$ is given by,

$$\Delta(b) = \frac{n^2(R)-1}{2} \exp\left(-\frac{b-R}{H}\right),$$

where $n(R)$ is the refractive index of the atmospheric gas at the bottom of the atmosphere. This formula is a higher order one than that given by [3].

Figures 1 and 2 show paths of light in the atmosphere and the refraction angle of the light obtained by numerical calculations and the analytic formula. In these calculations, an Earth-like model planet is used: the radius of the solid part of the model planet and the composition of its atmosphere are equal to those of the current Earth, and the temperature is 290K. We can see that the light passing through the planetary atmosphere can be refracted.

Figure 2: Refraction angle as a function of impact parameter.



parameter.

References: [1] Seager S. and Drake D. (2010) *ARA&A*, 48, 631–672. [2] Brown T. M. (2001) *ApJ*, 553, 1006–1026. [3] Sidis O. and Sari R. (2010) *ApJ*, 720, 904–911.

P0507. POSTER SESSION I

On atmospheric temperature inversions and the sizes of exoplanets. V. Parmentier¹, T. Guillot¹, A. P. Showman²

¹Université de Nice-Sophia Antipolis, Observatoire de la Côte d'Azur, CNRS UMR 6202, Nice, France – vivien.parmentier@oca.eu – tristan.guillot@oca.eu, ² Department of Planetary Sciences and Lunar and Planetary Laboratory, The University of Arizona, Tucson, USA - showman@lpl.arizona.edu

Summary : Simulations suggest that TiO can remain in the upper atmosphere of hot-Jupiters provided it condensates in grains smaller than 1 micrometer. The resulting temperature inversion would lead to smaller planets, an hypothesis that can be tested with Kepler.

Introduction: Temperature inversions leading to a hot stratosphere have been inferred in the atmosphere of several hot-Jupiters. The presence of titanium oxide (TiO) in the upper atmosphere of these planets is usually invoked to explain such a hot stratosphere. Thus a distinction between cold planets without either TiO or a temperature inversion (pL planets) and hot planets with both a temperature inversion and TiO (pM planets) have been proposed [1]. Nevertheless, the huge day-side temperature contrast of these planets coupled with a very dynamic atmosphere can lead to a depletion of TiO due to its condensation on the night-side. Here, we study how the dynamics affects the TiO abundance in the upper atmosphere and thus the presence or not of a temperature inversion. We then look at the influence of the temperature inversion on the evolution of the planet and its observational consequences in terms of radius.

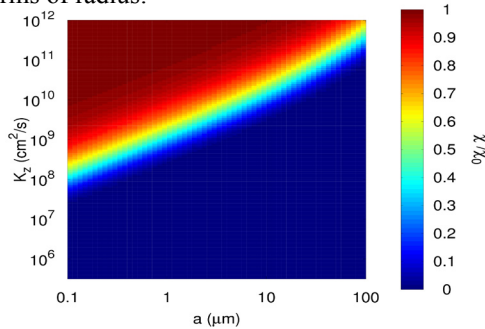


Figure 1 : Abundance of TiO at 1mbar as a function of the particle size and the vertical diffusion coefficient. An abundance of 0.5 is needed to maintain a hot stratosphere.

Day/night cold trap for TiO:

1D model : We derived a 1D analytical model to determine the equilibrium atmospheric TiO abundance from a balance between downward transport due to particle settling and upward transport due to turbulent transport. We obtain constraints on the diffusion coefficient necessary to maintain a high abundance of TiO in the upper atmosphere despite its depletion by the day-night temperature contrast. Our results (see figure 1) are very similar to the ones from Spiegel [2] for the

vertical cold trap but hold for all the planets, including the ones that are too hot for having a vertical cold trap.

3D model : The vertical diffusion coefficient being poorly known in hot-Jupiter atmospheres, we used a 3 dimensional global circulation model of HD209458b [3] to better constrain the TiO abundance. The simulated flows cause strong vertical mixing and suggest that TiO can remain suspended in the atmosphere if particle size are micrometer or less. The simulations moreover suggest the possibility of strong temporal variability in the dayside TiO abundance, which could cause significant time-dependence in the stratospheric temperature and thus in the observed spectrum of the planet.

Influence on the size of exoplanets: We expanded the 1-dimensional plane-parallel model for the atmosphere from [4] to a three-band model, which is accurate enough to model a temperature inversion due to TiO. We included this model into CEPAM, a code to model the internal structure and evolution of gas giant planets [5]. Then we performed evolution models for planets with a wide range of irradiation with and without temperature inversion. Planets with a temperature inversion appear to be smaller by 2 to 10% depending on the irradiation flux (figure 2). This could be tested with the high-precision Kepler measurements.

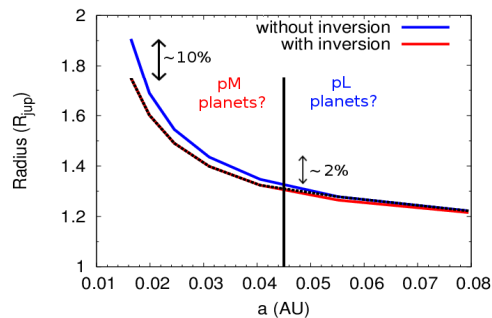


Figure 2 : Final radius of a 0.69M_j planet at different distances from a solar-type star. The vertical line is the hypothetical limit between pM and pL class planets as proposed by [1]. The dashed black line represents the possible radius-distance relationship for the planet under the pM/pL planets hypothesis

References : [1] Fortney J. et al. (2008) *ApJ*, 679,1419. [2] Spiegel, D. S. et al. (2009) *ApJ*, 699, 1487. [3] Showman, A. et al. (2009), *ApJ*, 699, 564 [4] Guillot T. (2010) *A&A*, Vol.150, A27. [5] Guillot, T. & Morel, P. (1995), *A&AS*, 109, 109.

Doppler beaming and Römer delay versus ellipsoidal modulation in the Kepler data of KOI-74.

S. Bloemen¹, T. R. Marsh² *et al.*

¹Instituut voor Sterrenkunde, Katholieke Universiteit Leuven, Celestijnenlaan 200D, B-3001 Leuven, Belgium, steven.bloemen@ster.kuleuven.be

²Department of Physics, University of Warwick, Coventry CV4 7AL, UK, t.r.marsh@warwick.ac.uk

We have analyzed the Q0, Q1 and Q2 data of the eclipsing binary KOI-74, which consists of an A star and a low mass white dwarf. The light curve shows clear Doppler beaming, ellipsoidal modulation and eclipses. In addition to these effects, we have detected an effect similar to the Römer delay. As shown in van Kerkwijk et al. (2010), the observed ellipsoidal modulation amplitude is not consistent with the mass ratio determined from the Doppler beaming amplitude. The amplitude of the observed Römer delay confirms that the mass ratio that one would derive from the ellipsoidal modulation amplitude cannot be the true mass ratio of the system. It has been suggested that the unexpected ellipsoidal modulation amplitude could be due to the rapid rotation rate of the primary. We have remodeled the light curve, trying to account for the effects of rapid rotation, but found this to only increase the discrepancy.

P0602. POSTER SESSION II

A very precise age for the old metal-rich open cluster NGC6791

K. Brogaard¹ and E. Sandquist² et al.^{3,4}

¹Department of Physics and Astronomy, University of Victoria, P.O. Box 3055, Victoria, BC V8W 3P6, Canada, kfb@phys.au.dk

²Department of Astronomy, San Diego State University, San Diego, CA 92182, USA, erics@mintaka.sdsu.edu

³The team behind Kepler Guest Observer programme 20044

⁴The KASC working group #2 on 'Oscillations in clusters'

Abstract:

Exploiting synergies among the measurements of cluster member eclipsing binaries [1], color-magnitude diagrams and ensemble asteroseismology of cluster stars [2,3] allows unprecedented constraints on stellar models and cluster parameters, including their ages.

We show here how *Kepler* is aiding such procedures and bringing us closer to a consistent understanding of stellar evolution in the old metal-rich open cluster NGC6791 [3,4].

The age of NGC6791 is determined more precisely than for any other old open cluster [4] and we ask the question whether this age is also accurate? As part of this, we demonstrate remaining inconsistencies and how *Kepler* will help solve them.

References:

- [1] Brogaard K. et al. (2011) *A&A*, 525, 2
- [2] Basu S. et al. (2011) *ApJL*, 729, 10
- [3] Miglio A. et al. (2011) *MNRAS*, accepted (ArXiv:1109.4723)
- [4] Brogaard K. et al. In preparation

LOW-MASS ECLIPSING BINARIES FROM KEPLER: REACHING THE NATURAL ROTATION RATE OF M AND K DWARFS. J. L. Coughlin¹, M. López-Morales², T. E. Harrison¹, and N. Ule¹,

¹Department of Astronomy, New Mexico State University, P.O. Box 30001, MSC 4500, Las Cruces, NM 88003-8001, jlcoughl@nmsu.edu, ²Institut de Ciències de l'Espai (CSIC-IEEC), mlopez@ieec.uab.es

Introduction: An outstanding problem in stellar astrophysics is that the radii of low-mass, main-sequence stars in eclipsing binary systems are consistently ~10-15% larger than predicted by stellar models. This inflation is hypothesized to be primarily due to enhanced magnetic activity as a result of their binarity, and thus artificially enhanced rotation rates. Thus, such an effect should diminish with increasing period, but only a small number of low-mass eclipsing binary systems are known in general, fewer are well-studied with precise light and radial-velocity curves, and barely any of these are at long periods. In addition to exploring the physics of low-mass stars, research into this area helps to better characterize the radii of extrasolar planets around low-mass stars, whose values are dependent on those assumed for the host star.

New Low-Mass EB's from Kepler: We have previously presented results from our search for new low-mass eclipsing binary systems via our Kepler Guest Observer programs and a search through the publicly available data [1][2]. We identified over 100⁺ low-mass eclipsing binaries suitable for ground-based follow-up, with 30 of them having periods greater than 10 days. We also modeled the Kepler light curves of these systems, and found preliminary evidence for a trend of decreasing stellar radii with increasing orbital period [1].

Ground-based Follow-Up: We present results of our ongoing effort to obtain ground-based multi-color light and radial velocity curves of these systems via the Kitt Peak National Observatory 4-meter, the Apache Point Observatory 3.5-meter, and New Mexico State University 1-meter telescopes. We also present preliminary modeling of these data combined with that from the Kepler mission, and examine what future work is needed to make progress in this area.

References: [1] Coughlin et al. (2011) AJ, 141, 78. [2] Harrison et al. (2011), AJ, Submitted.

P0604. POSTER SESSION II

Radial Velocity follow-up of Kepler Eclipsing Binaries on the Hobby-Eberly Telescope. Rohit Deshpande¹, Suvrath Mahadevan², Chad Bender³, Arpita Roy⁴, Scott Fleming⁵, Matthew Shetrone⁶, ¹Pennsylvania State University, 420 Davey Lab, University Park, PA 16802; rohit@psu.edu, ²Pennsylvania State University; suvrath@astro.psu.edu, ³Pennsylvania State University; cbender@psu.edu, ⁴Pennsylvania State University; aur17@psu.edu, ⁵Pennsylvania State University; scfleming@psu.edu, ⁶University of Texas at Austin; shetrone@astro.as.utexas.edu

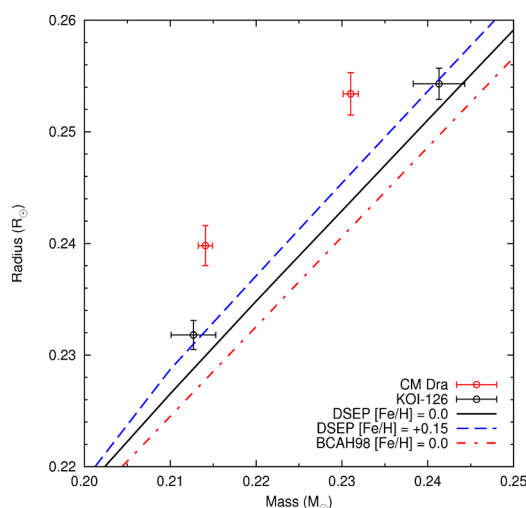
Introduction: We present first results from our radial velocity (RV) survey, carried out on the 10m Hobby Eberly Telescope (HET), to precisely measure mass and radii of Kepler eclipsing binaries. The observations were taken using the high resolution (R ~30,000) fiber-fed spectrograph in the V-band. We selected a sample of 30 detached binaries with varied periods and masses. Using information from the Kepler light curve modeling, the queue-based system on the HET enabled us to plan and observe targets at specific phases. This process thus reduced the total number of observations required to determine orbital parameters, and masses to six. With RV precision of ~ 50m/s and model parameter constraints from the Kepler photometry, we expect to determine masses and radii at the 1% level. We also discuss results from our follow-up observations of Kepler-16.

P0605. POSTER SESSION II

THE LOW-MASS, STELLAR MASS-RADIUS RELATIONSHIP. G. A. Feiden^{1,2} and B. Chaboyer³, ¹Department of Physics & Astronomy, Dartmouth College, 6127 Wilder Laboratory, Hanover, NH 03755. ²Neukom Graduate Fellow, gregory.a.feiden@dartmouth.edu, ³Dartmouth College, brian.chaboyer@dartmouth.edu

The characterization of exoplanets detected by the Kepler Space Telescope requires an accurate knowledge of the fundamental physical parameters of the host stars. Obtaining the properties of the host stars is, generally, a model dependent task relying on the predictions of stellar evolution theory [1]. Thus, to ensure a proper characterization, we need verification that stellar models are able to accurately reproduce the physical properties of stars. This verification can be achieved using results from studies of eclipsing binaries (EBs).

Up until now, results of EB studies have indicated that below 0.8 solar masses, stellar evolution models are unable to correctly predict the observed mass-radius relation [2]. Recently, however, models of the KOI-126 [3] stars were found to be in agreement with observations (see Figure) [4] and early results indicate that models of the Kepler-16 [5] components may also be consistent with observations. Both systems contain at least one component below fully convective boundary. In the case of KOI-126, both stars have masses around 0.2 solar masses and the models had the added constraint that they must also be able to reproduce the properties of a third metal rich star, which has started to evolve off the main sequence. Interestingly, it was only when super-solar metallicity models were considered that agreement was obtained between the models and the observed parameters. These results have led us to reevaluate the current state of low-mass stellar evolution theory.



Here, we present the results of an extensive comparison of EB systems with models from the Dart-

mouth Stellar Evolution Program (DSEP). The latest version of DSEP utilizes non-grey PHOENIX atmosphere surface boundary conditions [6] and a robust equation of state, FreeEOS [7], allowing DSEP to reliably model stars down close to the hydrogen burning minimum mass with an arbitrary metal abundance. Our results indicate that stars which show discrepancies with models are not as common as previously believed and that DSEP is capable of deriving physical parameters consistent with most observations. It is likely that the better agreement seen with DSEP is due to its equation of state, which allows it to model super-solar metallicity stars more reliably. With exoplanet parameters having such a strong model dependence, the results suggest that adopting DSEP models could potentially have important ramifications for identification of potential Earth-sized or habitable planets [1].

While Kepler has only provided two confirmed low-mass EB systems, there are over 2,100 candidate EB systems identified, many with estimated effective temperatures placing them in the low-mass regime [8]. In the future, this wealth of data will place tight constraints on low-mass stellar evolution models. To facilitate these studies, DSEP isochrones and theoretical stellar evolution tracks are publicly available at <http://stellar.dartmouth.edu/~models/> and in the near future a web-interface will be implemented to allow for individual models to be generated with any set of user-specified input parameters.

Acknowledgments: GAF and BC are grateful for the National Science Foundation (NSF) grant AST-0908345. GAF would also like to acknowledge support from the William H. Neukom 1964 Institute for Computational Science.

References:

- [1] Muirhead, P. S. et al. (2011) *arXiv:1109.1819*.
- [2] Torres, G. et al. (2010) *A&AR*, 18, 67. [3] Carter et al. (2011) *Sci*, 331, 562. [4] Feiden, G. A. et al. (2011) *ApJ*, 740, L25. [5] Doyle et al. (2011) *Sci*, 333, 1602. [6] Hauschildt et al. (1999) *ApJ*, 512, 377. [7] by Alan Irwin: <http://freeeos.sourceforge.net>
- [8] Slawson, R. W. et al. (2011) *arXiv:1103.1659*.

P0606. POSTER SESSION II

APOGEE Near-IR Radial Velocity Measurements of Kepler Eclipsing Binaries. S. W. Fleming¹ and R. Deshpande² and S. Mahadevan³ and C. Bender⁴ and A. Roy⁵ and R. Terrien⁶ and F. Hearty⁷ and D. Nidever⁸, ¹Dept. of Astronomy, Penn State University, 525 Davey Lab, University Park, PA 16802 (scfleming@psu.edu), ²Penn State University (rsd15@psu.edu), ³Penn State University (suvrath@astro.psu.edu), ⁴Penn State University (cbender@psu.edu), ⁵Penn State University (aur17@psu.edu), ⁶Penn State University (rct151@psu.edu), ⁷University of Virginia (frh3z@virginia.edu), ⁸University of Virginia (dln5q@virginia.edu)

We present the latest results from our APOGEE ancillary science project to measure radial velocities of Kepler eclipsing binaries and, after combining with Kepler photometry, derive precise masses and radii. The multi-object, fiber-fed APOGEE spectrograph operates in the H band and provides a spectral resolution of ~ 20000 . A total of 110 eclipsing binaries will be observed from two fields at three or six epochs, depending on the field. The order-of-magnitude improvement in contrast ratio by observing in the H band, combined with a two-dimensional cross-correlation technique and model parameter constraints from the Kepler photometry will enable stellar masses and radii to be measured at the $\sim 1\%$ level. With orbital periods ranging from a few days to a few months, a large number of benchmark systems will be defined spanning a range of orbital periods and stellar masses. These systems will provide critical observational constraints to next-generation stellar models that seek to include the effects of magnetic fields on convective stellar atmospheres.

CATAclysmic VARIABLES IN THE SUPER METAL-RICH CLUSTER NGC 6791. P. M. Garnavich, Physics Department, University of Notre Dame, Notre Dame, IN 46566; pgarnavi@nd.edu

Introduction: NGC 6791 is a remarkable open cluster. A number of photometric and spectroscopic studies have shown that it is both very old (~10 Gyr) and extremely metal rich (~3 times Solar [1]). This combination is rare in the Milky Way and it provides a laboratory to study stellar physics in a unique environment.

The high metallicity of NGC 6791 means it has a rich red-clump, but oddly it also has a well-populated blue horizontal branch. Variability searches in the cluster have identified two blue stars, named B7 and B8, as cataclysmic candidates and spectroscopy confirmed their nature [2]. Kepler monitored these two CVs over Cycle 2.

NGC6791-B7: Ground-based monitoring of B7 showed irregular variations with an amplitude of 0.5 mag., although a 3 magnitude drop over ten days was seen on one occasion [3]. The Kepler light curve is difficult to interpret. The variations are not periodic, but do show correlations on scales of 30 to 50 days. No orbital modulation is apparent in the 30-minute cadence observations.

NGC6791-B8: The faintness of B8 has made it difficult to study and its orbital period was unknown. Ground-based light curves of B8 displayed dwarf nova outbursts [3]. Kepler light curves confirm the dwarf nova outbursts with a typical recurrence time of 20 days and an amplitude of 1.5 mag. In Q8 the CV went into superoutburst providing clues to its class and orbital period [4]. The superoutburst lasted two weeks with an amplitude of 3 mag. Superhumps with an average period of 2.097 ± 0.003 hours are clearly seen. This suggests that the orbital period is just under the period gap and that B8 belongs to the SU UMa class of CV. In the first two days of the outburst the superhump peak-to-peak amplitude is 0.3 mag and the period is 2.109 ± 0.003 hours. The superhump period decreases with time at a rate of $\dot{P} = 2 \times 10^{-4}$.

References: [1] Garnavich, P. M., et al. 1994, AJ, 107, 1097; [2] Kaluzny, J., Stanek, K. Z., Garnavich, P., & Challis, P. 1997, ApJ, 491, 153 ; [3] Mochejska, B. J., Stanek, K. Z., & Kaluzny, J. 2003, AJ, 125, 3175 ; [4] Garnavich, P., Still, M., & Barclay, T. 2011, ATel 3507.

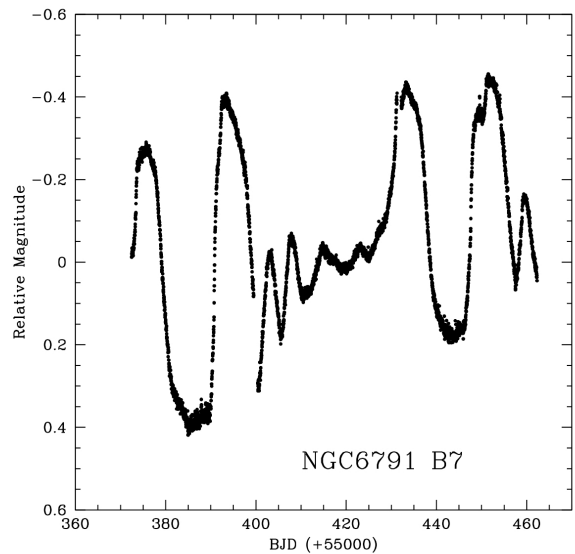


Fig 1- The Q6 light curve of star B7. Note the similarity of the variations separated by 55 days.

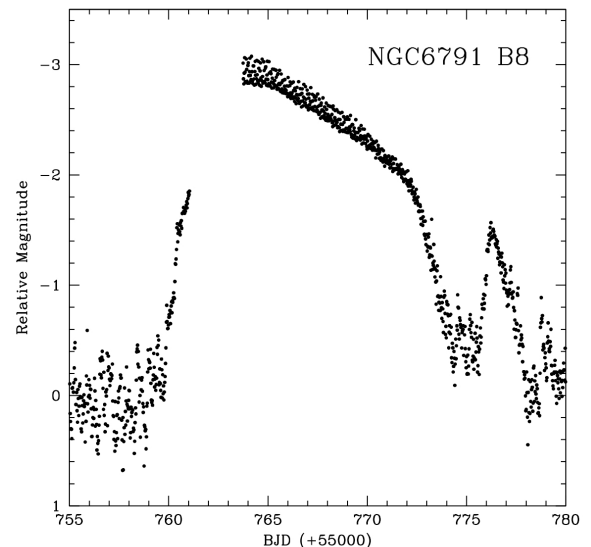


Fig 2- Part of the Q8 light curve of star B8 centered on the superoutburst. The variations during the outburst are the 2.1 hour period superhumps.

P0608. POSTER SESSION II

KIC 4544587: An Asteroseismically Interesting, Eccentric, Short Period Binary. K. Hambleton,¹ D. Kurtz², A. Prsa³, S. Bloeman⁴, and J. Soutworth⁵, ¹University of Central Lancashire, Preston, Lancashire, PR1 2HE, kmhambleton@googlemail.com, ²University of Texas at San Antonio, donald.kurtz@utsa.edu, ³Villanova University, andrej.prsa@villanova.edu, ⁴Instituut voor Sterrenkunde, Steven.Bloemen@ster.kuleuven.be, ⁵Keele University, jkt@astro.keele.ac.uk.

KIC 4544587 is an eclipsing binary star with rapid apsidal motion, tidal excitation of g modes, and p modes modulated by the Doppler shift. The primary component is an early A-type δ Scuti variable, with a temperature of 8270 ± 250 K, whilst the secondary component is an early G-type main sequence star with a temperature of 6500 ± 310 K. The orbital period of this system is 2.18911(1) d, with the light curve demonstrating a hump after secondary minimum due to proximity effects. The frequency spectrum of the residual data (the original data with the binary characteristics removed) shows the presence of both pressure (p) and gravity (g) modes. Eight of the g modes are precise multiples of the orbital frequency, with statistical confidence greater than 3σ . This is a signature of resonant excitation. Furthermore, many of the p modes that are not orbital harmonics are separated by the orbital frequency. We present our working hypothesis that the Doppler effect, caused by the orbital motion, has generated side lobes on the prominent p mode oscillations, which are of comparable amplitude to the oscillations themselves.

P0609. POSTER SESSION II

ADVANCED ANALYSIS OF SURFACE FEATURES ON ACTIVE CLOSE BINARIES. G. J. Peters¹ and R. E. Wilson², ¹Space Sciences Center & Department of Physics & Astronomy, University of Southern California, 835 W. 37 St., Los Angeles, CA 90089-1341, gjpeters@mucen.usc.edu, ²Department of Astronomy, University of Florida, wilson@astro.ufl.edu.

Introduction: Close binaries show photometric and spectroscopic activity that includes mass transfer in direct impact Algol systems and magnetic spot variability in some cooler systems. Although the generic process of mass transfer in Algol binaries has been understood now for about a half century, little is known about the detailed physics. For example, how is the mass actually deposited on the mass gainer? What is the extent of shock-induced heating in the photosphere and circumstellar material? Are there accretion-induced pulsations on the photosphere of the mass gainer? Is the mass transfer rate uniform, or is the gas stream clumpy? What are typical fluctuations in amount and location of matter deposition due to source and stream fluctuations? How much mass and angular momentum is lost from the system? The latter is important for computing the evolutionary tracks of Algols [1]. The physics of magnetic spot activity on the mass losers in Algol systems or in cool systems such as RS CVn binaries is a topic of current interest because of implications for convective envelope structure.

The Kepler Program on Active Binaries: Among our targets are the Algol systems that have separations close enough that the gas stream impacts the photosphere of the mass gainer. The seven systems listed in Table 1 were identified as possible Algol binaries from the online Catalogue of Variable Stars in the *Kepler* Field of View [2]. Stars designated as EA with periods greater than 1.3^d were considered, as these are likely direct-impact Algols. Each system has been monitored at the long cadence for the duration of *Kepler* Cycle 2 to investigate the basic variability in the light curves. Short cadence observations were obtained of each system for a duration of one month to look for micro-flaring and other short-term activity.

Table 1 - Program Stars

| Star | Period ¹ (days) | Spectral Types ¹ | Kepler Mag. |
|----------|-------------------------------|-----------------------------|----------------|
| BR Cyg | 1.3326 | A3 V + G IV: | 10.028 |
| WX Dra | 1.8020 | A8 V + K0 IV: | 12.796 |
| UZ Lyr | 1.8913 | B9V + G-K1 IV: | 10.672 |
| V995 Cyg | 3.5565 | B8: + G6 IV | 11.882 |
| V461 Lyr | 3.7217 | A2 V: + K3 IV | 12.746 |
| V810 Cyg | 3.7363 | A0 V: + G6 IV | 13.931 |
| V850 Cyg | 4.5645 | A-B: + ? | 11.246 |

¹From catalogs of Budding [3] and Malkov et al. [4] and Simbad database.

Light Curve Analysis: The light curves are being analyzed with an updated version the Wilson & Devinney code [5],[6],[7],[8]. The most recent addition is a thorough makeover of the program's spot capability, including major precision improvement for spotted star light (and velocity) curves, spot motions due to drift and star rotation, and spot growth and decay [9]. These enhancements apply to both accretion hot spots and magnetic cool spots. The program's analysis capability includes parameters for times of spot appearance, development, and disappearance. Important is that the information input is *Kepler* light curve data that exist in long, essentially continuous, trains. A sample calculation from the new program is shown below (Fig.1). One type of variability that is often seen is unequal flux levels at the quadrature points that slowly disappears (or grows) during the course of a few orbital cycles. We have modeled this with a decaying hot spot that initially has a temperature of twice that of the local photosphere. It should be mentioned that each of the program binaries has a unique light curve with its own variability pattern. UZ Lyr and BR Cyg are typical short-period Algol systems. V850 Cyg appears to consist of a cool pair with spectacular spot behavior. The *Kepler* light curves are revealing activity in short-period systems that has never before been observed.

We appreciate support from NASA NNX11AC78G.

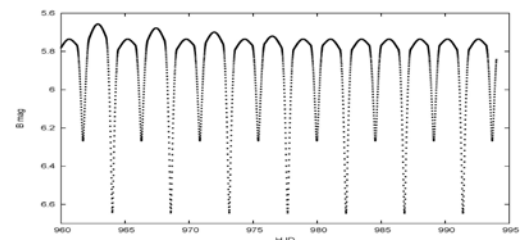


Fig. 1 - Calculated light curve for a 4.5^d binary with Teff =18000/14000 K and a decaying hot spot on the trailing hemisphere.

References: [1] Van Rensbergen W. et al. (2008) *A&A*, 487, 1129-1138. [2] Pigulski A. et al. (2009), <http://www.astrouw.edu.pl/asas/?page=kepler>. [3] Budding E. et al. (2004) *A&A*, 417, 263-268. [4] Malkov O. Y., et al. (2006) *A&A*, 446, 785-789. [5] Wilson R. E. (1979) *ApJ*, 234, 1054-1066. [6] Wilson R. E. (1990) *ApJ*, 356, 613-622. [7] Wilson R. E. (2008) *ApJ*, 672, 575-589. [8] Wilson R. E. & Devinney E. J. (1971) *ApJ*, 166, 605-619. [9] Wilson, R. E. (2012) in prep.

P0610. POSTER SESSION II

Two Unusual Binaries in the Old, Metal-Rich Open Cluster NGC 6791

Peterson R.C., Institution: Astrophysical Advances, peterston@ucolick.org

The cluster NGC 6791 is a template for old elliptical galaxies, being 8 Gyr old, metal-rich, and containing blue stars formed in binaries that may lead to spuriously low ages for old galaxies. Understanding the cluster's stellar and binary constituents will help to characterize how such stars are formed and evolve, and what role they play in shaping the spectral energy distribution of old galaxies. Within this old cluster, our GO-13 Kepler program has uncovered two unusual binaries. One is a triplyeclipsing system of near-main-sequence stars with a ~ 1.5 -day period. The light curve is complex, but with spectral monitoring, could constrain geometry, masses, and radii as well as provide the temperatures of detectable components and the distance to the system. This should significantly tighten comparisons of the cluster color-magnitude diagram to the stellar main sequence and turnoff. The other binary is a ~ 15 -day pair of stars midway up the giant branch that are near or beyond Roche-lobe overflow, whose characterization should elucidate when and how mass is transferred between evolved stars.

P0611. POSTER SESSION II

KEPLER OBSERVATIONS OF THE SU UMA CATAclySMIC VARIABLES V344 LYR, V1504 CYG, AND V447 LYR. M. A. Wood¹, M. D. Still^{2,3}, S. B. Howell², J. K. Cannizzo^{4,5}, and A. P. Smale⁶, ¹Department of Physics and Space Sciences, Florida Institute of Technology, Melbourne, FL 32901 (wood@fit.edu), ²NASA Ames Research Center (martin.still@nasa.gov; steve.b.howell@nasa.gov), ³Bay Area Environmental Research Institute, ⁴CRESST and Astroparticle Physics Laboratory (john.k.cannizzo@nasa.gov), NASA/GSFC, ⁵University of Maryland, Baltimore County, ⁶NASA/Goddard Space Flight Center (alan.p.smale@nasa.gov)

We report on the analysis of the *Kepler* short-cadence (SC) light curve of V344 Lyr ($P_{\text{orb}} = 2.11$ hr) and V1504 Cyg ($P_{\text{orb}} = 1.67$ hr) obtained during Q2—Q8, and the SC and long-cadence (LC) light curves of V447 Lyr ($P_{\text{orb}} = 3.73$ hr) during Q6-Q8. All three systems are SU UMa cataclysmic variables showing superoutbursts and superhumps. V344 Lyr and V1504 Cyg both show P_{orb} as well as positive and negative superhump periodicities. Positive superhumps occur during superoutbursts and are the result of a disk oscillation driven to resonance when the disk expands to the 3:1 Keplerian co-rotation resonance. The oscillating disk precesses in the prograde direction, resulting in a fractional period excess a few percent longer than P_{orb} and increasing with P_{orb} . The *Kepler* data are consistent with the two-source model for positive superhumps, where early in the superoutburst the signal is generated by viscous dissipation in the flexing disk itself, and later once the disk has returned to quiescence is caused by the periodically varying dissipation at the accretion stream impact point as it sweeps around the rim of the still flexing and asymmetric disk. The negative superhumps are the result of

accretion onto an accretion disk tilted out of the orbital plane and precessing in the retrograde direction. The modulation of the brightness in this case is a function of the variable depth in the primary potential well of the accretion stream bright spot as it sweeps across the face of the tilted accretion disk. For the first time, *Kepler* data reveal that the precession period of the tilted accretion disk increases between dwarf nova outbursts, and jumps rapidly to shorter period during dwarf nova outbursts (see Figure 1), providing a probe of the changing mass distribution and viscosity of the accretion disk as a function of time. Finally, V447 Lyr is an eclipsing binary system that shows positive superhumps. It is one of the longest-period eclipsing SU UMa systems, and as such provides a solid anchor to the superhump period excess versus P_{orb} relation at large P_{orb} .

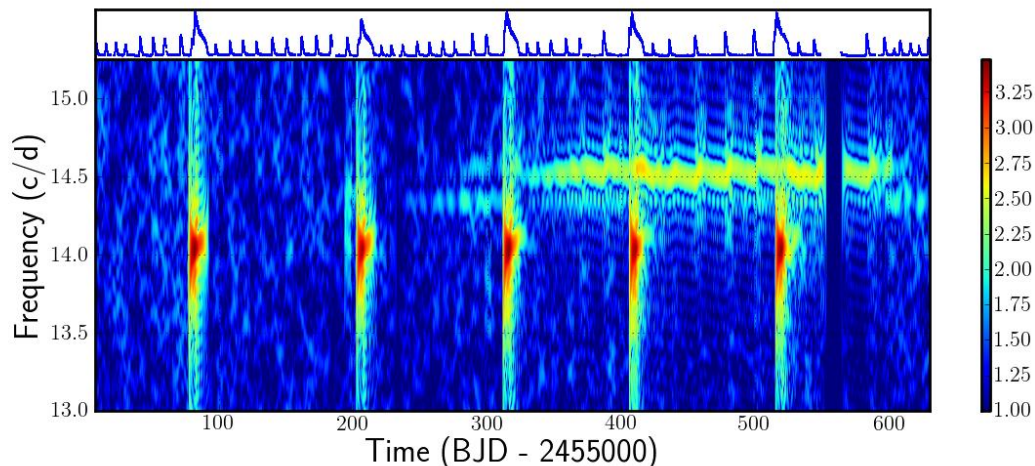


Figure 1: Spectrogram of V1504 Cyg for quarters Q2-Q8. The color scale shows the amplitude of \log of the residual counts once the large amplitude dwarf nova outbursts and superoutburst have been subtracted. Note that during the second year of *Kepler* observations, the negative superhump signal at ~ 14.5 c/d is excited and persists for over 4000 orbits. During that time, the period increases between dwarf nova outbursts and rapidly jumps to shorter period during outbursts, reflecting the changing moment of inertia of the tilted precessing disk as the disk mass increases and drains, respectively. Intensive studies of the *Kepler*-field cataclysmic variables hold the promise significant advancement in our understanding of the nature of astrophysical viscosity.

P0701. POSTER SESSION II

The Exact Solution of The Pioneer Anomaly According to The General Theory of Relativity and The Hubble's Law

By Azzam AlMosallami

University of Malaya

Az_almosallami@yahoo.com

Abstract

Radio metric data from Pioneer 10/11 indicate an apparent anomalous, constant, acceleration acting on the spacecraft with a magnitude $\sim 8 \times 10^{-10} \text{ m/s}^2$, directed towards the Sun[1,2].

Turyshev [7] examined the constancy and direction of the Pioneer anomaly, and concluded that the data a temporally decaying anomalous acceleration $-2 \times 10^{-11} \frac{\text{m}}{\text{s}^2 \cdot \text{yr}}$ with an over 10%

improvement in the residuals compared to a constant acceleration model. Anderson, who is retired from NASA's Jet Propulsion Laboratory (JPL), is that study's first author. He finds, so "it's either new physics or old physics we haven't discovered yet." New physics could be a variation on Newton's laws, whereas an example of as-yet-to-be-discovered old physics would be a cloud of dark matter trapped around the sun[12].

In this paper I introduce the exact solution for the Pioneer anomaly depending on the general theory of relativity and the Hubble's law. According to my solution, there are two terms of decelerations that controls the Pioneer anomaly. The first is produced by moving the Pioneer spacecraft through the gravitational field of the Sun, which causes the velocity of the spacecraft to be decreased according to the Schwarzschild Geometry of freely infalling particle. This deceleration is responsible for varying behaviour of the Pioneer anomaly in Turyshev [7], depending on $1/r^{2.5}$ the distance from the sun. The second term is produced by the attractive force of the dark matter which is constant and equals to the Hubble's constant multiplied by the speed of light in vacuum.

SURVEYING MAGNETIC ACTIVITY ON LATE-TYPE STARS: STARSPOT ROTATIONAL MODULATION AND EVOLUTION AND OTHER TEMPORAL VARIABILITY IN *KEPLER* PHOTOMETRY.

A. Brown¹, J. E. Neff², A. F. Kowalski³, S. L. Hawley³, H. Korhonen⁴, S. V. Berdyugina⁵, G. M. Harper⁶, L. Walkowicz⁷, T. R. Ayres¹, B. Tofany¹, N. Piskunov⁸, G. Basri⁹, S. Saar¹⁰, and L. Ramsey¹¹, ¹ CASA, 593 UCB, University of Colorado, Boulder, CO 80309-0593, USA, alexander.brown@colorado.edu; thomas.ayres@colorado.edu; ² College of Charleston, neffj@cofc.edu; ³ University of Washington, kowalski@astro.uw.edu, slh@astro.uw.edu; ⁴ Niels Bohr Institute, University of Copenhagen, Denmark, heidi.korhonen@nbi.ku.dk; ⁵ KIS, Freiburg, Germany, svetlana.berdyugina@kis.uni-freiburg.de; ⁶ Trinity College Dublin, Ireland, graham.harper@tcd.ie; ⁷ Princeton University, lucianne@astro.princeton.edu; ⁸ Uppsala University, Sweden, piskunov@fysast.uu.se; ⁹ UC Berkeley, basri@astro.berkeley.edu; ¹⁰ SAO, ssaar@cfa.harvard.edu; ¹¹ Penn State University, lwr@astro.psu.edu

Introduction: Starspots are direct tracers of regions of strong magnetic fields in the photospheres of late-type (F-G-K-M) stars. Starspots are dark, and thus conspicuous, because their intense magnetic fields suppress convective heat flux locally, resulting in a cooler atmosphere within the spot. These magnetic fields originate from an internal “dynamo” process powered by the interaction of subphotospheric convection and differential rotation. Observations of the surface distribution of starspots and how it evolves can provide important information on the dynamo process and the magnetic activity that it generates.

The *Kepler* satellite is providing spectacular optical photometric light curves of unprecedented precision and duration that routinely allow detailed studies of stellar magnetic activity on late-type stars that were difficult, if not impossible, to attempt previously. Rotational modulation due to starspots is commonly seen in the *Kepler* light-curves of late-type stars, allowing detailed study of the surface distribution of their photospheric magnetic activity. *Kepler* is providing multi-year duration light-curves that allow us to investigate how activity phenomena -- such as the growth, migration, and decay of starspots, differential rotation, activity cycles, and flaring -- operate on single and binary stars with a wide range of mass and convection zone depth.

Our *Kepler* GO program: We are observing a sample of F-G-K-type stars in our *Kepler* Cycles 1/2/3 Guest Observer programs that consists of over 220 stars that were selected for strong stellar activity using *GALEX* FUV and NUV photometry. These stars have V magnitudes between 9 and 15. The sample shows a wide variety of variability, as is illustrated in Fig.1, including starspot modulation and flaring.

We present data for a range of stars that illustrate the detailed variability found in *Kepler* light-curves and show how starspots evolve on a wide range of timescales for stars with typical rotation periods of a few days to a week. The physical properties of the stars are being measured using high resolution optical spectroscopy, which allows the *Kepler* results to be

placed within the existing framework of knowledge regarding stellar magnetic activity. These results demonstrate the powerful diagnostic capability provided by tracking starspot evolution essentially continuously for more than 18 months. The starspots are clearly sampling the stellar rotation rate at different latitudes, enabling us to measure the differential rotation and starspot lifetimes. We describe the methods by which we are investigating the detailed physical properties of these stars using multi-spectral region observations.

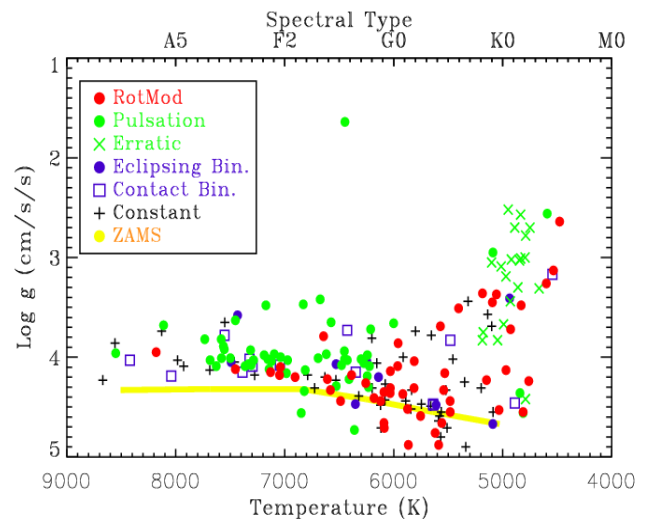


Fig. 1 T_{eff} vs $\log g$ H-R diagram displaying the dominant form of variability shown by our *Kepler* Cycles 1 and 2 GO sample, based on *Kepler* Input Catalog parameters.

P0703. POSTER SESSION II

ROTATION OF CLUSTER DWARFS AND SPECTROSCOPIC DIAGNOSTICS. Andrea K. Dupree,¹ Elisabeth R. Adams¹, and Andy Szentgyorgyi¹: Harvard-Smithsonian Center for Astrophysics, 60 Garden St., Cambridge, MA 02138; (dupree@cfa.harvard.edu, eadams@cfa.harvard.edu, aszentgyorgyi@cfa.harvard.edu)

Optical spectroscopic diagnostics (Ca II H and K, H- α , Ca IRT, Li I) are widely used to infer stellar properties such as age, magnetic activity, and winds from cool stars. Rotation of a cool star affects the strength of a magnetic dynamo which in turn determines the strength of magnetically associated spectral diagnostics.

We calibrate these diagnostics against rotation periods from Kepler using spectra from the multi-object spectrograph Hectochelle on the MMT [1]. Hectochelle provides echelle resolution ($\sim 35,000$) for selected wavelength regions spanning $\sim 150\text{\AA}$.

NGC 6811, an open cluster of age 1 Gyr in the Kepler field has stellar rotation periods derived for single dwarf stars [2] from Q1-Q4 of Kepler photometry. Here, we compare these rotation periods to several diagnostics from the optical spectra to establish the relations generally applied to individual stars in the field and evaluate their consistency. This cluster is part of a study of a larger sample of open clusters studied with Hectochelle spanning ages of 450 Myr (Melotte 111) to 4.4 Gyr (NGC 6791, also in the Kepler field).

References: [1] Szentgyorgi, A. et al. 2011, PASP, in press [2] Meibom, S. et al. 2011, Ap.J., 733, L9

P0704. POSTER SESSION II

Cycle 1 Observations of Low Mass Stars: New Eclipsing Binaries, Single Star Rotation Rates, and the Nature and Frequency of Starspots Thomas E Harrison¹, J. L. Coughlin¹, Nick M. Ule¹, and Mercedes Lopez-Morales²,
¹Astronomy Department, New Mexico State University, Las Cruces, NM 88003, tharriso@nmsu.edu, jl-cough@nmsu.edu, nmule@nmsu.edu, ²Institut de Ciencies de L'Espai (CSIC-IEEC), mlopez@ieec.uab.es

Introduction: We have analyzed *Kepler* light curves for 849 stars with $T_{\text{eff}} \leq 5200$ K from our Cycle 1 Guest Observer program. We identify six new eclipsing binaries, one of which has an orbital period of 29.91 d, and two of which are probable W UMa variables. In addition, we identify a candidate “warm Jupiter” exoplanet. We further examine a subset of 670 sources for variability. Of these objects, 265 stars clearly show periodic variability that we assign to rotation of the low-mass star. At the photometric precision level provided by *Kepler*, 251 of our objects showed no evidence for variability. We were unable to determine periods for 154 variable objects. We find that 79% of stars with $T_{\text{eff}} \leq 5200$ K are variable. The rotation periods we derive for the periodic variables span the range $0.31 \leq P_{\text{rot}} \leq 126.5$ d. A considerable number of stars with rotation periods similar to the solar value show activity levels that are 100 times higher than the Sun. This is consistent with results for solar-like field stars. As has been found in previous studies, stars with shorter rotation periods generally exhibit larger modulations. This trend flattens beyond $P_{\text{rot}} = 25$ d, demonstrating that even long period binaries may still have components with high levels of activity and investigating whether the masses and radii of the stellar components in these systems are consistent with stellar models could remain problematic. Surprisingly, our modeling of the light curves suggests that the active regions on these cool stars are either preferentially located near the rotational poles, or that there are two spot groups located at lower latitudes, but in opposing hemispheres.

P0705. POSTER SESSION II

THE FLARING ACTIVITY OF THE M DWARF GJ 1243. S. L. Hawley¹, J. R. A. Davenport¹, A. F. Kowalski¹, E. J. Hilton², J. P. Wisniewski¹, A. Brown³, L. Walkowicz⁴, ¹Astronomy Department, Box 351580, University of Washington, Seattle, WA 98195, slh@astro.washington.edu, jrad@astro.washington.edu, kowalski@astro.washington.edu, wisniewski@astro.washington.edu, ²University of Hawaii, hilton@ifa.hawaii.edu, ³University of Colorado, alexander.brown@colorado.edu, ⁴Princeton University, lucianne@astro.princeton.edu

Abstract: We analyze high time resolution (one minute cadence) data from our Kepler Cycle 2 GO program to investigate flares on the active M dwarf GJ 1243. In our preliminary analysis for one month of data (shown in Figure 1), we find a significant periodic variation in the light curve, as well as more than 270 flares. Neither the flare energy nor the number of flares appears to correlate with the phase of the 0.6 day periodic variation. We will present further results that incorporate the second month of Kepler data and our ground-based followup spectroscopy using the ARC 3.5m telescope at Apache Point Observatory. We will also discuss the flare frequency distribution for the GJ 1243 Kepler data and compare with ground-based data for similar stars. Finally, we will describe our analysis of the variability structure function for the Kepler data.

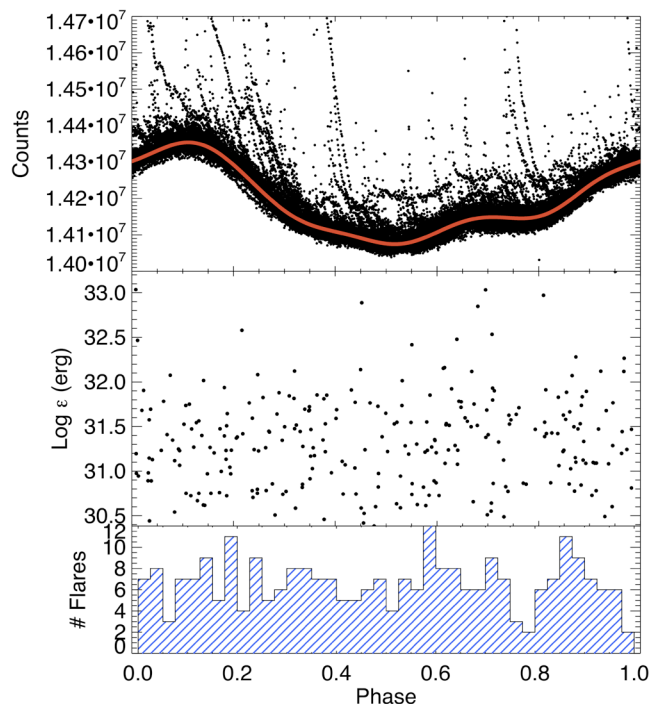


Figure 1: Top panel – the phase folded light curve for one month of 1-minute cadence Kepler data on GJ 1243. The periodic variation is evident, as are the flare excursions. Flare energies (middle panel) and number of flares (bottom panel) show no obvious correlation with phase.

P0706. POSTER SESSION II

USING KEPLER DATA TO CHARACTERIZE THE FLARE PROPERTIES OF GK STARS A. F. Kowalski¹, A. Brown², J. R. A. Davenport¹, R. Deitrick¹, S. L. Hawley¹, E. J. Hilton³, T. Ayres², S. V. Berdyugina⁴, G. M. Harper⁵, H. Korhonen⁶, L. Walkowicz⁷, ¹University of Washington, USA, adamfk@u.washington.edu, jrad@astro.washington.edu, slh@astro.washington.edu, deitrr@u.washington.edu; ²University of Colorado, USA, alexander.brown@colorado.edu, thomas.ayres@colorado.edu; ³Department of Geology and Geophysics and the Institute for Astronomy, University of Hawaii, USA, hilton@ifa.hawaii.edu; ⁴Kiepenheuer Institut fuer Sonnenphysik, Germany, svetlana.berdyugina@kis.uni-freiburg.de; ⁵Trinity College Dublin, Ireland, graham.harper@tcd.ie; ⁶Niels-Bohr Institute, University of Copenhagen, Denmark, heidi.korhonen@nbi.ku.dk; ⁷Princeton University, USA, lucianne@astro.princeton.edu

Due to their high occurrence rate and large contrast against the background stellar emission, white-light flares on a handful of young, rapidly rotating, low-mass M stars have been the primary source for our understanding of optical flare emission. *Kepler*'s high-precision, long baseline lightcurves have opened up the characterization of white-light emission to new domains of stars with various rotation rates, masses, and magnetic dynamo strengths. We present the properties of white-light flares on GALEX-selected solar-type stars from GO data in Q1-Q7. The flares are discussed in relation to intrinsic stellar properties, which are constrained by a vast amount of follow-up characterization of the sample. We compare the flare properties with those previously studied on M dwarfs and the Sun; such comparisons will provide important constraints for models of internal magnetic dynamos and atmospheric radiative-hydrodynamic flare simulations. An example light curve of a flare star from our sample is shown in Figure 1.

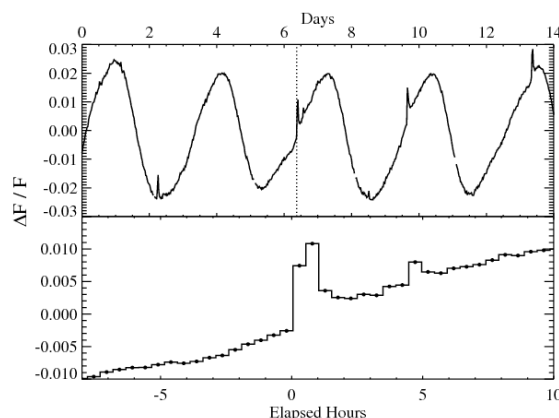


Figure 1: *Kepler* (30-minute cadence) data for a dG2 star reveals a handful of flares superposed on underlying rotational modulation. The vertical dotted line in the top panel indicates the flare event showcased in the bottom panel. A movie of an entire light curve (for this star and for two other flare stars) is located at the following link: www.astro.washington.edu/kowalski/flare_stars_movie.mpeg

P0707. POSTER SESSION II

STATISTICS OF STELLAR VARIABILITY IN KEPLER DATA WITH ARC SYSTEMATICS REMOVAL

A. McQuillan¹, S. Aigrain², S. Roberts³, ¹ University of Oxford, Oxford Astrophysics, Keble Road, Oxford OX1 3RH, UK, amy.mcquillan@astro.ox.ac.uk, ² University of Oxford, suzanne.aigrain@astro.ox.ac.uk, ³ University of Oxford, sjrob@robots.ox.ac.uk

Systematics Correction: We investigate the variability properties of main sequence stars in the public Kepler data. The Kepler pipeline (PDC), like other current reduction methods, is unsuitable for the study of stellar variability so a new Astrophysically Robust Correction for systematics (ARC) was developed. The key feature of our reduction is the removal of a set of basis functions that are determined to be present in small amounts across many light curves, therefore effectively removing systematics while leaving the true variability signal unchanged. Full details of this method can be found in Roberts et al. [1]. The improvement can be seen in Figure 1, which shows an apparent bimodality in variability where the PDC has removed intrinsic stellar signals at medium variability levels, while the ARC preserves them.

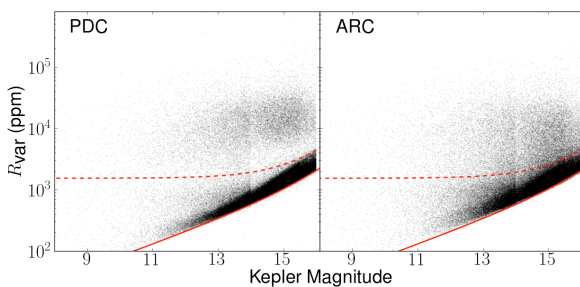


Figure 1. Variability (defined as 5th – 95th percentile of normalized flux) for the PDC and ARC data, with the photometric uncertainty (red solid line) and twice the solar value (red dashed line).

Variability Statistics: Using the ARC data we revisit and confirm many of the relationships presented by Basri et al. [2],[3] and Ciardi et al. [4], and extend this work to a more thorough study of the periodic and stochastic nature of the variability.

We divide the targets into high- and low-variability groups by comparison to the active Sun (dashed red line in Figure 1), allowing us to examine the stellar properties of each sample. Using this method, 36% of dwarf stars observed by Kepler appear more variable than the active Sun on a 33 day timescale.

We determine the variability statistics per spectral type, and show tenuous evidence that that the high-variability sample typically have lower proper motion. Variability is seen to increase with decreasing temperature and there exist significant differences in the nature of variability between spectral types.

The frequency content of the light curves shows evidence for periodic or quasi-periodic behaviour in 16% of dwarf stars. The fraction and typical period vary between spectral types, as shown in Figure 2. It should be noted that there are specific caveats that apply to this distribution, based on the length of the dataset and the period selection method. Full details of this can be found in McQuillan et al. [5].

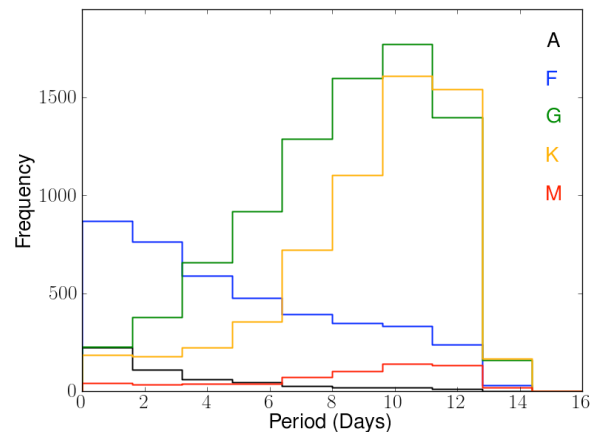


Figure 2. Period distribution for each spectral type, for stars displaying a significant period, showing a clear trend towards longer periods for later type stars. See McQuillan et al. [5] for caveats.

The stochastic component of variability associated with each spectral type was parameterised by fitting autoregressive models to the periodograms, as used by Aigrain et al. [6]. This analysis shows a trend of increasing amplitude and timescale towards later spectral types.

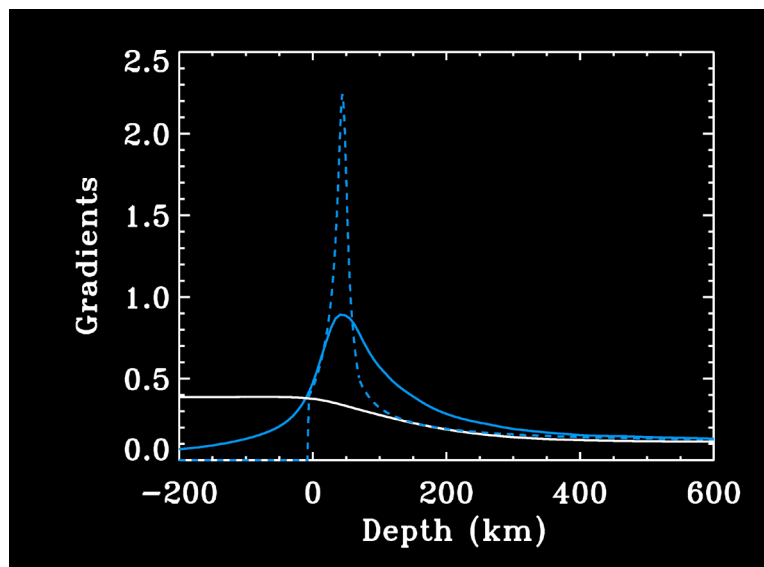
Most A and F stars have short periods (< 2 days) and highly sinusoidal variability, suggestive of pulsations. Their spectral density distribution implies they are accompanied by small scale, short-lived active regions. G, K and M stars tend to have longer periods (> 5 days, with a trend towards longer periods at later spectral types) and show a mixture of periodic and stochastic variability, indicative of activity. For these late type stars the activity regions also appear larger and more stable.

References: [1] Roberts et al. (in prep.). [2] Basri et al. (2010) *ApJ Letters*, 713, L155. [3] Basri et al. (2011) *AJ*, 141, 20. [4] Ciardi et al. (2011) *AJ*, 141, 108. [5] McQuillan et al. (in prep). [6] Aigrain et al. (2004) *A&A*, 414, 1139.

Impact of magnetic field on oscillation frequencies of solar type stars

L. Piau¹, R. F. Stein², P. Morel³, R. Collet⁴, R. Trampedach⁵ and S. Turck-Chieze⁶,
¹Laboratoire Atmospheres Milieux Observations Spatiales, 11 Boulevard D'Alembert, 78280 Guyancourt France; ²Michigan State University, Department of Physics & Astronomy, East Lansing, MI 48824-2320, USA ; ³OCA, Boulevard de L'Observatoire, BP 4229 F06304 Nice Cedex 4, France ; ⁴Max-Planck-Institut fur Astrophysik, Postfach 1317, D-85741 Garching b. Muenchen, Germany ; ⁵JILA, University of Colorado, 440 UCB, Boulder, CO 80309-0440 USA; ⁶CEA-Saclay DSM/IRFU/SaP, L'Orme des Merisiers 91191 Gif-sur-Yvette, France

We combine 3D simulations of the surface convection and 1D secular modeling of the whole Sun. The 3D hydrodynamical simulations are performed in a box domain of a few thousand kilometers of horizontal and vertical extension around the solar surface. They are made with and without magnetic field to mimic the solar activity. Thus we compute the thermal gradient and the turbulent pressure in the superadiabatic region and we estimate how they are affected by the surface activity. In a second step, horizontal averages of these quantities are introduced as boundary conditions of the 1D models that we use to calculate the eigenmodes. We compare the absolute seismic frequencies with those coming from more classical 1D models i.e. relying on the usual phenomenologies of surface convection: the mixing length theory and the full spectrum of turbulence phenomenology. We compare the oscillations frequencies we compute with the observed ones. Finally we show how the absolute oscillations frequencies change in presence of a magnetic field.



Thermal gradients $\partial \ln T / \partial \ln P$ around the stellar surface (solar conditions) : solid blue line : horizontal & time average of 3D simulation; dotted blue line : Canuto and Mazzitelli 1D phenomenology, solid white line : adiabatic gradient.

P0709. POSTER SESSION II

DIFFERENTIAL ROTATION IN KEPLER OPEN CLUSTER STARS.

S. H. Saar¹ and S Meibom¹, ¹SAO 60 Garden Street Cambridge, MA 02138 saar@cfa.harvard.edu; smeibom@cfa.harvard.edu

Starspots are regions of magnetic flux on cool stars that is so concentrated convective heat transport is locally suppressed. The precision and cadence of *Kepler* make it a superb instrument for studying the rotation and temporal/spatial evolution of starspots. Analysis of these starspot properties can yield important information on how the magnetic dynamo that generates them actually operates. Open clusters are ideal laboratories for stellar studies since they comprise stars of roughly fixed age and metallicity. We report on our observations of spots on cool stars in two open clusters in the *Kepler* field; NGC 6811 (age ~1 Gyr) and NGC 6819 (age ~2.5 Gyr). Rotation, differential rotation, and spot growth/decay are all clearly seen by eye in the data, but other sources of variability introduce some confusion. We use a principle components analysis PDC MAP to remove non-intrinsic variability in our sources, and then apply a number of methods (periodogram, gapped wavelet, and modeling) to measure differential rotation and growth/decay timescales for the observed spots. We present our first results, and compare our measurements with other stellar properties and previous results.

Stellar Variability From DASCH vs. Kepler Data

Sumin Tang*, Jonathan Grindlay and Soren Meibom

Harvard-Smithsonian Center for Astrophysics, 60 Garden Street, MA 02138

*stang@cfa.harvard.edu

DASCH (Digital Access to a Sky Century@Harvard) has similar magnitude range to Kepler, and therefore Kepler targets are also covered by DASCH over 100 years. Combining the long-term variations from DASCH, and the short-term variations from Kepler of great accuracy, enables a unique study of stellar variability on the widest range of timescale. Here we present our study of a group of peculiar long-term K giant variables with slow variations over decades. Most of them show strong star spots and flaring activities in the Kepler light curves, which suggests that the mysterious long-term variations may be related to strong star spots and magnetic activities which may be a new mechanism for dust formation or ejection. Preliminary study of a few other unusual variables are also presented.

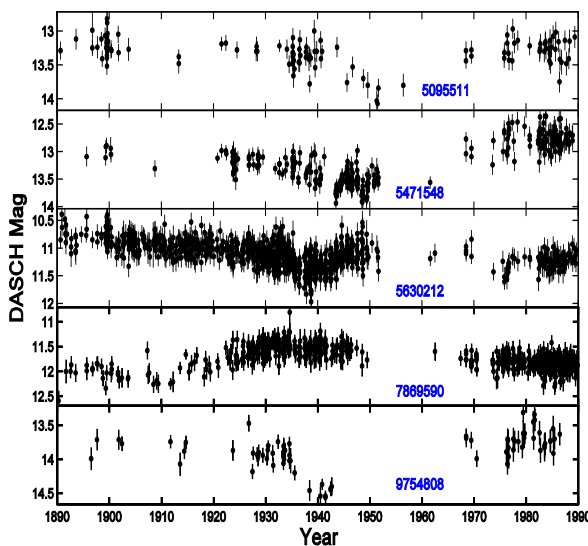


Figure 1: DASCH light curves of 5 long-term K giant variables in the Kepler FOV.

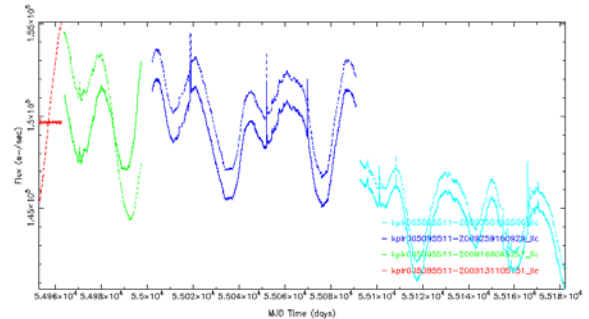


Figure 2: Kepler light curve of 5095511.

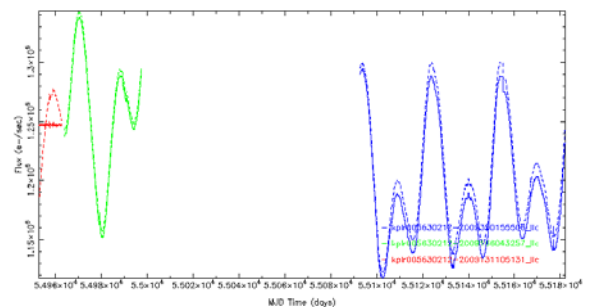


Figure 3: Kepler light curve of 5630212.

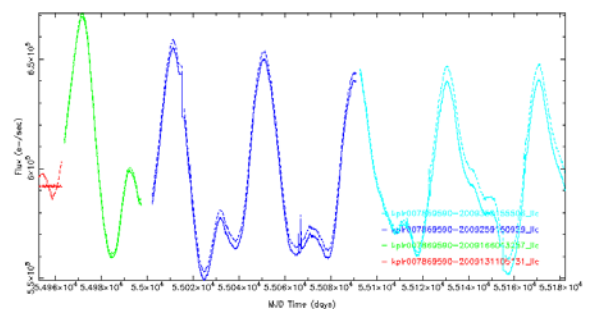


Figure 4: Kepler light curve of 7869590.

This work was supported in part by NSF grants AST-0407380 and AST-0909073 and now also the *Cornel and Cynthia K.Sarosdy Fund for DASCH*.

P0711. POSTER SESSION II

STELLAR DIFFERENTIAL ROTATION ESTIMATES FROM PLANETARY TRANSITS Adriana Valio¹

¹Center for Radio Astronomy and Astrophysics Mackenzie, Mackenzie University, Rua da Consolacao, 896, Sao Paulo, Brazil, avalio@craam.mackenzie.br

About 25% of the extra solar planets discovered so far transit their host star. During the eclipse of star by its orbiting planet, spots on the surface of the star may be occulted, causing small variation in the transit light-curve. These variations can be modeled using the method described in [1] that yields the starspots physical properties such as size, position, and temperature (or intensity). Presently, the transit light curves of HD 209458 [1], CoRoT-2 [2,3,4], CoRoT-4 [5], CoRoT-5, CoRoT-6 [5], CoRoT-8, CoRoT-11, CoRoT-12, and CoRoT-17 have been analyzed, and their spots characteristics determined.

Just like Galileo did four centuries ago for the Sun, from the spot analysis it is also possible to calculate the stellar rotation period and whether it presents or not differential rotation. The mean rotation period of the star is obtained from the out-of-transit light curve, whereas the differential rotation is estimated from the successive transits of the supposedly same spot. Hence we obtain the value of the rotation period at the latitude of the transit. Moreover, using the known value of the average rotation period (the out-of-transit rotation period), it is possible to determine the profile of stellar rotation as a function of latitude. So far, I have considered a profile similar to that of the Sun:

$$P(\alpha) = \frac{360^\circ}{A - B \sin^2(\alpha)} \quad (1)$$

where α is the latitude, A and B are constants to be determined for each star. The relative differential rotation is defined as:

$$\frac{\Delta\Omega}{\Omega} = \frac{P_{pole} - P_{eq}}{\bar{P}} \quad (2)$$

where \bar{P} is the average rotation period. The estimated relative differential rotation of the stars studied thus far varies from 3 to 50%.

For systems with multiple planets such as those that Kepler has discovered [6,7], that transit their host star on different projected stellar latitudes, it is possible to confirm if the differential rotation profiles are similar or not to the solar profile given by Eq.(1).

References:

[1] Silva, A. V. R. 2003, ApJL, 585, 147
 [2] Silva-Valio, A., Lanza, A. F.; Alonso, R.; Barge, P. 2010, A&A, 510, 25
 [3] Silva-Valio, A. & Lanza, A. F. 2011, A&A 529, 36

[4] Lanza, A. F., Bonomo, A. S., Pagano, I. et al. 2011, A&A, 525, 14
 [5] Valio, A. & Lanza, A. F. 2011, ApJ (submitted)
 [6] Lissauer, J. J., Fabrycky, d. C., Ford, E. B. 2011, Nature, 470, 53
 [7] Borucki, W. J., Koch, D. G., Basri, G. 2011, ApJ, 736, 19

Kepler & Blazhko Effect: mission (im)possible? M. Chadid

Université Nice Sophia-Antipolis, Observatoire de la Côte d'Azur, UMR 6525, Parc Valrose, 06108 Nice Cedex 02, France (Chadid@unice.fr).

Antarctica Reaserch Station, South Pole, TAAF, Antarctica.

A large fraction of RR Lyrae stars has been known to exhibit amplitude and phase modulations – the Blazhko effect [1] – for about a century. We still lack quantitative constraints of the physical mechanisms driving and governing the Blazhko effect, thus limiting our understanding of the pulsation characteristics of RR Lyrae stars.

Thanks to extensive ground based observations, and those from the Antarctica [2] and the satellite mission, CoRoT [3] & [4], a continuous stream of data have been obtained to monitor in detail light curve changes during various Blazhko cycles. The ground based observations clearly show that consecutive Blazhko cycles are not exactly periodic and also that the Blazhko period differs from cycle-to-cycle. The CoRoT data, have found that the Blazhko phenomenon manifests itself as equidistantly spaced multiplets around the main pulsation frequency and its harmonics, which are not only triplet and quintuplet (as detected in ground based observations) but also tenth order side peaks. Strong cycle-to-cycle changes in the Blazhko modulation have been reported as well (Fig. 1). These findings place strong constraints on the theoretical models proposed to explain the Blazhko effect. Stothers [6] & [7] suggested that the turbulent/rotational dynamo mechanism generates, in some RR Lyrae stars, the magnetic fields that grow over the Blazhko cycle and suppress turbulent convection, and in turn small changes in the period of the fundamental radial mode. The physical mechanism suggested by Stothers appears promising, however no magnetic field has been detected in RR Lyrae stars [5].

Here, I discuss recent photometric results of Kepler Blazhko & non-Blazhko RR ab stars towards an understanding of the Blazhko enigma.

References:

- [1] Blazhko, S. 1907, *Astr. Nachr.*, 175, 325.
- [2] Chadid, M., Vernin, J., et al. 2010, *A&A*, 516, 15.
- [3] Chadid, M. et al. 2010, *A&A*, 510, 39.
- [4] Chadid, M., Perini, C., et al, 2011, *A&A*, 527, 146.
- [5] Chadid, M., Wade, G. A., Shorlin, S. L. S., Landstreet, J. D. 2004, *A&A*, 413, 1087.
- [6] Stothers, R. B. 2006, *ApJ*, 652, 643.
- [7] Stothers, R. B. 2010, *PASP*, 122, 536.

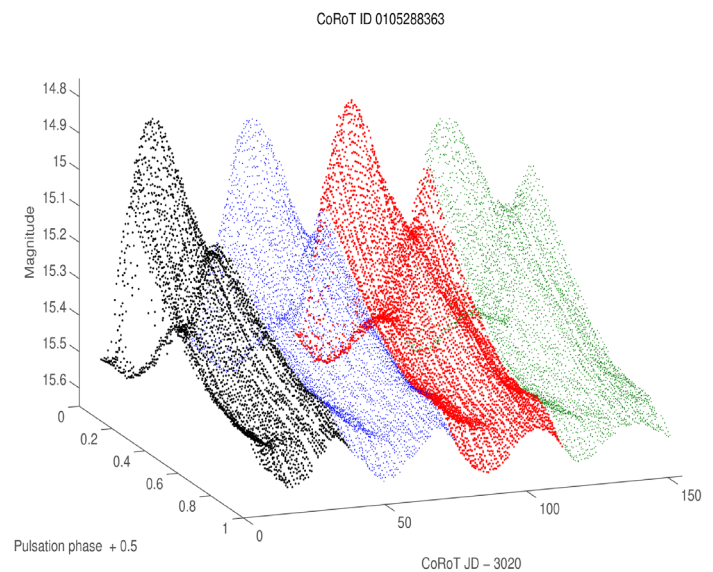


Fig. 1 Two-dimensional CoRoT light curve of CoRoT ID 0105288363 folded with the pulsation period (0.5676d) over four Blazhko cycles. Strong cycle-to-cycle changes in the Blazhko modulation [4].

P0802. POSTER SESSION II

Solar type pulsators on and near the Main Sequence E. Michel¹, ¹Observatoire de Paris, LESIA, pl. J. Janssen, F92195 Meudon, France, Eric.Michel@obspm.fr.

Introduction: Since acoustic oscillations have been observed in the Sun and their excitation mechanism understood, it has been clear that such oscillations had to be present in a noticeably large domain of mass and age covering low-mass stars to intermediate ones and all the Main Sequence evolution phase at least. The great success of helioseismology thus has logically motivated a great interest for extending this technique to such stars. While first detections have been achieved from the ground, first precise measurements of the modes in terms of eigenfrequencies, amplitudes and lifetimes, came only recently with space photometry observations. After more than four years in orbit, CoRoT has observed and measured oscillations in about a dozen of such stars, most of them on the Main Sequence, from early F stars to objects very close to our Sun in terms of effective temperature and evolution stage. This sample is being enlarged by new CoRoT observations and by the Kepler data.

I will discuss these results and show to which extent they satisfy the expectation of the community in terms of precision on the determination of the oscillation modes parameters. I will also use this sample to discuss what we already learned from them in terms of stellar physics and beyond, for instance in the case of stars hosting planets.

Asteroseismology of the solar-like star HAT-P-7: impact on the characterisation of its exoplanet companion

A. Grigahcène, M. Oshagh, O. BenOmar, M.-A. Dupret and M. J. P. F. G. Monteiro

HAT-P-7 is a very interesting star for more than one reason. First, it is a pulsating solar-like star, which allows us to characterize it and probe its interior through the study of its pulsations. Second, it lies within the field of view of the NASA spacecraft Kepler. Which is a great advantage since it allows us to access to very high quality and continuous observational data. In these conditions, a seismological study of this star is expected to give very good estimations of the star parameters, such as its mass, age, radius, ... These results can be used as input for the characterisation of the exoplanet orbiting it, which is the third reason to be interested by this star.

In this work:

- 1- we use the public Kepler data to estimate the star pulsation frequencies;
- 2- we perform an asteroseismic study of the pulsating star using Time-Dependent-Convection models;
- 3- and we make a revision of the planet properties using the asteroseismic results.

P0804. POSTER SESSION II

The Frequency Spectra of B Stars in Kepler. J. McKeever,¹ J. Jackiewicz,¹ B. McNamara,¹ R.T.J. McAteer,¹ L. Boucheron,² H. Cao,³ D. Voelz,² M. Kirk,¹ G. Taylor,¹ K. Degrave,¹ A. Al-Ghraibah,² A. Petsov,¹ and B. Calabro,¹
¹New Mexico State University, Department of Astronomy, PO Box 30001, MSC 4500, Las Cruces, NM 88003-8001, jeanm12@nmsu.edu, ²New Mexico State University, Department of Computer and Electrical Engineering, ³New Mexico State University, Department of Computer Sciences

Abstract: Balona et al. [1] has surveyed 48 B stars in the Kepler field and have noted that with space based observations, unprecedented details in the power spectra can be seen. We are expanding upon this study with a larger sample of approximately 200 B stars, of which only about 10% overlap with their sample. Here we present the results of our analysis, detailing the types of B star pulsations we find and the properties of their power spectra.

[1] Balona et al. (2011) *MNRAS*, 413, 2403-2420

P0805. POSTER SESSION II

Are the constant *Kepler* A-stars chemically peculiar? Simon. J. Murphy, Jeremiah Horrocks Institute, University of Central Lancashire, Preston, PR1 2HE, UK; email: smurphy6@uclan.ac.uk

Introduction: The delta Scuti instability strip lies at the junction between the classical Cepheid instability strip and the main sequence. Amongst the delta Scuti stars in this region lie the rather more constant metallic-lined (Am) stars. These represent a significant fraction of A stars – up to 50% at A8 [1]. Of the ten known Am stars in the *Kepler* field, six are known to pulsate [2].

Now that it is known that some Am stars do pulsate, we must question whether the constant A-stars *all* have Am spectra. Given that 70% of non-chemically peculiar stars are delta Scuti stars and are therefore variable (based on pre-*Kepler* photometric sensitivity levels; [3]), we might expect almost all of the non-variable stars in the *Kepler* field of view to be chemically peculiar.

The unprecedented precision of the *Kepler* spacecraft allows stars to be studied photometrically at the micro-magnitude variability level. Stars that are constant at this level are unusual indeed. Pulsation, spots and activity all contribute to total variability, hence these A-stars are probably the *only* stars in the HR-diagram that are truly constant.

Method: This study uses Q3 long-cadence *Kepler* data to investigate nine of the most constant A-stars in the *Kepler* field of view. This is accompanied by spectroscopic observations to investigate atmospheric parameters and chemical peculiarity.

References: [1] Smalley B. et al., 2011, *A&A*, 535, A3+ [2] Balona L. A. et al., 2011, *MNRAS*, 396 [3] Turcotte S., Richer J., Michaud G., Christensen-Dalsgaard J., 2000, *A&A*, 360, 603.

P0806. POSTER SESSION II

STANDARD PHOTOMETRY OF KEPLER ASTEROSEISMIC TARGETS. M. Steŝlicki¹, D. Drobek¹, M. Jerzykiewicz¹, J. Molenda-Źakowicz¹, K. Uytterhoeven^{2,3,5,6}, O. Creevey^{3,4}, J. Gutierrez-Soto⁷, P. Pappics⁸ and J. C. Suárez⁷, ¹Institut Astronomiczny Uniwersytetu Wrocławskiego, ul. Kopernika 11, 51-622 Wrocław, Poland (steslicki@astro.uni.wroc.pl), ²Departamento de Astrofísica, Universidad de La Laguna, 38205 La Laguna, Tenerife, Spain (TF), Spain, ³Instituto de Astrofísica de Canarias, C/Via Lactea s/n, E-38200 Tenerife, Spain, ⁴Universidad de La Laguna, Avda. Astrofísico Francisco Sánchez s/n, 38206 La Laguna, Tenerife, Spain, ⁵Laboratoire AIM, CEA/DSM-CNRS-Université Paris Diderot; CEA, IRFU, SAp, Centre de Saclay, 91191, Gif-sur-Yvette, France, ⁶Kiepenheuer-Institut für Sonnenphysik, Schöneckstraße 6, 79104 Freiburg im Breisgau, Germany, ⁷Instituto de Astrofísica de Andalucía (CSIC), Glorieta de la Astronomía s/n 18008, Granada, Spain, ⁸Instituut voor Sterrenkunde, K.U. Leuven, Celestijnenlaan 200D, 3001 Leuven, Belgium

Introduction: The main scientific goal of the NASA space mission Kepler is to discover Earth-sized planets. Kepler photometry is also used for detecting pulsations in thousands of stars selected as asteroseismic targets by the Kepler Asteroseismic Science Consortium. Unfortunately the Kepler data does not provide colour information. Moreover, the majority of the Kepler targets is poorly studied in the literature and the precision of T_{eff} , $\log g$, and $E(B-V)$ available in the Kepler Input Catalogue (KIC-10) is generally too low for asteroseismic modelling, especially for hot and peculiar stars. We report the status of ground-based multi-colour standard photometry of Kepler targets acquired in 2010 and 2011.

P0807. POSTER SESSION II

SPECTROSCOPIC AND PHOTOMETRIC OBSERVATIONS OF LARGE SAMPLE OF THE KEPLER TARGETS. M. Stęślicki¹, E. Niemczura¹, K. Uytterhoeven^{2,3,4,5} et al., ¹Instytut Astronomiczny Uniwersytetu Wrocławskiego, ul. Kopernika 11, 51-622 Wrocław, Poland (steslicki@astro.uni.wroc.pl), ²Departamento de Astrofísica, Universidad de La Laguna, 38205 La Laguna, Tenerife, Spain (TF), Spain, ³Instituto de Astrofísica de Canarias, C/Via Lactea s/n, E-38200 Tenerife, Spain, ⁴Laboratoire AIM, CEA/DSM-CNRS-Université Paris Diderot; CEA, IRFU, SAp, Centre de Saclay, 91191, Gif-sur-Yvette, France, ⁵Kiepenheuer-Institut für Sonnenphysik, Schöneckstraße 6, 79104 Freiburg im Breisgau, Germany

Introduction: The Kepler space mission is providing continuous and high-precision photometry of thousands of stars. Such data are essential for asteroseismic studies. However, the Kepler data do not provide information on the stellar physical parameters, which are also crucial for successful seismic modeling. Therefore, additional ground-based data are needed. We report the status of spectroscopic and photometric observations of middle main sequence stars (spectral types A-F) from the Kepler field. For a large sample of stars observed by various instruments we obtained effective temperatures, surface gravities, projected rotational velocities and abundances of chemical elements. These determinations are fundamental for seismic modeling of these objects.

P0901. POSTER SESSION II

A CYCLE 2 STUDY OF RV TAURI AND SEMI-REGULAR VARIABLES USING KEPLER. J. L. Cash¹ D.K. Walter² and S. B. Howell³, ¹ SC State University, Dept of Biological and Physical Science, Orangeburg, SC 29117, jcash@physics.scsu.edu, ²SC State University, dkw@physics.scsu.edu, ³NASA Ames, steve.b.howell@nasa.gov

Introduction: We present the results of our analysis of Cycle 2 observations of eleven (11) previously classified Semi-Regular and one (1) RV Tauri star in the Kepler Field of View. The high precision photometry and continuous monitoring capability of Kepler have allowed us to examine the light curves of these objects in unprecedented detail. We discuss the variety of behavior exhibited in the light curves of these stars. Some of our objects show very small or effectively no variation in their light output, while others show distinct variation over a magnitude or more. The light curve of the one previously classified RV Tauri type in our sample exhibits the well known alternating deep and shallow minima while one of the Semi-Regular types also hints at similar behavior. Several other stars show clear patterns of oscillation, and we present our results of the period determination along with the light curve fits and residuals for these stars. Over the time span of available observations, some of the light curves are highly irregular and longer timescales will be needed to resolve any multi-periodicity or determine the underlying semi-regular nature of the variability.

Support for this work has been provided to South Carolina State University through NASA award NNX11AB82G and NSF award AST-070814.

P0902. POSTER SESSION II

GRANULATION PROPERTIES IN RED GIANTS OBSERVED BY KEPLER. S. Mathur¹, S. Hekker^{2,3}, R. Trampedach⁴, J. Ballot^{5,6}, T. Kallinger^{7,8}, D. Buzasi⁹, R. A. García¹⁰, D. Huber¹¹, A. Jiménez^{12,13}, B. Mosser¹⁴, T. R. Bedding¹¹, Y. Elsworth³, C. Régulo^{12,13}, D. Stello¹¹, W. J. Chaplin³, J. De Ridder⁸, S. J. Hale³, K. Kinemuchi¹⁵, H. Kjeldsen¹⁶, F. Mullaly¹⁷ and S. E. Thompson¹⁷, ¹High Altitude Observatory, NCAR, P.O. Box 3000, Boulder, CO 80307, USA. (savita@ucar.edu) ²Astronomical Institute "Anton Pannekoek", University of Amsterdam, PO Box 94249, 1090 GE Amsterdam, The Netherlands. ³School of Physics and Astronomy, University of Birmingham, Edgbaston, Birmingham B15 2TT, UK. ⁴JILA, University of Colorado and National Institute of Standards and Technology, 440 UCB, Boulder, CO 80309, USA. ⁵Institut de Recherche en Astrophysique et Planétologie, Université de Toulouse, CNRS, 14 avenue E. Belin, 31400 Toulouse, France. ⁶Université de Toulouse, UPS-OMP, IRAP, 31400 Toulouse, France. ⁷Institute for Astronomy (IfA), University of Vienna, Turken-schanzstrasse 17, 1180 Vienna, Austria. ⁸Instituut voor Sterrenkunde, K.U. Leuven, Celestijnenlaan 200D, 3001 Leuven, Belgium. ⁹Eureka Scientific, 2452 Delmer Street Suite 100, Oakland, CA 94602-3017, USA. ¹⁰Laboratoire AIM, CEA/DSM – CNRS – Université Paris Diderot – IRFU/SAP, 91191 Gif-sur- Yvette Cedex, France. ¹¹Sydney Institute for Astronomy, School of Physics, University of Sydney, NSW 2006, Australia. ¹²Universidad de La Laguna, Dpto de Astrofísica, 38206, Tenerife, Spain. ¹³Instituto de Astrofísica de Canarias, 38205, La Laguna, Tenerife, Spain. ¹⁴LESIA, UMR8109, Université Pierre et Marie Curie, Université Denis Diderot, Obs. de Paris, 92195 Meudon Cedex, France. ¹⁵Bay Area Environmental Research Inst./NASA Ames Research Center, Moffett Field, CA 94035, USA. ¹⁶Danish AsteroSeismology Centre, Department of Physics and Astronomy, University of Aarhus, 8000 Aarhus C, Denmark. ¹⁷SETI Institute/NASA Ames Research Center, Moffett Field, CA 94035, USA.

Introduction: The Kepler mission has been observing more than 1000 red giants during a nearly continuous period of ~13 months. With the resulting frequency resolution ($< 0.03 \mu\text{Hz}$), we were able to study the granulation properties of these stars [1]. The granulation pattern is the visible manifestation of the convection taking place in the outer layers of the stars. Briefly, it is due to hot plasma from the interior rising to the photosphere where it cools down, and descends back into the interior at the edges of the granules. To estimate the granulation time scale and amplitude, Harvey-like functions [2] are fitted to the power spectra.

We found relations between the granulation parameters and acoustic-mode global parameters as well as with fundamental stellar parameters. These relations agree with what is expected from theory [3]. We also compared the observed granulation parameters with 3D hydrodynamics simulations of the convection [4]. Observations and simulations present similar trends though the absolute values still show some discrepancies.

References: [1] Mathur S. et al. (2011) *ApJ*, in press. [2] Harvey J. (1985) *ESASP*, 235, 199. [3] Kjeldsen H. and Bedding T. R. (2011) *A&A*, 529, L8. [4] Trampedach R. and Stein R. F. (2011) *ApJ*, 731, 78.

P1001. POSTER SESSION II

Kepler Data Analysis Tools Developed by the Guest Observer Office

Tom Barclay^{1,2} and Martin Still^{1,2}.

¹NASA Ames Research Center, MS 244-30, Moffett Field, CA 94035, ²Bay Area Environmental Research Institute.

*thomas.barclay@nasa.gov

Introduction: The Kepler Guest Observer Office has developed a suite of software tools for the reduction and analysis of Kepler pixel-level, light curve and full-frame image data. Most-critically, these tools can extract new light curves from pixel level data using manually-derived pixel apertures, and mitigate for instrumental artifacts using both detrending and cotrending algorithms.

Target Pixel Files: Pixel level data consists of a series of images of a target star and is distributed with each archived light curve. We have developed tools that allow the user to inspect pixel data, define new pixel extraction apertures and extract new light curves. Fig. 1 illustrates a case where a background eclipsing binary contaminates the archived light curve of a survey target. By employing two different apertures, two entirely different light curves are extracted.

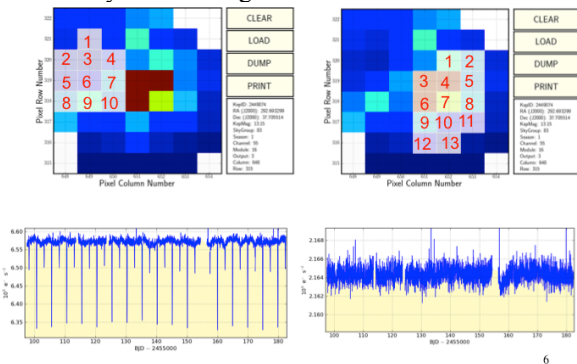


Figure 1: The upper panels showcase the pixel image of a star. The white pixels are employed to extract the time series photometry in the lower panels. The right-hand panel contains the extraction of just the target star, which the light curve reveals to be approximately non-variable. The left-hand panels reveal that there is an eclipsing binary star blended with, and to the left of, the target.

Cotrending Basis Vectors: The Kepler Mission has released data products to the public archive at MAST containing time-tagged characterizations of the instrumental systematics identified in the ensemble time-series of hundreds of intrinsically quiet stars collected each operational quarter. This product is known as the Cotrending Basis Vectors. We have developed a tool which fits these data to light curves and removes or reduces the instrumental structure, leaving calibrated photometric time series dominated by astrophysical variability.

Fig. 2 showcases 16 light curves chosen at random from a single CCD channel collected over quarter 5. The upper panel contains the archived data obtained from simple aperture photometry. All light curves contain both intrinsic astrophysical signal and instrumental systematics. The plots in the lower panel contain the same data after Cotrending Basis Vectors have been fit and removed. This leaves light curves with significantly reduced systematics.

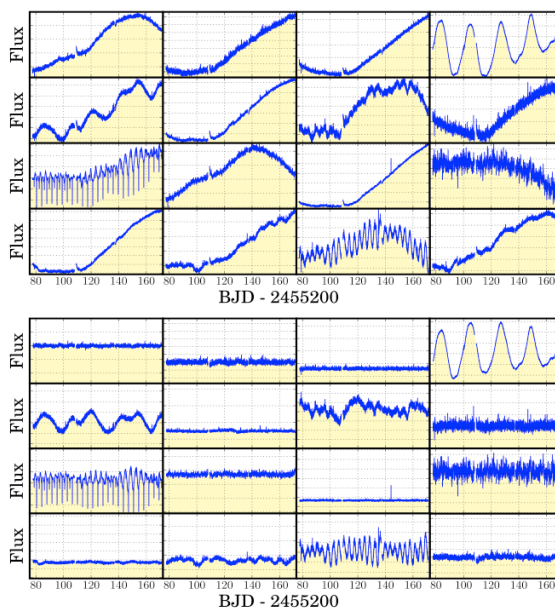


Figure 2: The upper panel exhibits 16 typical, long cadence light curves from the Kepler archive, constructed from calibrated, simple aperture photometry. The lower panel contains these same 16 light curves but with instrumental systematics reduced by fitting and subtracting Cotrending Basis Vectors.

Where to find these products and tools: The light curve and target pixel files are available from MAST: archive.stsci.edu/kepler. The Cotrending Basis Vectors are available from archive.stsci.edu/kepler/cbv.html. The Kepler data analysis tools come in the form of a PyRAF/IRAF package called PyKE, available from keplergo.arc.nasa.gov/ContributedSoftware.shtml

Summary: The Kepler Guest Observer and Science Offices continue to make available data and software tools that facilitate more accurate exploitation of Kepler photometry.

P1002. POSTER SESSION II

RECENT OPERATIONAL IMPROVEMENTS TO HIGH PRECISION PHOTOMETRIC OBSERVATIONS WITH WARM IRAC. S. Carey¹, J. Krick¹, J. Ingalls¹, K. von Braun², J. Stauffer¹, D. Charbonneau³, S. Ballard³, M. Fisher⁴, R. Olds⁴, ¹Spitzer Science Center, MS 220-6 Caltech, Pasadena, CA 91125; carey@ipac.caltech.edu, ²IPAC, ³Harvard-Smithsonian Center for Astrophysics, ⁴Lockheed Martin Denver.

The Spitzer project has recently made several improvements to the warm IRAC staring mode observations. This type of observation is critical not only for confirming Kepler planet candidates [1], but also for measuring transiting exoplanet atmospheric thermal profiles [2], atmospheric chemical compositions [3], and global wind and energy transport mechanisms. The IRAC 3.6 and 4.5 μm observations have significant photometric systematics due to a coupling of telescope motions with intra-pixel gain variations. These systematics are being trended with increasingly sophisticated techniques [4,5]. To mitigate the effect of these systematics in the data themselves, a cycling of an on-board heater was modified to reduce by $\sim 50\%$ both the amplitude and period of the pointing wobble, thereby reducing the aliasing of transits and improving photometric accuracy.

Most recently, we have commissioned a peakup mode to improve pointing for IRAC observations. Figure 1 displays the results of an experiment testing the repeatability and stability of the peakup mode. As shown, almost all of the ten individual observations land in the same 0.2×0.2 pixel region (which has minimal gain variation, the sweet-spot) with each epoch having excellent scatter (0.03 arcsec, 1σ radial rms over 2 minutes). This is a factor of 10 improvement over blind pointing. The peakup uses the optical peakup instrument (PCRS [6]) on the cryogenic focal plane previously used with great effectiveness with the IRS spectrometer. Preliminary high-precision ($\sim 10^{-4}$) gain maps of the sweet-spots will be presented. Coupled with science data taken at these sweet-spots, the gain maps permit observers to remove systematics in the photometry due to intra-pixel gain without self-calibrating their observations. Not only will this improve the removal of the systematics and precision of the observations, but it also lessens the likelihood of modifying scientifically interesting signatures such as atmospheric variations of the exoplanet or host star.

The peakup mode has been demonstrated for target stars with visible magnitude between 7 and 12.5 with fainter targets limited by the amount of data that can be stored and processed by the on-board computer while brighter sources saturate the PCRS detector. For sources outside of the peakup magnitude limits, preliminary tests have shown that the available PCRS guide stars can be used to accurately place the target on the IRAC arrays. These tests suggest that the

peakup will be available for the full magnitude range of Kepler exoplanets. We present results of a recent demonstration using KOI-069.

Use of the peakup mode should prove beneficial for full-phase light curve observations and other stares of greater than 24 hours. By performing peakups every ~ 8 hours, the ~ 0.3 arcsec/day pointing drift seen in long stares can be mitigated, while other solutions continue to be explored. In addition, tests are ongoing to demonstrate that light curves can be sampled sparsely and still recover phase variations. Sparse sampling has two benefits over traditional full-phase monitoring; 1) the curve can be sampled using $\sim 50\%$ of the observing time, and 2) the observations can be scheduled more flexibly, improving the likelihood of having the observation executed.

Full commissioning of the mode is ongoing with the expectation that all high-precision photometric observations will use peakups by the beginning of 2012. Use of the mode can continue as long as Spitzer is operating and should permit photon-limited follow-up and characterization of all Kepler discoveries.

References: [1] Fressin et al. (2011) arXiv:1105.4647. [2] Beerer et al. (2011) ApJ, 727, 23. [3] Fortney et al. (2011) arXiv:1109.1611. [4] Ballard et al. (2010) PASP, 122, 897. [5] Demory et al. (2011) A&A, 533, A114. [6] Mainzer & Young (2004) SPIE, 5487, 93.

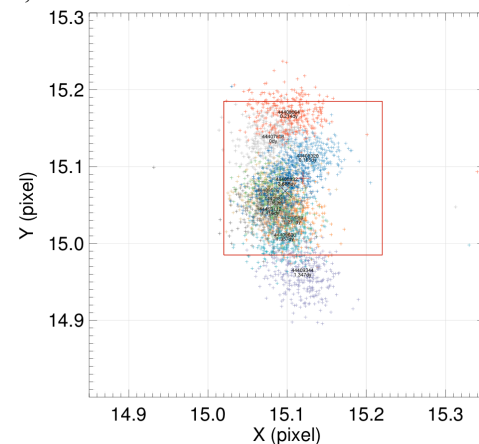


Figure 1: Centroid positions for ten epochs of the 4.5 μm subarray PCRS peakup test. Each epoch (represented by a different color) consists of an initial slew to the PCRS, peakup on the PCRS, offset to IRAC and 2.25 minutes of 0.4 second frames while staring. The box indicates the 0.2×0.2 region of the pixel with minimal gain variations that (sweet-spot).

P1003. POSTER SESSION II

Kepler Observations of II ZW 229.015 M.T. Carini¹, W.T. Ryle², ¹Western Kentucky University, Department of Physics and Astronomy, 1906 College Heights Blvd. Bowling Green, KY. 42103, mike.carini@wku.edu, ²Thomas More College, wesley.ryle@thomasmore.edu.

Introduction: The seyfert 1 galaxy II ZW 229.015 has been observed with the Kepler spacecraft since quarter 4 of Kepler science operations. The results of the quarters 4-7 (1 year) Kepler observations will be presented. We find the source to be highly variable, with discrete variations occurring on timescales as short as days and with amplitudes as small as 0.5%. Such small amplitude, rapid variability was previously undetected in seyfert galaxies. We compare the Kepler results with contemporaneous ground based optical observations derived from the literature[1]. The results of a PSRESP analysis searching for a break in the PDS and the resulting characteristic timescale and corresponding mass estimate will be presented.

References:

[1] Barth, A. J. et al. ApJ 732,121

P1004. POSTER SESSION II

KEPLER AND THE NEXT GENERATION: EFFECTIVE APPLICATION OF EDUCATION/PUBLIC OUTREACH IN THE HIGH SCHOOL SCIENCE CLASSROOM. N. M. Chambers¹, West High School, 20401 Victor Street, Torrance, CA 905030, nchambers@etusd.org.

Introduction: One goal of the Kepler Mission's Education and Public Outreach is effective and meaningful communication of the concepts, process, and outcomes of the mission to high school age students in a formal education setting. After the author's participation in the 2009 E/PO workshop at the Jet Propulsion Laboratory, the Transit Tracks activity [1] was incorporated into a high school astrobiology curriculum at two different learning levels (9th/10th grade introductory, and 11th/12th grade advanced). The author will discuss initial success stories and explain how the activity was modified, extended and enriched with additional outside resources and original ideas in 2010 and 2011.

The original activity, which is taught in a knowledge forming context, is revisited and incorporated into a unit-summarizing final assessment of student understanding. This final assessment incorporates the use of transit light curves and absorption spectroscopy to simulate the identification of a potentially habitable extrasolar planet. Concept mastery, data analysis, and synthesis of evidence-based conclusions are an expected outcome of this project. The author will present both the assignment and student products.

General feedback on the E/PO effort, including what elements translate successfully into a 9-12 classroom as well as suggestions for improvement, will be included.

References:

[1] <http://kepler.nasa.gov/education/activities/transitTracks/>

P1005. POSTER SESSION II

FOLLOW-UP OF THE WTS/ROPACS CANDIDATES: DETECTION OF FALSE POSITIVES. P. Cruz¹, D. Barrado^{1,2}, S. Hodgkin³, J. Birkby⁴, and the RoPACS Consortium. ¹Center of Astrobiology (CAB/INTA-CSIC), ESA P.O Box 78, 28691 Villanueva de la Canada, Madrid, Spain e-mail: pcruz@cab.inta-csic.es , ²Calar Alto Observatory, German-Spanish Astronomical Center (CAHA) e-mail: barrado@cab.inta-csic.es , ³Institute of Astronomy, Cambridge e-mail: sth@ast.cam.ac.uk , ⁴Leiden Observatory, Leiden University email: birkby@strw.leidenuniv.nl .

Abstract: This work is dedicated to identify false positives within the list of planet-host candidates from the WFCAM Transit Survey (WTS). The RoPACS* network utilizes WTS to discover and study planets around cool stars, at infrared wavelengths, via the transit method.

Spectroscopic follow-up has been performed for some of the planet-host candidates to find their spectral types and to exclude non-planetary companions. Those candidates from late-type stars undergo a more detailed follow-up with intermediate resolution spectroscopy in order to detect changes in their radial velocities that could correspond to a more massive object such as brown-dwarfs or low-mass stars.

Partial results from observations taken with the 3.5-meter telescope at the Calar Alto Observatory will be presented in this poster. Future plans are to apply the same technique to the Kepler candidates that have Jupiter-like radius.

* The RoPACS Project is a Marie Curie Initial Training Network funded by the European Commission's Seventh Framework Programme (<http://star.herts.ac.uk/RoPACS/>).

P1006. POSTER SESSION II

Searching for Earth’s Twin and STEM Education—the *Kepler Mission’s* Education and Public Outreach Program. E. K. DeVore¹, A. G. Gould², P. K. Harman¹, D. G. Koch³, and S. B. Howell³, ¹SETI Institute, 189 Bernardo Ave, Mountain View, CA 94043, edevore@seti.org, ²Lawrence Hall of Science, University of California at Berkeley, CA 94720, ³Kepler Science Office, NASA Ames Research Center, Moffett Field, CA 94035

Introduction: Are we alone? Are there other worlds like our own? Astronomers are discovering many exoplanets, but can smaller planets - new Earths - be found? These are powerful and exciting questions that motivate student learning and public interest in the *Kepler* search for planets. The *Kepler Mission* Education and Public Outreach (EPO) program capitalizes on the excitement of discovering Earth-size planets in the habitable zone, stimulating student learning and public interest in Science, Technology, Engineering and Mathematics (STEM) education, particularly astronomy and physics.

Who is the Audience for *Kepler Mission* EPO? The EPO program aims to bring *Kepler* science and discoveries to multiple audiences: students and teachers in formal educational institutions, the general public in informal settings such as museums and planetariums, and the general public through the media and outreach activities such as radio programs, star parties and a robust website. See Figure 1.

EPO expertise plus existing networks of educators and outreach agents to the *Kepler Mission*, which amplify the EPO program’s reach to students, teachers and the public. Examples: *Kepler* lessons are reaching thousands of schools across the nation through the Lawrence Hall of Science’s GEMS *Space Science Sequence for grades 3-5 and 6-8*, and the FOSS *Planetary Science* unit for middle schools. The production and distribution of the *Kepler Mission* poster with published articles via science education organizations brings *Kepler* to about 80,000 US STEM teachers in middle and high schools, plus planetarium directors internationally[1]. The *Shadows and Silhouettes* kit for amateur astronomers supports outreach to the public as well as schools, and has been used by hundreds of clubs in every state (reaching more than 100,000 people) to explain lunar phases, eclipses and planetary transits; it was developed and distributed in partnership with the Astronomical Society of the Pacific, which leads the Night Sky Network. A partnership with the Space Science Institute (Boulder, CO), created a set of museum exhibits that features the search for life beyond Earth, *Alien Earths*, that toured the national for five years, and are now a part of the permanent exhibits at the Virginia Air and Space Museum. These projects and others that leverage the *Kepler* EPO program will be discussed as models for NASA EPO programs. Partnerships offer both a greater impact in terms of the reach of programs and the effectiveness of NASA funding in enhancing STEM education.

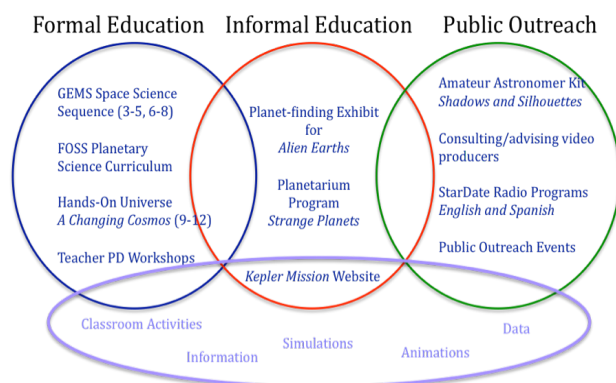


Figure 1: The Scope of *Kepler* EPO Program

High Impact Leverage and Partnerships: The *Kepler* EPO goals are to increase public awareness and understanding of the *Kepler Mission* by embodying key principles set forth in *NASA’s Partners in Education and Implementing the OSS Education/ Public Outreach Strategy*: involve scientists and contractors in EPO efforts, establish collaborations with planetarium programs and science museums, and build on existing programs and networks that maximize the leverage of NASA EPO funding in this project. The *Kepler* EPO plan is designed to take advantage of existing collaborations, networks, experience, and relationships to optimize the impact of EPO. These partnerships bring

Reflections on Long-Duration EPO Programs: The *Kepler* mission EPO program has been in existence the entire duration of the *Kepler Mission*. The long-duration of the program has required that the EPO program team adapt to new opportunities and to new challenges. These include spin-off projects developed with *Kepler* data that engage the public in citizen science. The presentation will close with a brief discussion on the evolution of the *Kepler* EPO program.

References: [1] Koch, D. G., DeVore, E., Gould, A., Harman, P. Seeking Other Worlds, Vol. 33 No. 4, 2009 Science Scope, NSTA. and Koch, D. G., DeVore, E., Gould, A., Harman, P. Take Off With NASA’s Kepler Mission! V. 76 No. 1, 2009 Science Teacher, NSTA. and Gould, A., Komatso T., DeVore, E., Harman, P., Koch, D. G., Share the Hunt for Other Earths, March 2009, The Planetarian, IPS.

P1007. POSTER SESSION II

A UBV Photometric Survey of the Kepler Field. M. E. Everett¹, S. B. Howell² and K. Kinemuchi², ¹NOAO (950 N. Cherry Ave., Tucson, AZ 85719; everett@noao.edu), ²NASA Ames.

Abstract: We present first results from an optical photometric survey of the Kepler field in the Johnson UB_v filters. The primary goal of the survey is to produce a catalog that identifies blue objects for spectroscopic follow-up studies and inclusion as Kepler targets. We have used the NOAO Mosaic 1.1 CCD camera at the WIYN 0.9m telescope to cover the field in a series of 207 overlapping pointings. Each pointing was observed using consecutive 40s exposures in B and V and 180s in U. Calibration is done by setting our magnitudes and colors according to the transformed KIC magnitudes of selected stars in each pointing and by minimizing any remaining differences in sources observed in areas of image overlap. The UB_v colors reveal a rich set of blue sources that include objects such as hot subdwarfs and white dwarfs, planetary nebula nuclei, and cataclysmic variables.

Extragalactic Science With Kepler

Michael N. Fanelli¹, Pamela M. Marcum² and Cassidy Newton³,

¹NASA-Ames Research Center, MS 244-30, Moffett Field, CA, michael.n.fanelli@nasa.gov; ²NASA-Ames Research Center, pamela.m.marcum@nasa.gov; ³Texas Christian University, csmith2@tcu.edu

Although designed as an exoplanet and stellar astrophysics experiment, the Kepler mission provides a unique capability to explore the essentially unknown photometric stability of galactic systems at millimag levels using Kepler's blend of high precision and continuous monitoring. Time series observations of galaxies are sensitive to both quasi-continuous variability, especially low-level variations from embedded active nuclei, and random, episodic events, such as supernovae. In general, galaxies lacking active nuclei are not expected to be variable on the timescales and amplitudes observed in stellar sources and are free of source motions that affect stars (e.g., parallax). These sources can serve as a population of quiescent, non-variable sources, which can be used to quantify the photometric stability and noise characteristics of the Kepler photometer.

A factor limiting robust galaxy source selections in the Kepler FOV is the lack of detailed quantitative information about the galaxy population. The only systematic census of galaxies in this low galactic latitude field is the 2MASS extended source catalog, which list ~11K sources at *JHK* magnitudes. Optical photometric and spectroscopic information is lacking, constraining for example the identification of AGN candidates in this field.

Despite these limitations, a significant and growing number of galaxies are being observed, forming the Kepler Galaxy Archive. Galaxy time series were/are being obtained by dedicated Guest Observer programs in Cycle 1-3 along with a small number of serendipitous sources found in the exoplanet survey. Observed sources total approximately 100, 250, and 700 in Cycles 1-3 (Cycle 3 began in June 2011).

In this poster we interpret the properties of a set of ~20 galaxies monitored during quarters 4-8, their associated light curves, photometric and astrometric precision and potential variability as revealed by periodograms. Data analysis issues relevant to extended sources and available software tools will be discussed. In addition, we detail ongoing surveys which are providing new photometric and morphological information on galaxies over the entire field. These new datasets will both aid the interpretation of the time series and improve source selection, e.g., help identify candidate AGNs and starburst systems, for further monitoring.

P1009. POSTER SESSION II

EChO: an exoplanetary mission under study

K. G. Isaak¹, the EChO study science team (P. Drossart², O. Krause³, C. Lovis⁴, M. Ollivier⁵, I. Ribas⁶, I. Snellen⁷, B. Swinyard⁸, G. Tinetti⁹) and the ESA EChO study team (L. Puig¹⁰, I. Escudero Sanz¹¹, P-E. Crouzet¹², D. Martin¹³, N. Rando¹⁴)

¹ESA/ESTEC, Keplerlaan 1, Noordwijk 2201-AZ, Netherlands: kate.isaak@esa.int , ²LESIA, France: pierre.drossart@obspm.fr , ³MPIA, Germany: krause@mpia.de , ⁴Observatoire Astronomique de l'Université de Genève, Switzerland: christophe.lovis@unige.ch , ⁵IAS, France; marc.ollivier@ias.u-psud.fr , ⁶CSIC/IEEC, Spain: iribas@ice.csic.es , ⁷Leiden University, Netherlands: snellen@strw.leidenuniv.nl, ⁸RAL, UK: bruce.swinyard@stfc.ac.uk, ⁹University College London, UK: g.tinetti@ucl.ac.uk , ¹⁰ESA/ESTEC, Netherlands: ludovic.puig@esa.int , ¹¹ESA/ESTEC, Netherlands: isabel.escudero.sanz@esa.int, ¹²ESA/ESTEC, Netherlands: pierre-elie.crouzet@esa.int, ¹³ESA/ESTEC, Netherlands: didier.martin@esa.int, ¹⁴ESA/ESTEC, Netherlands: nicola.rando@esa.int.

Introduction:

The Exoplanet Characterization Observatory (EChO) is a medium class mission under study within the framework of the Cosmic Vision 2015-2025 program of the European Space Agency. It is one of four candidates currently competing for the M3 launch slot in the 2020-2022 timeframe. EChO will be dedicated to, and optimized for, transit spectroscopy, and will characterise the atmospheres of exoplanets ranging from hot Jupiters down to more temperate, super Earths through measurement of transmission, reflection and absorption spectra covering the 0.4 - 16 micron wavelength range.

In this poster we outline the primary science goals of the EChO mission, detail the high-level science requirements necessary to achieve these goals and present a preliminary mission reference concept that has been developed during a recent assessment activity within the ESA Concurrent Design Facility.

Prof. Adil. H Khan

Jiwagi University India Govt. Kasturba Girls College Guna M.P.India

Atmospheric Pollution "A cause study of Air plane Space Shuttle & Rockets Pollution & Space disaster

In the space disaster January 28, 1986, the space shuttle Challenger damaged seventy three seconds into its flight in air , killing the seven members . This accident was believed the temperature of the day .Actually, the space shuttle main engines run based on hydrogen and oxygen as stated above, which are mixed together to form good old fashioned H₂O. Space shuttle launched produces tons of carbon dioxide and Its derivatives. About lot of tons harmful particulate matter settle around the launch area and nearly tons of acid kill animals. Air operation has carbon dioxide emissions of nearly tons a month and data shows the 66000 airplanes that fly in and out of the airport each month emit about 16,00000 tons of carbon dioxide.

P1011. POSTER SESSION II

Prof. Adil. H Khan

Jiwagi University India Govt. Kasturba Girls College Guna M.P.India

ATMOSPHERE: Origin Of Atmosphere & Space Pollution (Aerosols, Clouds , Water Cycle) and study of key sources of satellites , Space Shuttle & Rockets "

Aerosols is the smallest part of the atmosphere it's activity creating unbalanced the atmospheric composition . The composition of the clouds Aerosols and hydrological cycle are connected with radiation In single word we can say that it's a reaction of various excited and non excited Chemical in the atmosphere . Aerosols origin based on soil erosion , dust particles , Vol cones ,forest and the activity of the wild life animals , human activities(Industry , Vehicle Pollution, & etc.) , such as the burning of fossil fuel , dust storms ,Sea spray etc. In similarly the origin of aerosols is effecting to all the part of pollution in other word we can say that aerosols is the smallest unit of the pollution .In the origin of aerosols is the starting process of pollution . The tiny particles (aerosols) origin depend in to the human activity in the atmospheric planet . These aerosols start the absorption of radiation or in other word we can say that start the reaction between the aerosols and radiation because both origin are chemically and the similarity is that both are the excited state of the chemical's in the atmosphere . They also produce brighter clouds that are less efficient at releasing precipitation. These in turn lead to large reductions in the parts of the radiation reaching Earth's surface, these radiation's heating of the atmosphere, changes the composition of the atmospheric temperature, unbalanced rainfall, and small amount removal of pollutants. These aerosol are creating the weaker hydrological cycle in day by day , which is connecting directly to availability and quality of water in the river and other sources of water , a major environmental problem of the today scenario.

P1012. POSTER SESSION II

Selecting New Variable Star Targets from the Kepler Full Frame Image Variability Catalog. K. Kinemuchi^{1,2}, M. Still^{1,2}, S. Howell¹ and R. Szabo³ (¹NASA-Ames Research Center, Mail Stop 244-30, Moffett Field, CA 94035, ² Bay Area Environmental Research Institute, 560 Third St. West, Sonoma, CA 95476, ³ Konkoly Observatory of the Hungarian Academy of Sciences, P.O. Box 67, H-1525 Budapest, Hungary.)

Abstract: Kepler provides an unique and powerful resource for performing serendipitous time-domain astrophysics. However, due to telemetry restrictions, only 170,000 targets are observed each quarter, of which 4% are reserved through the Guest Observer and Kepler Asteroseismic Science Consortium (KASC) programs for targets of specific stellar and extragalactic interest. There exists 10^7 sources within the Kepler field of view brighter than $K_p=21$ confusion limit. For providing Kepler with the highest impact to astrophysics, survey resources are needed to aid the community in selecting the highest value targets through multiwavelength, color, and timing information.

One method for identifying targets of high potential astrophysical interest is to extract variable stars from the Kepler Full Frame Images (FFIs). These images are taken principally for engineering purposes at one month intervals with 30-minute exposure times. We can find variable objects in the Kepler field of view from the FFI frames through difference imaging, and we performed aperture photometry to those stars. We used the eight FFI frames collected during the spacecraft commissioning phase (Quarter 0) to create a catalog of variable objects.

We find over 200,000 variable objects in the Kepler field, and there are a variety of pulsators, rotators, eruptive, or eclipsing stars, as well as other exotic variable stars exhibiting subtle or large brightness changes over a short timescale. Kepler is currently not observing approximately 50% of the detected variable stars from our catalog.

The FFI catalog increases the number of known variable stars in the Kepler field and provides new targets for astrophysical studies. It will also provide a target selection resource of high value for Kepler astrophysics projects through the KASC, the Guest Observer Program, or Guest Observer Director's Discretionary Time during an extended Kepler mission. The catalog will be made available through the Multi-Mission Archive at STScI (MAST).

P1013. POSTER SESSION II

Science from Kepler Collateral Data: 50 ksec/year from 13 million stars. J. J. Kolodziejczak¹ and D. A. Caldwell², ¹Space Science Office, NASA Marshall Space Flight Center, Huntsville, AL 35812; kolodz@nasa.gov, ²SETI Institute, NASA Ames Research Center; Douglas.Caldwell@nasa.gov.

Introduction: As each Kepler frame is read out unshuttered, light from each star in a CCD column accumulates in successive pixels as they wait for the next row to be read out. This accumulation is the same in the masked rows at the start of the readout and virtual rows at the end of the readout as it is in the science data. A range of these "smear" rows are added together for each long cadence and sent to the ground for calibration purposes. We will introduce and describe this smear collateral data, discuss and demonstrate its potential use for scientific studies exclusive of Kepler calibration,[1,2] including global characteristics of stellar variability, which are influenced by parameters of galactic evolution.

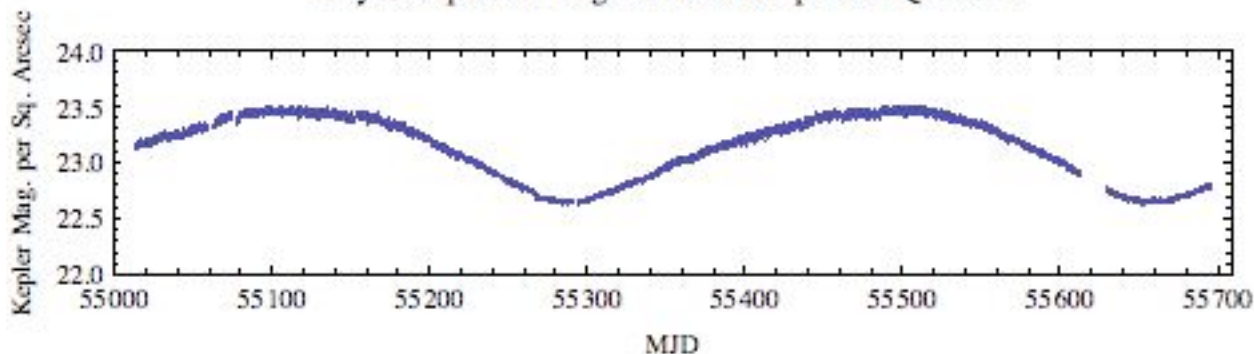
Photometric Precision: The smear data consists of individual column data for 24 rows, which represents a 0.178% duty cycle or ~50 ksec of observing time / year on every star in the Kepler field. This amounts to continuous 1/2 hour sampling of all stars at a sensitivity

level 1/23rd that of the regular science targets with the significant limitation that stars sharing the same CCD column are summed.

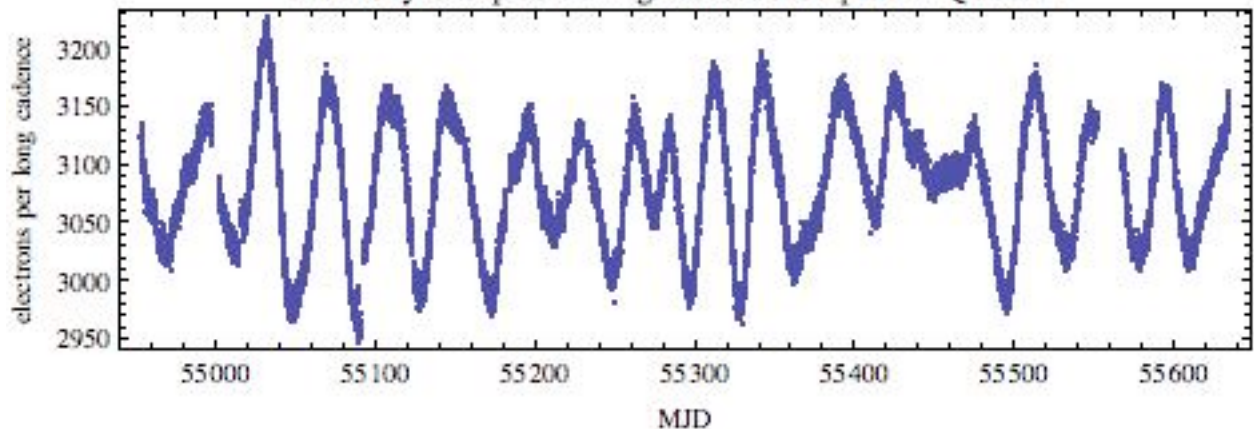
Applications: The smear data contain projected information on zodiacal light and background, variable stars, variability of stellar populations. The figures below show an example of background estimation, and a sample light curve including data from a bright variable star during Q0-Q8 from the sky group cycling through Ch. 7.3, 17.3, 19.3, and 9.3 during Q1-Q4, respectively. Additional examples will be show along with discussion of the necessary steps required to analyze this unique data set, methods for accounting for image artifacts[3], and peculiar limitations arising from the short exposures and projected nature of the data.

References: [1] J. M. Jenkins, et al. (2010) *ApJ*, 713, L87. [2] D. A. Caldwell et al. (2010) *ApJ*, 713, L92. [3] J. J. Kolodziejczak. (2010) *Proc. SPIE*, 7742, 38.

Preliminary Estimate of Sky Brightness for Sky Group containing Module 7 Output 3 in Quarter 1



Preliminary 2-Year Smear Light Curve for an Example (KepMag = 9.2) Variable Star from Sky Group containing Module 7 Output 3 in Quarter 1



Kepler Science Operations Center Software Infrastructure

. S. McCauliff¹, T. C. Klaus²

1. Orbital Sciences Corporation/NASA Ames Research Center, Moffett Field, CA 94035, USA, sean.d.mccauliff@nasa.gov

2. Orbital Sciences Corporation/NASA Ames Research Center, Moffett Field, CA 94035, USA, todd.klaus@nasa.gov

Introduction: We discuss several software infrastructure components of the Kepler Science Operations Center (SOC) data reduction pipeline. The pipeline infrastructure (PI)[1] job descriptions and execution environment allow for execution of science algorithm implementations in a variety of languages. PI scales well from laptops with single processors to the Pleiades supercomputer at NASA/Ames. The Kepler mission’s focus on time series data has required the creation of a new database management system, Kepler DB[2]. Kepler DB is a database management system for storing arrays, sparse arrays and arbitrary binary data. Modifications to data stored in Kepler DB are atomic and consistent. We conclude with an overview of the hardware needed to process Kepler data.

Pipeline Infrastructure: The SOC pipeline infrastructure (PI) abstracts distributed execution and work description across a cluster of machines on which the pipeline runs. Work is described by space and time constraints which can vary between different processing stages. For example, photometric analysis is performed for all the targets on the same CCD output, but transiting planet search[3] (TPS) is performed for individual targets. The SOC 7.0 release has added the ability to execute jobs on remote machines, in this case the Pleiades supercomputer at NASA/Ames. This has been instrumental in the processing of the multi-quarter TPS on ~ 200,000 distinct targets the Kepler mission has observed over all quarters.

Kepler DB: Kepler DB is a database management system to manage data as arrays and sparse arrays. It differs from relational databases in that it does not store data in terms of tuples and their relations. This is similar to approaches taken by other database management systems such as SciDB[4]. Besides being a more natural data storage representation for the Kepler science data, this representation is also more efficient than a relational database. Kepler DB currently manages 7.1TiB of data spread among tens of millions of arrays and sparse arrays. PI provides some infrastructure for sending the science data stored in Kepler DB to the computing nodes of the Pleiades supercomputer.

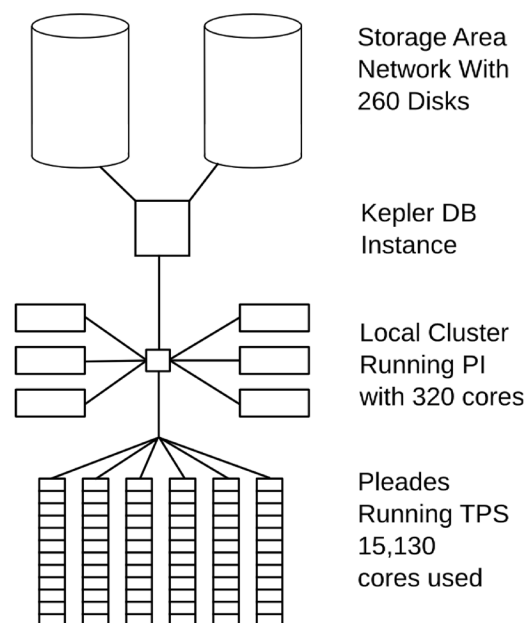


Illustration 1: SOC data flow for TPS processing on the Pleiades supercomputer. Links between components represent bidirectional data flow.

References:

[1] T. C. Klaus, et. al., (2010), Proc. SPIE, Vol. 7740, 77401B. [2] S. McCauliff, et. al. (2010), Proc. SPIE, Vol. 7740, 77400M. [3] P. Tenenbaum, et. al., (2010) Proc. SPIE 7740. [4] Cudre-Mauroux, P. et. al., (2009) Proc. VLDB.

P1015. POSTER SESSION II

USING MULTICOLOR PHOTOMETRY TO CONFIRM TRANSITING PLANET CANDIDATES.

H. Parviainen¹, B. Tingley² and H. Deeg³. Instituto de Astrofísica de Canarias, C/ Vía Láctea, s/n, E38205 - La Laguna (Tenerife). España. ¹hannu@iac.es, ²btingley@iac.es, ³hdeeg@iac.es

Introduction: If transits of planets are observed in multiple colors, a color signature is revealed that is very distinct from those produced by eclipsing binaries, blended or otherwise. It arises due to the interplay between the comparatively small size of the planets relative to its parent star and differential limb darkening. While this technique has its limitations, it can provide relatively quick confirmations without heavy consumption of telescope resources for some candidates.

In addition to this use, these same observations can also be used to test model stellar atmospheres, both to determine if their accuracy is sufficient for PLATO mission goals and to evaluate if the one-dimension models currently used to generate limb-darkening coefficients are sufficient to explain the observations. If not, the new 3-D model stellar atmospheres might need to be used, which has implications that extend far beyond the exoplanet field.

In this talk, we also present high cadence multi-color observations of two Kepler candidates with the GTC that demonstrate the usefulness -- and limits -- of this technique.

P1016. POSTER SESSION II

Demystifying Kepler Data: A Beginner's Guide

Joshua Pepper (1), Karen Kinemuchi (2), Martin Still (2), Michael Fanelli (2), Thomas Barclay (2)
(1) Vanderbilt University (2) NASA Ames Research Center & Bay Area Environmental Research Institute
joshua.pepper.v@vanderbilt.edu

Kepler is producing the best photometric data ever recorded. However, the sheer detail of the data, combined with the technical challenges and characteristics of a space-based mission, has resulted in a data set and accompanying metadata that can be difficult for astronomers who are used to ground-based photometry to start working with. The extensive Kepler documentation does not offer an easy place to begin learning how to employ the Kepler lightcurves. Our paper is designed to be a useful primer for the average astronomer to understand the characteristics and capabilities of the Kepler data, metadata, mission, documentation, and websites.

P1017. POSTER SESSION II

A deep, high cadence photometric survey of the Kepler field.

Gavin Ramsay¹, Adam Brooks¹, Tom Barclay², Martin Still², Pasi Hakala^{3,1} Armagh Observatory, Northern Ireland, ²NASA Ames Research Center, USA, ²Finnish Center for Astronomy with ESO, FINCA, Finland.

This summer we commenced a deep, high cadence, photometric survey of the Kepler field using the 2.5m Isaac Newton Telescope and the Wide Field Camera on La Palma. We take a series of 20 sec exposures in the *g* band lasting one hour. Light curves are obtained for all sources in the field and those which are variable identified. We are sensitive to objects in the range $13.5 < g < 21$ and variability on timescale of 2 mins to one hour. Unlike other surveys, we aim to cover the whole of the Kepler field. Currently we have covered more than 1/4 of the field with further observations expected in the summer of 2012. Initial results suggests our existing data contains nearly 1000 sources which have variability timescales less than 40 mins. Our ultimate goal is to obtain photometry of our most astrophysically interesting sources using *Kepler* in Short Cadence mode. Our data has already led to one object, a PG1159 star, being scheduled for SC mode observations. We will make the results of our survey public.

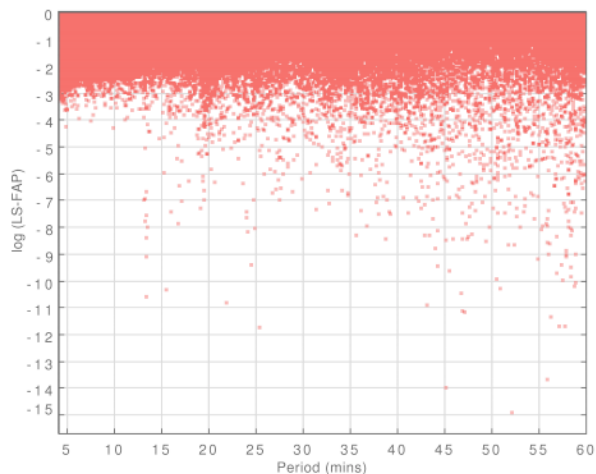


Figure 1: This shows the period of variability as a function of the Lomb-Scargle False Alarm Probability for nearly half a million stars in the Kepler field. The light curves were obtained using the INT and Wide Field Camera on La Palma. Strongly variable sources have more negative values. This figure contains only a sub-set of our existing data as further data is currently being analysed.

Removing the Noise While Preserving the Signal – An Empirical Bayesian Approach to Kepler Light Curve Systematic Error Correction.

Jeffrey C. Smith^{*1}, T. Barclay², M. N. Fanelli², J. M. Jenkins¹, J. Kolodziejczak³, R. Morris¹, Martin C. Stumpe¹, J. Twicken¹, J. Van Cleve¹,

^{*}jeffrey.smith@nasa.gov, ²SETI Institute/NASA Ames Research Center, MS 244-30, Moffett Field, CA 94035, USA, ³Bay Area Environmental Research Institute, ⁴NASA Marshall Space Flight Center,

Introduction: With the unprecedented photometric precision of the Kepler Spacecraft, significant systematic and stochastic errors on transit signal levels are observable in the Kepler photometric data [1]. These errors, which include discontinuities, outliers, systematic trends and other instrumental signatures obscure astrophysical signals. The Presearch Data Conditioning (PDC) module of the Kepler data analysis pipeline tries to remove these errors while preserving planet transits and other astrophysically interesting signals. The old implementation of PDC used for previous data releases performed well for simulated data with SoHo solar measurements but the completely new noise/stellar variability regime observed in Kepler data posed a significant problem [2]. These variable stars are often of particular astrophysical interest and the old PDC did not perform optimally by suppressing the variability. A completely new version of PDC has been developed and is included in the Kepler 8.0 pipeline software release.

We present a Bayesian Maximum A Posteriori (MAP) [3] approach where a subset of highly correlated and quiet stars is used to generate a cotrending basis vector set which is in turn used to establish a range of "reasonable" robust fit parameters. These robust fit parameters are then used to generate a "Bayesian Prior" and a "Bayesian Posterior" PDF (Probability Distribution Function). When maximized, the posterior PDF finds the best fit that simultaneously removes systematic effects while reducing the signal distortion and noise injection which commonly afflicts simple Least Squares (LS) fitting. A numerical and empirical approach is taken where the Bayesian Prior PDFs are generated from fits to the light curve distributions themselves versus an analytical approach.

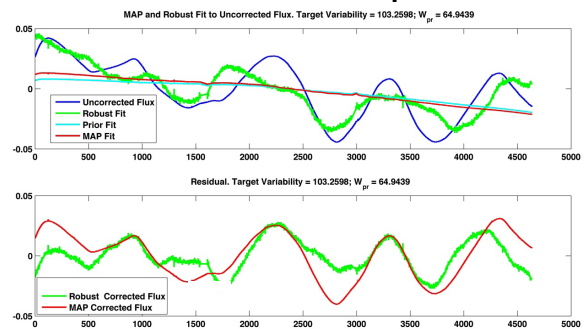
The figures below show examples of PDC-MAP performance on two variable stars. The blue curve is the uncorrected light curve, the green is a robust fit of the basis vectors to the data, the cyan is a fit based on the prior PDF of surrounding light curves and the red is the posterior PDF MAP fit which weighs both the prior and robust fit curves. The resultant removes the systematic trends yet preserves the intrinsic stellar variability without introducing noise. The new PDC drastically improves Kepler's ability to understand the properties of parent stars and therefore ultimately im-

prove Kepler's primary mission of detecting Earth-like planets. But PDC-MAP also improves the Kepler data's utility to the broader astrophysical community. Future improvements to the current design are presented in a companion poster by M. C. Stumpe et al. Also, along with the systematic effects there are Sudden Pixel Sensitivity Dropouts (SPSDs) resulting in abrupt steps in the light curves and its removal is presented in another companion poster by R. L. Morris et al.

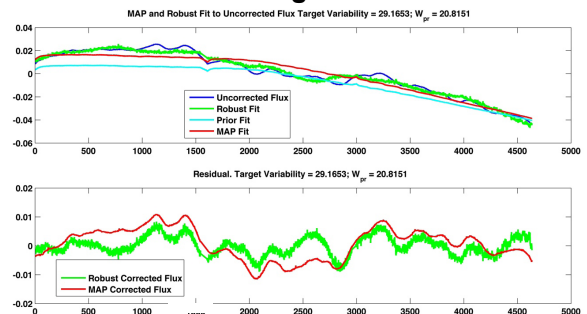
References:

- [1] Jenkins, J. M., et al., *ApJL* **713**, L87 (2010)
- [2] Ciardi, David R. et al. *AJ* **141** p. 108 (2010)
- [3] S. M. Kay. *Fundamentals of Statistical Signal Processing: Estimation Theory*. New Jersey: Prentice Hall PTR, 1993

MAP Preserves Stellar Variability Better than Robust Least Squares



MAP Guards Against Noise Injection Afflicting LS Fits



Celestial orbits: new theory

Necat Taşdelen: necattasdelen@ttmail.com

Abstract:

Kepler’s celestial theory is based on his 3 laws: elliptical orbits, swept out area equality in equal interval of time and interplanetary period law. I am claiming that, according Newton’s mechanical laws a new celestial theory should be considered.

Keywords:

Celestial orbits, Kepler laws, elliptic orbits, Newton laws, spiraled orbits

Introduction:

Consider Newton’s

$$(F*dt=m*dv) \text{ expression;} \tag{1}$$

Where F is a vector and its components are Fradial=Fr and Fperpendicular=Fp and,

$$\text{Work}=F*L \quad \text{where (L) is the displacement length} \tag{2}$$

$$dW_r=dF_r*L+F_r*dL$$

$$dW_p=dF_p*L+F_p*dL$$

and we write

$$dW_p=m*d(dV_p/dt)*L+m*dV_p/dt*dL$$

$$dL=r*da \quad \text{where (da) is the polar angular differential}$$

$$dW_p=m*d(dV_p/dt)*L+m*dV_p/dt*r*da$$

In physics “*the work in the perpendicular direction to the attraction field equal zero*”. So,

$$dW_p=0$$

$$d(dV_p/dt)*L+dV_p/dt*r*da=0$$

$$dV_p/dt=0 \quad \text{which means, when integrating} \tag{3}$$

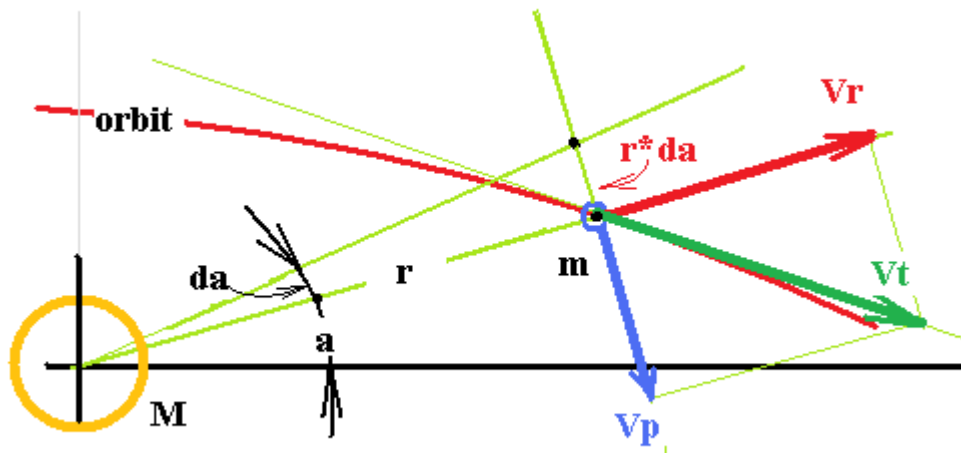
$$V_p=Ct \tag{4}$$

That is:

Kepler’s law about the equality of swept out area in equal time interval is not correct.

*Kepler says: (r*Vp=Ct) (area law which is pronounced as r and Vp variables)*

Newton says: (Vp=Ct) (no area law. even r is variable)



P1020. POSTER SESSION II

Ultracool dwarfs in Kepler Field of View R.Tata¹ and E.L. Martin², ¹Instituto de Astrofísica de Canarias; C/ Via Lactea s/n Tenerife Spain 38200; rrtata@iac.es, ²INTA-CSIC Centro de Astrobiología ege@cab.inta-csic.es

Introduction: Despite of the tremendous progress in the discovery and understanding of ultracool dwarfs (very low-mass stars and brown dwarfs with spectral types later than about M6) in the last 2 decades, only a handful of these objects have been detected at low galactic latitudes ($|b| < 5$), and little is known about their photometric variability properties. We use selection criteria based on photometry and proper motions to select ultracool dwarf candidates from the Kepler Input Catalog (KIC). We have obtained follow-up low-resolution optical spectroscopy for 5 of these candidates at the 4m Mayall telescope at KPNO which allow us to confirm that their spectral properties are those of ultracool dwarfs (4 late-M and one L-type). These candidates provide excellent targets for transit searches and variability studies at the ultracool end of the spectrum. We estimate that, given the Kepler precision expected, for their brightness and their small radii, a detection of earth sized planets is feasible around them.

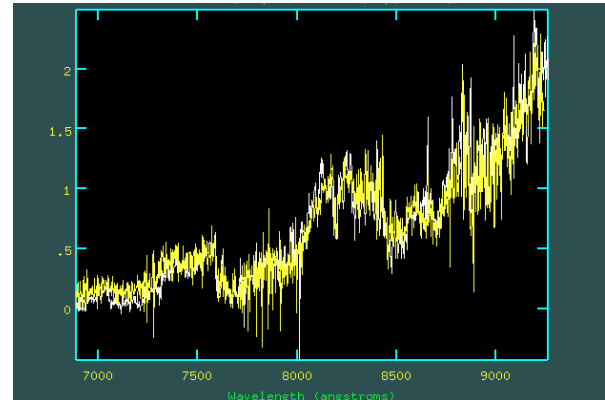


Figure : A plot showing an L0 dwarf from literature (in yellow) overplotted against the spectrum of a candidate observed at 4m Mayall Telescope (in white) in September 2011 using RcSPEC.

P1021. POSTER SESSION II

A Comparison of the Characteristics of the Central Stars of M57 and NGC 6826.

P. Temple, phxbird@hotmail.com, Western New Mexico University, P.O. Box 1235, Deming, NM 88031

Introduction: In scientific and popular literature there has been a question of whether the central stars of planetary nebulae are variable. Due to the difficulties of observing these objects from ground based telescopes the answer to this question is only now being investigated. Without a space based instrument like Kepler obtaining high precision photometry and determining variability required a precision photometer or specialized CCD techniques and software. Even with these limitations in mind progress was made.

Grauer and Bond 1984¹ used a high speed photometer to discover low amplitude pulsations in PN of Kohoutek I-16. This study led to further discovery of 16 PN and 5 pulsating PN with binary central stars Bond²³. Handler⁴ points out 3 kinds of variability in central stars. Variability seems to be common in the stars studied but these studies are limited to a very small percentage of known PN due to the difficulty of observation.

M57 and NGC 6826: In the fall of 2009 a short imaging run of 56 images was taken of PN M57 with the 11" AAVSONET⁵ telescope at Astrokolholz observatory in Cloudcroft, NM. Each image was a 90 second exposure using an I filter. The period is $\approx .19$ of a day, with a magnitude change of .6 magnitude. There are hints in the light curve of a possible close contact binary of a very short period, with lots of brightening and dimming that confuse the interpretation. However, the data run was of too short a duration and the telescope aperture too small to feel confident in the results on its own merits.

Now with recent Kepler data (4 runs at this time) there is enough information on NGC 6826 to compare it with the ground based M57 data. NGC 6826 has a period of .619 of a day and a magnitude change of 10 mmag. These figures are much more precise than what can be obtained by an 11" ground based telescope making direct comparison difficult. The time scale of the Kepler data stretches over days while the M57 data is only over 1.5 hours. However, there is still a similar pattern to the two light curves, a close approximation to a contact binary interspersed with chaotic light spikes of an unknown nature. Douchin et al⁶ confirms the binary properties of NGC6826 in a recent paper. This opens the possibility that M57 is also a binary system with a much faster period and greater magnitude fluctuation. With both M57 and NGC 6826 there is a familiar appearing pattern to the light curves but it does not comfortably fit any known models of variable stars at this time. Without much more ground and

space observations of more stars the astrophysics of these objects can only be speculated.

Conclusion: The question of variability has been definitively answered! There is obvious variability in many planetary nebulae. The next question is how widespread is this variability, as well as what is causing the variability. The current model of star formation and death may be challenged if it is found that a binary configuration is needed to cause the winds that define a planetary, Bond⁷.

With the 5 PN in the Kepler FOV it may be possible to start answering this second set of questions over the next several years. The mmag precision and 30 minute to 60 minute integration times over several months time should provide a great deal of data to process and from the subsequent light curves, better astrophysical information can be gleaned.

Further ground based and space based observations are needed to complete a picture of the physics of these most interesting stars. Careful ground based differential photometry or high speed photometry of a much larger sampling of PN are needed from ground and space. Time series taken over many nights of different PNe coupled with the precision of the Kepler data would at least begin to give a more complete model of the physics of the central stars of PN until more spaced based data is available.

References:

-
- ¹ Grauer and Bond 1984, APJ 277:211-215
 - ² Bond and Meakes 1990 AJ, v100 # 3
 - ³ Bond and Ciardullo 1990 ASPC 11:529B
 - ⁴ Handler 1997 IAUS 180:109H
 - ⁵ AAVSO Wright 28
 - ⁶ Douchin and Jacoby 2011 Proceedings IAU Symposium #283
 - ⁷ Bond 2000 ASPC 199:115B

P1022. POSTER SESSION II

DYNAMICS OF PROTOPLANETARY DISKS IN STELLAR CLUSTERS. S. Torres¹ and B. Pichardo²,
¹Instituto de Astronomía, Universidad Nacional Autónoma de México, Apdo. postal 70-264 Ciudad Universitaria, D.F., México, storres@astroscu.unam.mx, ²Instituto de Astronomía, Universidad Nacional Autónoma de México, barbara@astroscu.unam.mx.

Introduction: Most stars are born in stellar clusters [1],[2], these are environments where stellar density reaches $1M_{\odot}/pc^3$ to $10^4M_{\odot}/pc^3$.

Planetary disks around stars in these environments are affected by gravitational interactions along their passage through these stellar regions. Disk interactions with stars cause truncations of the disks. The most abundant stars in the Galaxy ($\sim 75\%$) are called very low mass stars, this is because the small stars $[0.013$ to $0.6] M_{\odot}$, burn their fuel slowly and stay a much longer time on the main sequence. With the development of technology, astronomers have been able to detect planets around other stars (688 (26/09/11)), a significant number of them corresponds to very low mass stars.

In this paper we analyzed the dynamics of planetary disks in very low mass stars that belong to the star clusters. We study orbital parameters (eccentricity, inclination, pericenter and apocenter) after the interaction between the host and the flyby stars. To achieve this goal we use a code of stellar encounters (EEC).

Methodology and Numerical Implementation:

The code of stellar encounters simulates the gravitational interaction between a planetary system characterized by a cold disk of test particles in a Keplerian potential and a hyperbolic orbit of the flyby star. In general, the EEC solves the equations of motion in the non-inertial reference system of the central star, providing the required orbital parameters.

The code is 3D. The sampling of orbits goes as $a \propto n^{-3/2}$, where a is the semimajor axis of the particle's orbit, and n is the number of orbits. Particles are under the influence of the stellar forces (main and flyby star), and the equations of motion are solved from the Sun's non-inertial frame of reference. The code calculates the main orbital characteristics of the debris disks after a flyby, such as eccentricity, pericenter, apocenter and inclinations. The Bulirsch-Stoer integrator gives a maximum relative error before the flyby of 10^{-14} and 10^{-13} in the energy and angular momentum integrals, respectively.

Simulations and Preliminary Results: To make the simulations we used the following parameters:

1. Host star: For brown dwarfs mass range is $[0.013-0.075]M_{\odot}$, for these simulations we take the upper limit, $0.075M_{\odot}$ this because they are the most abundant in star clusters. On the other hand, the case of red dwarf mass range is $[0.08$ to $0.6]M_{\odot}$ we know the average mass of stars in open clusters is $0.5M_{\odot}$ [3], that

correspond to red dwarfs so this mass taken for the simulations.

2. Flyby star: The most abundant stars in open clusters are red dwarfs with a mass of $0.5M_{\odot}$ average, we use this mass for the simulations.

3. Velocity dispersion: The typical velocity dispersion in open clusters is between $1-3km/s$. For these simulations we take $3km/s$ because this speed is more common in these environments [3]. While for the globular clusters, the range is from $5-15km/s$. For these simulations we worked with $8km/s$.

4. Interaction time: The code is structured as that the interaction of the perturbing star with the planetary disk is in a period of 10.000 years.

5. Disk: Since dwarf stars have little mass, its planetary disks have small radii $\sim 20 - 80AU$ (Bate et al. 2002), for brown dwarfs we take an interval $[0.1$ to $60] AU$, while for red dwarfs we work with $[0.5-70] AU$.

6. Interaction angle: We take $\phi = 0$, $\theta = 45$ and $\alpha = 45$.

7. Impact parameter: we working with: 1000, 500, 300, 200, 100 AU.

Brown Dwarfs (Open Clusters): For 1000AU impact parameter of the disc is not altered. For the impact parameter 300AU the particles in the range of 30-60 AU, obtained eccentricities up to 0.7 and inclinations at 35 degrees. On the other hand the particles at the periphery of the disk is ejected to more than 100AU.

Brown Dwarf (Globular Clusters): For 1000AU interaction the effect on the disk is negligible, while for 200AU the particles are ejected more than 100AU, attain inclinations at 30 degrees and eccentricities up to 0.7, the particles between 0 and 15 AU remain unchanged.

Red Dwarf (Open Clusters): For 500UA of impact parameter is not altered in the orbital parameters. At 200AU begins to be a significant change in the orbital parameters, since the particles are on the edge of the disk come to reach 0.5 eccentricities and inclinations of 40 degrees and are ejected to 100AU. The particles that remain unchanged are between 0.5 and 20UA.

Red Dwarf (Globular Clusters): For interactions of 500 AU, the effect is zero, while for 200AU the interaction of particles in the periphery of the disk (50-70) AU undergo changes in their orbital parameters obtained inclinations at 20 degrees and eccentricities of 0.2.

Conclusion: The Preliminary results show us that brown dwarfs stars are more vulnerable than red dwarfs stars to gravitational encounters in stellar clusters, which means it is more difficult the planet forma-

P1023. POSTER SESSION II

ZODIACAL DUST BANDS OBSERVED IN THE KEPLER BACKGROUND . J. E. Van Cleve^{*1}, W. T. Reach², F. C. Witteborn³, D. Caldwell¹, B. Clarke¹, W. Borucki⁴, and J. M. Jenkins¹
[*jeffrey.vanclave@nasa.gov](mailto:jeffrey.vanclave@nasa.gov), ¹SETI Institute/NASA-Ames Research Center, MS 244-30, Moffett Field, CA 94035, ²USRA/SOFIA, ³Orbital Sciences Corp., ⁴NASA-Ames Research Center

Introduction: *Kepler* measures the brightness of the background on each Long Cadence (LC) using a dedicated array of background pixels on each channel. This background is the sum of zodiacal light and unresolved stars in roughly equal proportion. Since the unresolved stellar contribution is unchanging in *Kepler*'s fixed field of view (FOV), the time-varying component of these background observations is due to the zodiacal light. Within this FOV, *Kepler* offers a combination of spatial and temporal resolution, precision, and data continuity not matched by any other single instrument for the study of the three-dimensional structure of zodiacal light. *Kepler* thus complements the all-sky maps of infrared survey missions such as IRAS, COBE, and WISE.

Detection and Imaging of Events: Early *Kepler* operations showed transient background phenomena lasting at most a few minutes, which were attributed to sunlight scattered from debris spalled off *Kepler* by micrometeoroids [1]. In the course of that earlier study, we also found a few transients on time scales of 2-48 hrs, with amplitude of a few percent of the large-scale background in the Kepler FOV, which move as coherent structures across the focal plane (Figures 1 and 2), which we interpreted as scattered light from dust particles of cometary or asteroidal origin in our Solar System.

Here we report a more thorough study of these slow events in the first two years of Kepler data, using a detection filter which is better matched spatially and temporally to these slower events than the one used for the debris events. We construct event images by subtracting background maps from times well-removed from the event from background maps based on pixels collected during the detected event. We then relate the heliocentric longitude and orientation of the structures observed at a given point in Kepler's earth-trailing orbit to those expected from known comet and asteroid dust trails [2, 3, 4], compare the low spatial and temporal frequency component of the observed zodiacal light to the predictions of the three dimensional model of Reach [4], and examine the year-to-year reproducibility of events at the same ecliptic longitude. Based on the early results shown in Witteborn [1], we expect to be able to detect events as faint as 0.5% of the large-scale zodiacal brightness, with spatial resolution of small as 0.25 degrees. An initial inspection of the background flux time series suggests 2 or 3 events per observing quarter will be found.

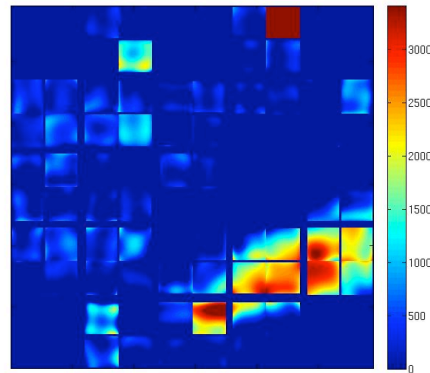


Figure 1: Early event image from LC #13395 of an elongated object that stayed in the focal plane for over 6 hours on MJD 55215. The image is 13.0x13.0 degrees; flux units are e-/cadence per pixel. The maximum on the scale corresponds to only 0.8% of the large-scale sky brightness.

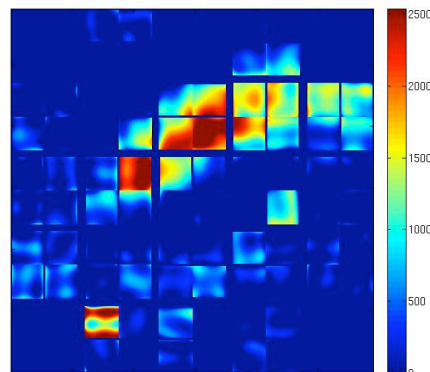


Figure 2: The elongated object as seen 6 hr later on LC #13407. It maintained about the same size and shape in all the intervening images, but slowly moved upward in the field-of-view as one would expect for an object, which Kepler passes “underneath” in the course of its earth-trailing heliocentric orbit. Image scale and flux units are the same as in Figure 1.

Funding for this work is provided by the NASA Science Mission Directorate.

References:

- [1] Witteborn F. C. et al. (2011) Proc. SPIE 8151
- [2] Nesvorny, D. et al. (2010) *ApJ* 713, 816. [3] Mainzer, A. et al. (2011) *ApJ* 731, 53. [4] Reach, W. T. (2010) *Icarus* 209, 848.

P1024. POSTER SESSION II

UNDERSTANDING QUASAR VARIABILITY THROUGH KEPLER. A. E. Wehrle¹, S. C. Unwin², P. J. Wita³, and D. Silano³, ¹Space Science Institute, 4750 Walnut Street, Suite 205, Boulder, CO 80301, awehrle@spacescience.org, ²JPL, Mail Code 301-170S, 4800 Oak Grove Drive, Pasadena, CA 91101, Stephen.c.unwin@jpl.nasa.gov, ³The College of New Jersey, Department of Physics, P.O. Box 7718, Ewing, NJ 08628, witap@tcnj.edu, silano2@tcnj.edu.

We are monitoring four flat spectrum radio quasars (blazars) and one powerful radio galaxy, Cygnus A, to search for variability on timescales comparable to the light crossing time of the accretion disk around the central supermassive black hole and the base of the relativistic jet. We want to see if some optical variability in quasars is due to a bright feature in the accretion disk as it approaches the last stable orbit, or if it is due to inhomogeneities in the jet, possibly in a helical structure. When the quasars are in quiescent, faint states, a quasi-periodic light curve indicates an accretion disk origin, and provides a dynamical means of measuring a lower limit to the mass of the supermassive black hole which may be compared to those derived by other methods, such as the shape of X-ray iron K α lines and stellar velocity dispersions. When the quasars are in bright states, then long-lived quasi-periodic oscillations (QPOs) are very probably from helical features in the jets, but if several different short-lived QPOs are seen in one quasar, then the emission is probably coming from turbulence behind a shock. If during a faint state, instead of QPOs, we detect aperiodic variations, including high and low breaks in the power spectrum density (PSD), then we may obtain the physical scales of the inner and outer edges of accretion disks and hence the BH mass. Aperiodic variations during a high state, with breaks in the PSD, could yield the smallest and largest physical scales corresponding to light travel times, modulo the Doppler factor, in the relativistic jet.

Kepler is ideally suited to the necessary measurements by delivering highly stable photometry continuously on timescales from minutes to days. The principal challenge of our Kepler data analysis is that the automatic pipeline removal of day-to-week-scale drifts also removes real astrophysical brightness variations. We will present preliminary results on short timescale variations.